공학박사학위논문

복합차원 열유동 해석 기법을 통한 가솔린 자동차용 엔진 폐열 회수 시스템 열교환기의 설계 최적화

Design Optimization of Heat Exchangers of an Engine Waste Heat Recovery System for a Gasoline Vehicle based on Combined-Dimensional Thermal Flow Analysis Approach

2015년 2월

서울대학교 대학원

기계항공공학부

배 석 정

복합차원 열유동 해석 기법을 통한 가솔린 자동차용 엔진 폐열 회수 시스템 열교환기의 설계 최적화

Design Optimization of Heat Exchangers of an Engine Waste Heat Recovery System for a Gasoline Vehicle based on Combined-Dimensional Thermal Flow Analysis Approach

지도교수 김 찬 중

이 논문을 공학박사학위논문으로 제출함

2014년 11월

서울대학교 대학원

기계항공공학부

배 석 정

배석정의 박사학위논문을 인준함

2014년 12월

위 원 장: 민 경 덕 (인)

부 위 원 장: 김 찬 중 (인)

위 원: 송 한 호 (인)

위 원: 송 정 호 (인)

위 원: 김 사 량 (인)

Abstract

Design Optimization of Heat Exchangers of an Engine Waste Heat Recovery System for a Gasoline Vehicle based on Combined-Dimensional Thermal Flow Analysis Approach

Sukjung Bae

Department of Mechanical and Aerospace Engineering

The Graduate School

Seoul National University

Strict regulations on emission and fuel consumption are expanding worldwide in response to the global warming and the depletion of natural resources. The improvement of fuel efficiency by development of power-train technology has reached its limit.

In this study, a waste heat recovery system based on Rankine cycle is constructed to improve the fuel efficiency of gasoline vehicles. A commercial CFD analysis tool is capable of predicting detailed flow distribution for complex geometries, but it cannot adequately simulate the phase change processes yet. On the other hand, the performance prediction code is one-dimensional, but it can take phase change into account, and enables a quick

verification of the effect of change in design factors. In this study, an optimized design process has been established by harmonizing the advantages of these two design techniques. The design of the waste heat recovery system have been performed through combined-dimensional analytical processes.

First of all, the system layout has been decided by the one-dimensional analysis. The cycle performance prediction program has been developed to select working fluids through the system performance prediction, design the cycle performance, and decide the design specification of core components. As a result, the system layout containing dual-loop cycles has been designed. The waste heat recovery system consists of an HT (high temperature) loop, in which water, as the HT working fluid, recovers waste heat from the exhaust gas, and an LT (low temperature) loop, in which a refrigerant, as the LT working fluid, recovers heat dissipation from the HT loop, and waste heat from the engine coolant of relatively low temperature.

A new design of HT boiler, which recovers waste heat from exhaust gas, has been conducted. The working fluid in the HT boiler experiences a phase change from liquid state to saturated state. At a liquid state, the specific volume of the working fluid is so small that the cross-sectional area must be small, otherwise it would not recover sufficiently the waste heat. On the other hand, at a saturated state, the specific volume of the working fluid grows with quality, i.e., the cross-sectional area of the heat

exchanger need to be considerably large compared to that of liquid state. Focusing on this point, three structural concepts have been established, designed via 1D and 3D analytical design process, embodied as prototypes, and assessed by experiments.

A novel design process model for an LT condenser has been built, so that the pressure drop is reduced, while the heat transfer performance is maintained close to a target value. The refrigerant has low enough evaporation temperature to recover the waste heat from engine coolant of about 100 ℃, but has small saturation enthalpy. Thus, excessive mass flow rate of the LT working fluid, e.g. over 150 g/s, causes a significant pressure drop to maintain the heat dissipation performance of more than 20 kW. An investigation for multi-pass structural design has been conducted by inspecting the number of passes, and the arrangement of the numbers of tubes, in order to enhance the flow uniformity and reduce the pressure drop of working fluid.

The cycle design technology and the combined-dimensional optimization design process for the core heat exchangers are expected to play a role of bridgehead to secure technological competitiveness in the future automotive waste heat recovery field.

keywords : **Waste Heat Recovery System, Rankine Cycle, Boiler, Condenser, Thermal Flow Analysis, Combined-dimensional Analysis**

Student Number : 2008-30855

Contents

List of Tables

List of Figures

Nomenclature

A : Area [m^2]

C : Heat capacity [W/K]

c_p : Isobaric specific heat [J/kgK]

D : Diameter [m]

d : Diameter [m]

De : Dean number [-]

f : Fanning friction factor [-]

G : Mass flux [kg/s-m^2]

H : (Spiral) depth [m]

h : Convection heat transfer coefficient [W/m^2K]

k : Conduction heat transfer coefficient [W/mK]

$\dot{m}$: Mass flow rate [kg/s]

N : Number of data [-]

NTU : Number of transfer unit [-]

Nu : Nusselt number [-]

P : Power [W]

p : pitch [m]

Pr : Prandtl number [-]

Q : Heat transfer rate [W]

q : Volume flow rate [m^3/s]

Re : Reynolds number [-]

s : Ratio of cross-sectional area [-]

T : Temperature [℃]

t : Thickness [m]

UA : Overall heat transfer coefficient [W/K]

W : Work [W]

X : Lockhart-Martinelli parameter [-]

δ : Tube thickness [m]

δx : longitudinal increment [m]

ϵ : Heat recovery rate [-]

η : Efficiency [-]

μ : viscosity [kg/m-s]

ξ : Heat recovery rate [-]

ρ : Density [kg/m^3]

σ : Flow uniformity [-]

Φ : Two-phase multiplier

ϕ : Severity factor [-]

Subscripts

C : Cross flow section

c : Sudden contraction

CE : End of cross flow section

$crit$: Critical

d : (Heat) dissipation

e : Sudden expansion

Chapter 1

Introduction

1.1 Background and Motivation

Recently, the environmental concerns on global warming and the depletion of fossil fuels have caused strict regulations limiting emissions and fuel economy. Regarding these issues and the trend of development in the world's automobile industry, the importance in the reduction of greenhouse gases and fuel efficiency improvement technology are highlighted at present [Ringler09, Endo07, Heo10].

European fuel consumption regulations have been enacted to limit carbon dioxide emissions to 130 g/km by 2012 and 95 g/km by 2020. Regulations have been announced in the US to reduce greenhouse gas emissions and improve fuel economy to 35.5 mpg by 2016. The regulations are presumed to significantly strengthen fuel economy to 50.0 mpg. The Korean government and the automotive industry are undergoing deliberations for the development of green cars to achieve a fuel economy target of 17.0 km/l by 2015. Such fuel consumption regulations have changed from self-regulation agreements to more aggressive

regulatory measures that impose penalties. There is also a trend of using the enhanced regulations as trade barriers by applying penalties to imported vehicles that do not meet the regulations [Heo10]. As a result, the world's car makers are tending toward the development of co-generation system technology as well as clean diesel cars, hybrid electric cars, and hydrogen fuel cell vehicles; these comprise the principal directions of research and development.

In contrast to new concept cars with fuel cells or hydrogen that entail a lot of time for infra-structural development, a co-generation system can be applied directly to hybrid electric vehicles as well as conventional internal combustion vehicles and is a good entity to focus on until comprehensive infra-structural developments in the future [Ringler09, Endo07, Teng4, Heo10]. In addition, since it is forecast that sales of new hybrid cars and electric vehicles will occupy no more than 14% of entire car sales by 2035, the development of an epoch-making fuel efficiency improvement technology for gasoline and diesel vehicles is expected to become increasingly important [Kee10].

Compared to the hitherto highlighted technologies to improve fuel economy such as optimization technologies for fuel mixing or combustion processes in power generation steps, a co-generation system is a system to recover the waste energy discharged from the engine coolant and exhaust gas into electric or mechanical energy [Ringler09, Endo07, Teng4, Heo10,

Stobart06]. The system is generally referred to as a co-generation system as it consists of both a fuel combustion system and a waste energy recovery system. The background of the development of technology for engine waste energy recovery systems is based on the consideration that the energy portion used in power generation is up to a maximum of 25 to 35 percent of the fuel energy of a vehicle; the energy used at the main operation range is only 10 to 20 percent. The energy used to drive the actual vehicle is less than 10 percent of the energy, when the drive power for engine auxiliary parts, air and rolling resistance are taken into consideration. It is therefore considered that most remaining energies are disposed of through exhaust gas and engine coolant [Ringler09, Endo07, Teng4, Heo10].

Engine waste energy recovery system technologies are divided into various technologies depending on the type of energy disposal and the method used to recover this energy. Currently, the turbo compound technology that recovers kinetic energy from exhaust gas, the thermo-electric generator technology and the Rankine cycle technology that recover waste heat from exhaust gas and engine coolant have the greatest potential for practical use and are therefore most often performed in studies.

Engine waste heat recovery system technology applying the Rankine cycle has a number of advantages, including the fact its efficiency is high and it is not sensitive to engine load change, unlike turbo compound technology. In addition, its dependency

on the rare elements required for thermoelectric power generation, which result in price increases, is low. Therefore, BMW in Germany, Honda in Japan, along with numerous other companies, are actively performing studies related to this technology [Ringler09, Endo07, Teng07].

The co-generation system technology has been started and being researched by several worldwide leading automobile manufacturers since the mid-2000s; however, the technology is still at the beginning stage that no one has been developed to a mass production stage. Therefore, diverse and profound researches are required on the optimization design of the cycle, the system layout, and the core components for actual vehicle package and cost reduction, the control strategy to maximize the effect of fuel economy improvement, and the design and evaluation technology for various actual vehicle conditions.

1.2 Previous Researches

1.2.1 Automotive Rankine Cycle

According to the prospects of the automobile industry, unlike the fuel efficiency improvement technologies developed up to now at the motive power generation stage, technologies capable of recovering wasted energy from the engine disposed of through exhaust gas and engine coolant without it being converted into motive energy recycled as electric energy or mechanical energy are actively being developed in the USA, Germany, Japan, etc. Currently, the Rankine cycle technology is considered to be the most practical one among various co-generation technologies [Heo5].

Teng *et al.* (2007) of AVL have dealt with the waste heat recovery of a heavy duty truck by organic Rankine cycle technology, in detailed investigation of the working fluids [Teng07].

Ringler *et al.* (2009) of BMW have been leading the technology for the last decade, referred to as 'Turbosteamer', adapting the combined cycle engine to a gasoline vehicle [Ringler09]. In 2012, the second generation 'Turbosteamer' has been unveiled, with a simplified single loop design adapted to a gasoline 2.0L class vehicle. The maximum pressure of the single loop Rankine cycle is set as 10 bar, whose working fluid is water. Reportedly, the

1-loop Rankine cycle promises a fuel efficiency improvement of 6% or more to be used as electric power source. An exhaust heat exchanger plays a role as a boiler in the cycle, which has several working fluid pipes bent between the exhaust flow channel with fins. A compact condenser is located near the engine coolant loop [Freymann12].

Endo *et al.* (2007) of Honda have been studying Rankine cycle technology, in view of maximizing the exergy in a gasoline hybrid electric vehicle. An evaporator is integrated into the engine cylinder head. The engine waste heat recovery system has a volumetric expander which has quite invariant efficiency characteristics at low speed and variation of the flow rate. The evaporator is mounted on the exterior of engine to minimize the modification of the existing engine model. Water, as the working fluid of the system, is heated as hot water (189 ℃, 15 bar) at engine jacket and evaporated as steam by exhaust gas (400 ℃, 80 bar). Automatic control system to adjust the temperature and pressure of steam (water) in accordance with variation of engine load. The fuel economy improved by application of the waste heat recovery system was announced as 13.2% at vehicle speed of 100 km/h [Endo07].

Nelson (2009) of Cummins have constructed a waste heat recovery system for heavy duty truck with 1-Loop Rankine cycle, which aims to improve fuel efficiency about 10% by obtaining electrical energy by a generator mounted on the turbine shaft.

The exhaust gas temperature of a diesel engine is relatively low than that of a gasoline one so that the refrigerant R245fa is used as the working fluid. R245fa, as for the working fluid, has low evaporation temperature and low system pressure than other refrigerants, however, it is not an eco-friendly refrigerant. The waste heat recovery system recovers not only from exhaust gas discharged into the atmosphere, but also from EGR gas and charge air as well [Nelson09].

1.2.2 Core Components for Rankine Cycle

Endo *et al.* (2007) have been integrated an evaporator into the engine cylinder head. The evaporator is mounted on the exterior of engine to minimize the modification of the existing engine model. The evaporator integrated in the cylinder head has stacked plates in which fins are arranged as a type of a built-in plate heat exchanger with serpentine pipes and fins. The working fluid, i.e., water flow is split into two channels at the entrance of the evaporator: one forms counterflow with exhaust gas and recovers waste heat from the exhaust gas; the other recovers waste heat from engine coolant at the cylinder head; and then both flow channel merges at the middle of the evaporator to recover waste heat from the hot exhaust gas and flow into the expander at the super-heated state [Endo07]. The heat sources are the exhaust gas and the engine coolant. However, there is not any bypass flow channel or flow controlling valve. The serpentine pipes and fins have less contact area than shell and tube type heat exchangers. Repeated bending of 180 degree of the pipes leads to a low productivity of the evaporator.

Nelson (2009), investigating the application of Rankine cycle technology onto the heavy duty truck, has been reduced the existing air cooled charge air cooler, and disposed a water cooled CAC in front of the air cooled CAC, in which the working fluid cools down the charge air heated at the compressor. The

superheater is located at the upstream side of EGR line at which the temperature of the exhaust gas is the highest. The condenser is a form of a water-cooled heat exchanger that has a separate low-temperature radiator and receiver integrated auxiliary sub-cooler [Nelson09].

Ye *et al.* (2009) developed a parallel multi-flow condenser for a vehicle air conditioning system that has flow-separating holes on baffles in headers, in order to enlarge the two-phase zone in the condenser. They focused only on the heat dissipation performance, which was increased by about 10% with increase in the mass flow rate of the working fluid. That means the pressure drop of the working fluid is increased rather than decreased [Ye09]. Sanaye et al. (2011) proposed an optimization algorithm for parallel flow condenser by balancing of heat dissipation and pressure drop [Sanaye11].

Lopes *et al.* (2012) reviewed the Rankine cycle core components such as heat recovery heat exchanger, expander, pump and condenser for waste heat recovery from hybrid engines. The types of shell and tube, plate heat exchanger, and metal foam have been introduced as the boiler, or heat recovery heat exchanger. The adequate type for the condenser has been claimed as the plate heat exchanger [Lopes12].

1.3 Thesis Objectives

Engine waste heat recovery systems applying the Rankine cycle for automobiles consist of a one-loop type system that recovers waste heat from exhaust gas and engine coolant or only from exhaust gas using just one working fluid, and a more or less complicated two-loop type system that recovers waste heat and regenerates motive power efficiently from two waste heat sources with different temperature levels through systematically divided usage of different working fluids, and thus maximizes fuel efficiency [Ringler09]. In the case of the two-loop type system, the loop at the high temperature exhaust side refers to the HT (high temperature) loop and the loop at the relatively low temperature engine coolant side refers to the LT (low temperature) loop.

In order to improve the fuel efficiency of automobiles, this study constructed a dual-loop waste heat recovery system, to apply the Rankine cycle to 3.3 liter gasoline vehicles. The waste heat recovery system consists of an HT loop, in which water, as the HT working fluid, recovers waste heat from the exhaust gas, and an LT loop, in which a refrigerant, as the LT working fluid, recovers heat dissipation from the HT loop, and waste heat from the engine coolant of relatively low temperature.

An engine waste heat recovery system consists of electric high

pressure pumps, heat exchangers, valves and controllers for temperatures and pressures of working fluids and is connected the existing exhaust system and engine cooling system so that the technology experience at the research and development procedures will diverge to variety of future technologies. Heat exchangers and pumps, which are core components of the engine waste heat recovery system, are different from ones of other existing system in view of operating conditions such as flow rate, temperature, and pressure. That is, the flow rate of the working fluid in HT loop is within 0.5 L/min, and the flow rate of the working fluid in LT loop is 4 times of the flow rate of refrigerant in the conventional vehicle air conditioning system. Thus, consideration of improvement of reliability in design, selection of the type of the core components, and design of efficiency improvement are significant.

The core components in both loops are superheaters, boilers, condensers, expanders, and pumps. In this study, design processes of HT boiler, HT condenser, LT boiler, and LT condenser have been investigated. Design of performance of the core components starts with selection of suitable types and design of structure of heat exchangers considering the conditions of high temperatures and high pressures. The thermal-flow analysis consists of one by 3D CFD and by 1D program developed for each component. The commercial CFD code is able to predict detailed flow distribution three-dimensionally, but it is not able to

realize the phase change. The 1D performance prediction program developed is one-dimensional, however, it is capable of simulating the phase change, and enables a quick verification of a design parameter. This study has conducted the unique structure design process, and validated with experimental data revealing the heat recovered and pressure drop characteristics.

1.4 Thesis Outline

In this study, the optimization design of the exhaust and engine coolant system layout has been performed for the maximization of engine waste heat recovery performance. As for the purpose of applying a dual-loop waste heat recovery system with Rankine cycles to an automobile, there are a variety of constrictions and limit conditions. The core components of the dual-loop waste heat recovery system are an HT electric pump, an HT boiler, an HT superheater, an HT expander, an HT condenser(LT superheater), an LT electric pump, an LT recuperator, an LT boiler, an LT expander, an LT condenser: two pumps, two expanders, and six heat exchangers.

In Chapter 2, the cycle performance prediction program has been developed to select working fluids through the system performance prediction, design the cycle performance, and decide the design specification of core components. Selection of the working fluids has been conducted by use of the cycle program. As a result, the system layout containing dual-loop cycles has been designed.

In Chapter 3, a process in search of the optimal design of HT boiler, one of the heat recovery heat exchangers in the system, has been conducted. The working fluid in the HT boiler experiences a phase change from liquid state to saturated state.

At a liquid state, the specific volume of the working fluid is so small that the cross-sectional area must be small, otherwise it would not recover sufficiently the waste heat. On the other hand, at a saturated state, the specific volume of the working fluid grows with the quality, i.e., the cross-sectional area of the heat exchanger can be larger than at a liquid state. Focusing on this point, the peculiar heat transfer structure of the HT boiler has been devised.

In Chapter 4, A novel design process model for an LT condenser has been built, so that the pressure drop is reduced, while the heat transfer performance is maintained at a target. An investigation for multi-pass structural design has been described by inspecting the number of passes, and the arrangement of the numbers of tubes, in order to enhance the flow uniformity, and reduce the pressure drop of the working fluid. The scheme of size reduction of the air-cooled LT condenser has been investigated.

In Chapter 5, overall conclusions of the configuration of the waste heat recovery system and the core heat exchangers, and future works to be resolved have been described.

Chapter 2

Design of Cycle and System Layout

2.1 Basic of Rankine Cycle

The co-generation system is defined as the system that the engine power is obtained primarily by combustion and auxiliary power is regenerated secondarily by recovering the waste heat, otherwise discarded. The working fluid in a liquid state is pressurized by high pressure pump, recovers waste heat in the heat exchanger(s) so as to be heated, evaporated, and super-heated, and enters the expander in a high temperature and high pressure vapor state. The system obtains shaft torque from expansion work of the working fluid at the expander.

The basic Rankine cycle consists of the four processes shown in Figure 2.1. Process 1-2 is the reversible adiabatic compression of liquid working fluid by a high-pressure pump. Process 2-3 is the isobaric heat transfer, heat recovery from the heat source by a heat exchanger, and generation of superheated vapor. In general, heat exchangers for heat recovery are sorted into heat exchangers generating two-phase vapor (boiler, evaporator, or steam generator) and heat exchangers generating superheated

vapor (superheater). Yet in some layout structures, one heat exchanger alone generates superheated vapor from liquid.

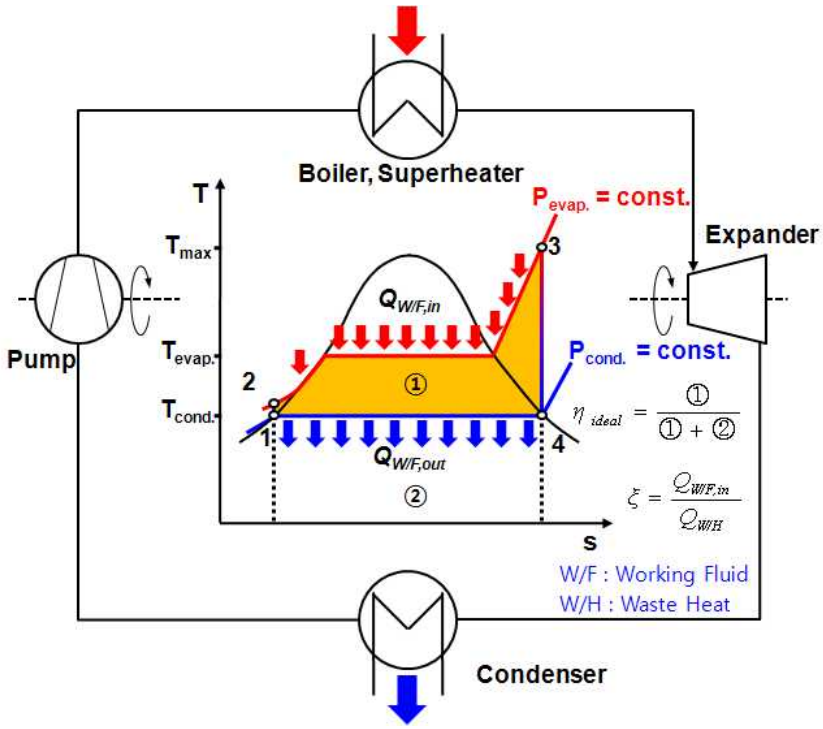

Figure 2.1 Basic Rankine cycle

Process 3-4 is the isentropic expansion of the working fluid vapor in an expander that generates mechanical power. In some cases, a generator is mounted on the expander shaft to convert mechanical energy into electrical energy. Process 4-1 is the isobaric condensation of the working fluid back to the liquid phase along with heat dissipation into the environment.

The ideal efficiency of the Rankine cycle, waste heat recovery,

and ideal regenerative power, respectively, are expressed in the following manner.

$$\eta_{ideal} = \frac{W_{expander} - W_{pump}}{Q_{w/f,in}} = 1 - \frac{Q_{w/f,out}}{Q_{w/f,in}} \quad (2.1)$$

$$\xi = \frac{Q_{w/f,in}}{Q_{w/h}} \quad (2.2)$$

$$P_{ideal} = Q_{w/h} \times \eta_{ideal} \times \xi \quad (2.3)$$

In the above, the waste heat ($Q_{w/h}$) is represented as the product of the mass flow rate of exhaust gas, the isobaric specific heat, and the temperature difference between the exhaust gas and ambient air for the cases where the heat source of the cycle is exhaust gas.

In general, the net work and the efficiency of the cycle increase when the high pressure (the supply pressure) increases and/or the low pressure (the discharge pressure) decreases. In addition, the efficiency of the cycle increases when the maximum temperature of the cycle increases. However, if the working fluid is an organic fluid, the excess overheating in the heat exchanger can deteriorate the cycle efficiency because the thermal instability of the fluid can cause thermal dissociation.

For the same working fluid, since raising the high pressure of the system, i.e., the evaporation pressure increases the evaporation temperature, the cycle efficiency increases, while the

temperature difference between the heat source and the working fluid decreases so that the heat recovery rate worsens. If the system pressure increases, the stability of the system and enhanced reliability design of component parts such as the expander and heat exchangers are required; they are connected directly to the cost of the system. Therefore, it is important to determine the optimal operating conditions considering these issues. The maximum temperature of the system may be limited by problems regarding the stability of the system, the cost of the temperature-resistant material of the component parts, and pollution when leaks occur somewhere in the system [Endo07].

The cycle efficiency increases when the low pressure of the system, i.e., the condensation pressure in the condenser, decreases, but if the low pressure is set below the atmospheric pressure, problems can occur again in terms of the reliability of the system and the core components. The function of the condenser is to release heat to the ambient air. Therefore, the temperature of the working fluid in the condenser needs to be higher than the ambient temperature. Thus, at the low-pressure side, both the pressure and the temperature of the working fluid act as the design constraints; however, if one of the two is determined, then the other is automatically determined since most of the working fluid in the condenser is in the saturation state. Therefore, either of them works as a significant design parameter.

2.2 Selection of the Working Fluid

The selection of the working fluid in the Rankine cycle is a very important first step in system design. That is, the selection or the development of the working fluid requires consideration of the waste heat recovery, cycle efficiency, size of the core components, reliability design, system cost, and safety and environmental aspects.

Generally, the working fluids for Rankine cycle are classified by the slope of the saturation curve as three types: wet fluids, isentropic fluids, and dry fluids. Wet fluid, such as ammonia, water, carbon dioxide, has a negative slope of vapor side of the saturation curve. Dry fluid, such as R11, R12, R134a, has a positive one; Isentropic fluid, such as benzene, R113, R245fa, has almost infinite one.

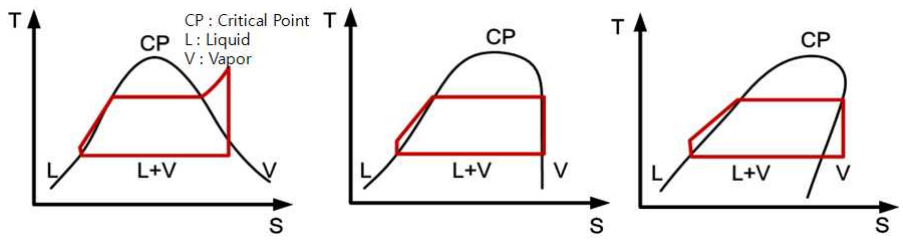

Figure 2.2 Types of working fluids

It is not proper for the wet fluid to be the working fluid where the temperature of the heat source is low, e.g., the exhaust gas of diesel engine, engine coolant, et cetera, since the heat

recovery performance drops off. For the turbine expander, the exit quality of the wet fluid less 0.9 decreases the efficiency, causes the corrosion and damage of the blades. Thus, for the wet type working fluid, the volumetric expander is appropriate.

A cycle analysis program has been developed calculate the heat recovery performance by use of Visual Basic. The input data into the program are the type of working fluid, the cycle high and low pressure conditions, heat source conditions.

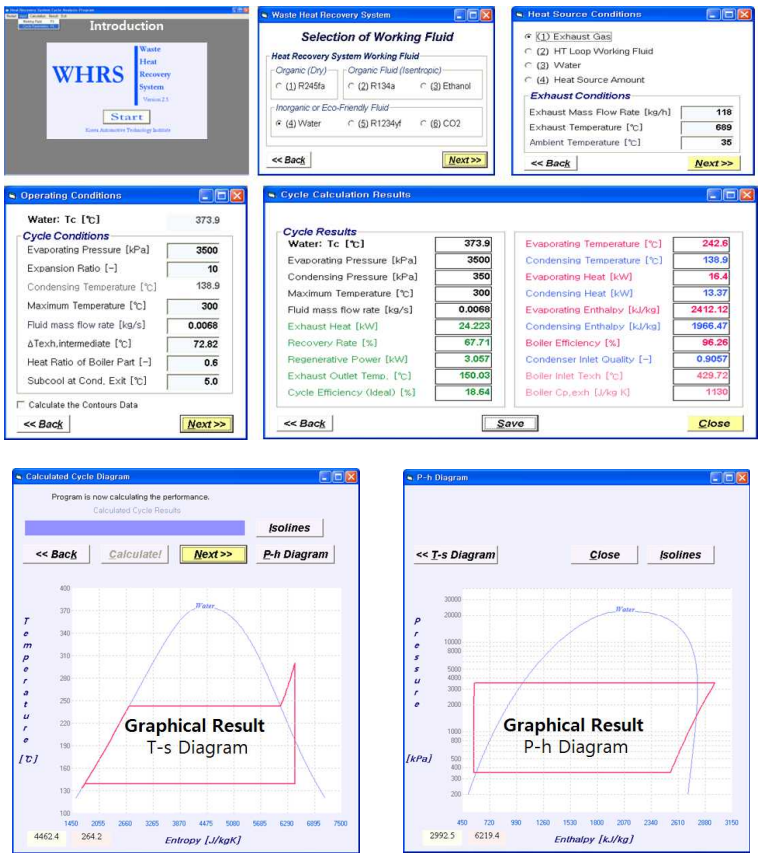

Figure 2.3 The Rankine cycle analysis program

The program simulates the behavior of the working fluid in a Rankine cycle and decides the properties at all the processes(Figure 2.3). The output data from the program are cycle performance data such as the heat recovered, the heat dissipated from the system, the heat recovery rate, the cycle efficiency, the regenerated power, and the outlet exhaust temperature. The physical properties of the states of the working fluid are calculated by use of Refprop 8 in the cycle analysis program. The Rankine cycle heat recovery and regenerated power are calculated from equations (2.2) and (2.3).

2.2.1 HT Working Fluid

In the case of water, the latent heat of evaporation is superior to that of other fluids, and the mass flow rate needed for the recovery of the same amount of waste heat is relatively very small. Regarding the size of the core components, a review of the mass flow rate as well as the specific volume of the working fluid is also required since a smaller volumetric flow rate of the working fluid enables the size reduction design. Thus, water has the merit that it has a somewhat larger specific volume than general refrigerants, but the relatively high latent heat of evaporation enables to reduce the size of the component parts. Moreover, being a natural refrigerant, water is safe in terms of environmental and safety aspects, and the high compatibility of materials facilitates the selection of the materials of components in terms of cost and weight. Furthermore, the thermal stability of water is advantageous in terms of system durability and the choice of the operating range. However, because of its high evaporation temperature, if the temperature of the heat source is low, the heat recovery can be small, and due to the high freezing point, water should be used in the form of a mixture with antifreeze.

Ethanol has a relatively large latent heat, but requires a larger mass flow rate than water for the same waste heat recovery rate. And because of its larger specific volume compared to general

refrigerants, the size of the component parts has to increase. Besides, ethanol is a flammable material with an ignition point of about 13℃, which also serves as a disadvantage.

Most of the refrigerants, which are organic compounds, have very low evaporation temperatures; this is beneficial for the recovery rate, while they have such small latent heats that they require very large mass flow rates for the same heat recovery. Whether or not the refrigerant of concern is an eco-friendly refrigerant (global warming potential of 150 or less) is the primary consideration in the selection of the working fluid for waste heat recovery in a Rankine cycle. A secondary consideration is that the condenser is at the low-pressure side rather than the high-pressure side, as in an air-conditioning system. In other words, if the condensation temperature is set at 60℃, which is estimated roughly from the consideration of a condensation temperature that is higher than that of the ambient air or low-temperature fluid, most of the condensation pressure (the low pressure of the system) of the refrigerant is very high at 20 bar or thereabouts. Hence, although the expansion ratio at the expander is 10, the evaporation pressure is very high at about 200 bar, which can be an additional weak point. Thirdly, the temperatures of the system should be reviewed in light of the thermal dissociation phenomena over a certain temperature range.

A comparison of the characteristics of the working fluid is represented in Table 2.1. R1234yf is an alternative refrigerant, and

has similar thermodynamic properties to R134a. In this study, the working fluid for heat recovery from the high-temperature exhaust gas side was determined readily as water, as described above, with various benefits. For the relatively low temperature coolant side, the environmentally friendly refrigerant R1234yf rather than R245fa, ethanol, etc., was determined as the working fluid taking into consideration the conditions of the temperature of evaporation and the pressure of condensation, and the efficiency of the cycle. Ethanol was a competitor to R1234yf, but had a volumetric flow rate into the expander that was 118 times that of R1234yf. The resulting expander would be enormously large; hence, the fluid was excluded in the light of the possible evaporation and condensation temperatures of the cycle for waste heat recovery.

Table 2.1 Comparison of working fluids for exhaust gas

	Fluid type	GWP (-)	$T_{b,atm}$ (℃)	L_{atm} (kJ/kg)	v_{atm} (m^3/kg)
Water	Wet	Natural ref.	100	2256.5	1.6939
R134a	Isentropic	1,300	-26.1	217.0	0.1926
R1234yf	Isentropic	4	-29.2	178.2	0.1694
R245fa	Dry	950	14.9	196.7	0.1698
Ethanol	Wet	Natural ref.	78.4	820.0	0.6147

2.2.2 LT Working Fluid

The design conditions of the engine coolant for the LT loop cycle design are 40 L/min and 100℃. Working fluid was selected taking into consideration cycle efficiency, size and unit price of the core components, as well as safety and environmental aspects, etc., within the limit conditions of the LT loop cycle design. The limit conditions of the LT loop cycle design include condensation and vaporization temperature. That is, since the air cooled LT condenser at the low pressure side plays the role of condensing the working fluid by discharging heat to the atmosphere, the condensation temperature at the low pressure side must be higher than the ambient temperature (set to 60℃) and the vaporization temperature at the high pressure side must be lower than that of the engine coolant. Taking this into consideration, this study set the vaporization temperature of the working fluid to 93.2℃ under the design point conditions of the engine coolant.

Figure 2.4 shows the theoretical cycle efficiency of working fluids when considering such limit conditions. When applying 60℃ as the condensation temperature of ethanol, the condensation pressure becomes too low, causing a problem in the aspect of part reliability. Therefore, this study applied its saturation temperature, 69.1℃, as condensation temperature at a condensation pressure of 0.7 bar (absolute pressure).

Table 2.2 Comparison of working fluids for engine coolant

	GWP (-)	P_s^* (bar)	L^* (kJ/kg)	$c_{p,x=1}^*$ (kJ/kg-K)	$v_{x=1}^*$ (m^3/kg)
R1234yf	4	33.82	33.5	16.342	0.00301
R245fa	950	10.84	141.0	12.964	0.01626
Ethanol	natural ref.	1.78	823.1	1.889	0.35565

* : values at 93.2℃

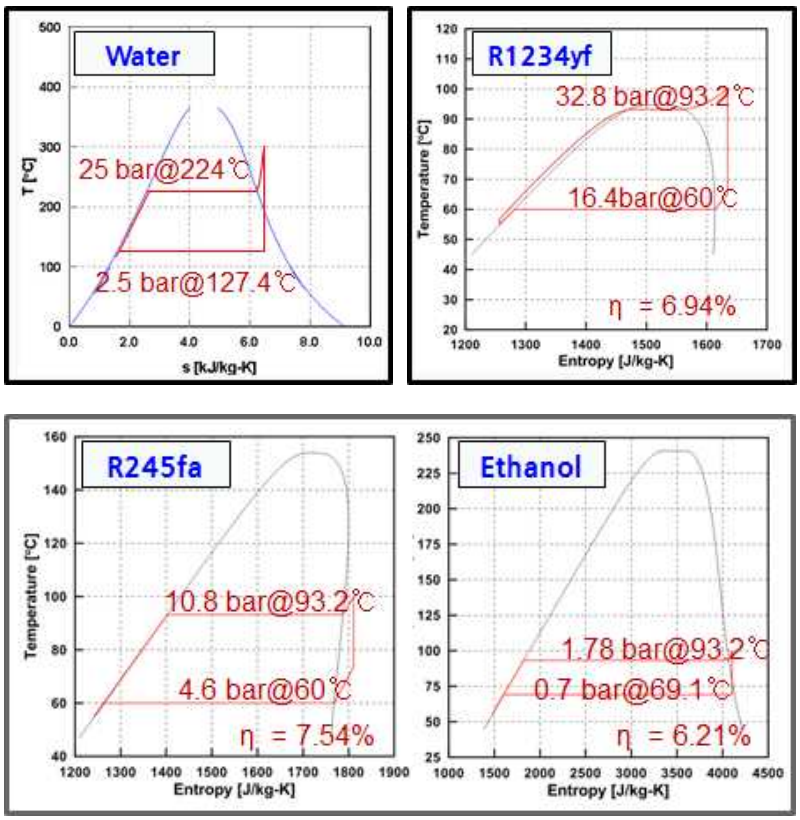

Figure 2.4 T-s diagram according to working fluids

In the case of R1234yf, the system pressure of 32.8 bar is the highest. However, it is thought that this causes no problems as far as pressure design. R245fa exhibits the highest cycle efficiency, but is not environmentally friendly (below GWP 150), as shown in Table 2.2. R1234yf, an environmentally friendly refrigerant considered as a suitable substitute for the current refrigerant R134a for automobile air conditioners, has physical properties similar to those of R134a. Ethanol has the highest latent evaporation heat. However, since its specific volume is 118 times greater than that of R1234yf, it has the disadvantage that the size of key parts, such as the expander, is larger. In addition, one of its disadvantages is that it is a flammable substance with an ignition point of approximately 13℃. Therefore, when considering cycle efficiency and expander size, R1234yf and R245fa can be considered as fluids that work to recover waste heat from the engine coolant. Consequently, R1234yf, an environmentally friendly refrigerant is selected as the working fluid. However, the refrigerant R1234yf is not so easy to be supplied to the system investigated that the refrigerant R134a which has similar properties to R1234yf has been used for the experiments.

2.3 Configuration of the System Layout

2.3.1 Heat Recovery Conditions

The target vehicle is HG Grandeur 3.3 L class vehicle. The Rankine cycle program developed has been utilized for analysis of cycle performance characteristics in the range of the design conditions of exhaust gas.

Table 2.3 Exhaust gas conditions of the target vehicle

Vehicle Speed (km/h)	Engine speed (rpm)	Fuel consumption (kg/h)	Power output (kW)	Exhaust flow rate (kg/h)	Exhaust temperature (℃)	Q_{exh} (kW)
60	1,203	2.45	6.7	38.0	507	5.7
80	1,503	3.82	12.7	59.2	555	9.9
100	2,002	5.10	16.4	79.4	623	15.1
120	2,402	7.58	26.7	118.0	689	25.2

Table 2.3 shows the characteristics of the heat energy of the exhaust gas of the target vehicle. The variation in vehicle conditions is considered to design the engine waste heat recovery system. However, in view of high criteria of the performance and the reliability, the heat source conditions at vehicle speed of 120 km/h have been selected as the design point of the core components. In other words, the requirements for the

performance of the components, and the cycle furthermore, are sufficiently satisfied over the system operation range when requirements are satisfied at the design point. The heat energy is calculated as 25.2 kW at the flow rate of 118 kg/h, and the temperature of 689 ℃ of the exhaust gas, assuming the ambient temperature to be 25 ℃.

The design criteria are selected as the heat energy of the target vehicle over the range of the speed of 60 to 120 km/h for the LT loop heat recovery. The reference temperature is set as 81, 85, 88, and 90 ℃ at which engine coolant at 85, 90, 95, and 100 ℃, respectively, is cooled sufficiently in the conventional engine cooling system.

Table 2.4 Engine coolant conditions of the target vehicle

Vehicle Speed (km/h)	Coolant flow rate (L/min)	Coolant temperature (℃)	Specific heat, c_p (kJ/kg-K)	$Q_{coolant}$ (kW)
60	25	85	4.203	6.8
80	30	90	4.204	10.2
100	35	95	4.205	16.5
120	40	100	4.206	27.0

2.3.2 Limit Conditions for Cycle Design

The constraints for cycle design are, firstly, the expander inlet steam temperature, which is set as 300 ℃. The expansion ratio is set as 10. In case of the expansion ratio of 10 and the evaporating pressure of 25 bar, the pressure and temperature at condensation are 2.5 bar and 127.4℃, respectively.

As shown in Figure 2.5, which presents the expected temperature distribution of exhaust gas and the working fluid at the positions, the temperature of exhaust gas is lowered passing through the HT superheater, the catalytic converter, and the HT boiler. The working fluid flows in the counterflow direction of the exhaust gas flow, and undergoes phase change processes by recovering the waste heat.

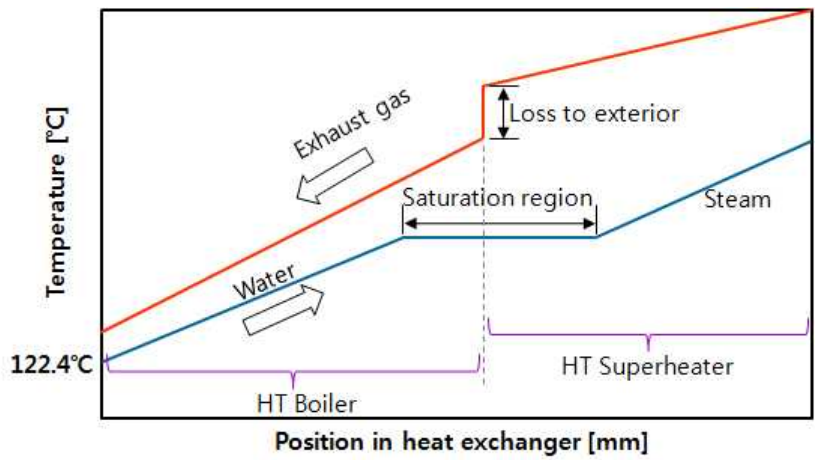

Figure 2.5 Temperature distribution of HT loop side heat waste recovery system

The section assumed to be an exterior loss is one that the exhaust gas loses heat from the exhaust pipe between the HT superheater and the HT boiler. The overall temperature loss is assumed to be up to 60℃ in the cycle analysis.

When the sub-cool at the exit of the condenser is 5℃, the working fluid temperature entering the pump is 122.4 ℃. Thus, the final temperature of the exhaust gas cannot be lower than 122.4 ℃, which is the exit temperature of the working fluid from the HT condenser to the HT boiler.

2.3.3 Design of the HT and LT loop cycles

In order to design the Rankine cycles, the prediction of cycle performance for the working fluids is a matter of primary importance. The mass flow rate of the working fluid affects the system re-generative power and the outlet temperature of the heat source, the exhaust gas for HT loop herein, finally affects the LT loop cycle. The system evaporation pressure determines the cycle efficiency with the fixed expansion ratio. Considering possible cases, the range of the evaporation pressure has been decided as 10 to 45 bar. The range of the mass flow rate of the working fluid has been decided as 5.7 to 7.3 g/s taking into account of the range of exhaust gas outlet temperature around 140 ~ 160 ℃, which is higher than the LT loop maximum temperature.

Figure 2.6 shows the calculation results for HT loop Rankine cycle design recovering the waste heat at the vehicle speed of 120 km/h by use of the cycle analysis program. Figure 2.6 (a) indicates the variation of the exhaust gas outlet temperature from the HT boiler according to the working fluid mass flow rate and the evaporation pressure assumption with the fixed expansion ratio of 10. Even if the mass flow rate of the working fluid is identical, low evaporation pressure decreases the density of the working fluid and increases the volume flow rate so that the volume of the expander should be increased.

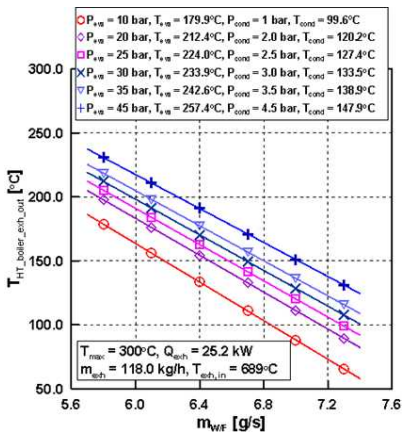

(a) Exhaust outlet temperature

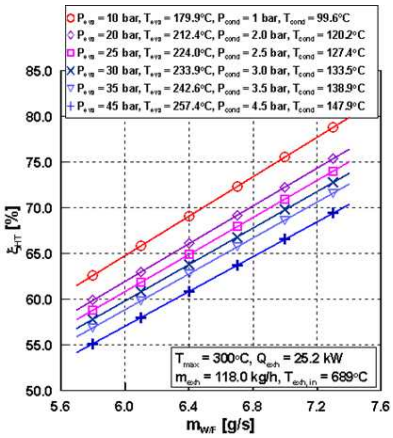

(b) Heat recovery rate

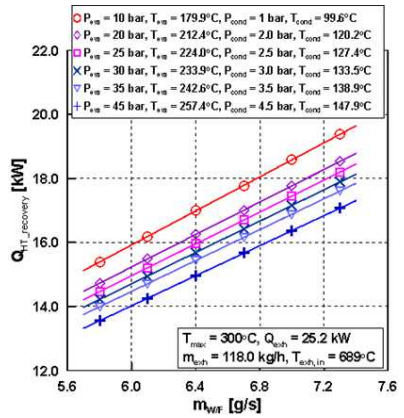

(c) Heat recovery

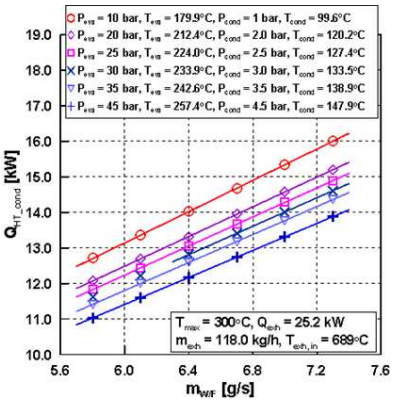

(d) Heat dissipation

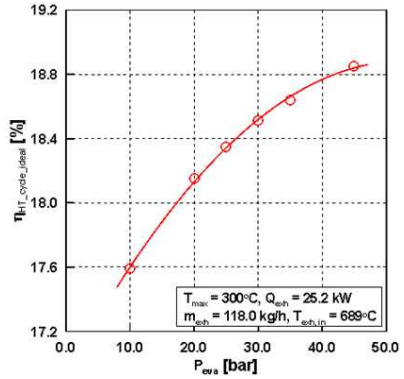

(e) Cycle efficiency

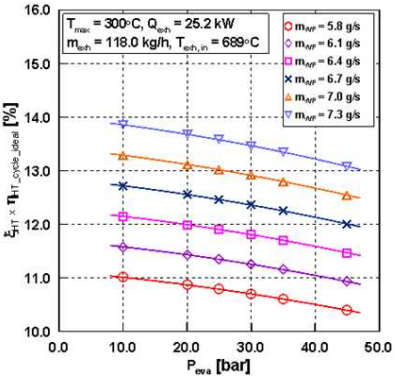

(f) Re-generative power ratio

Figure 2.6 Calculation results for HT loop design (120 km/h)

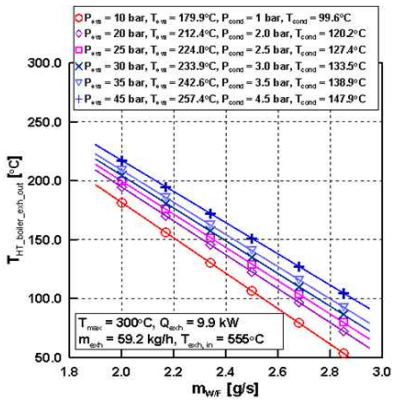

(a) Exhaust outlet temperature

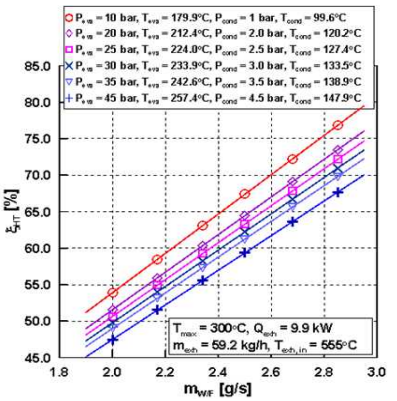

(b) Heat recovery rate

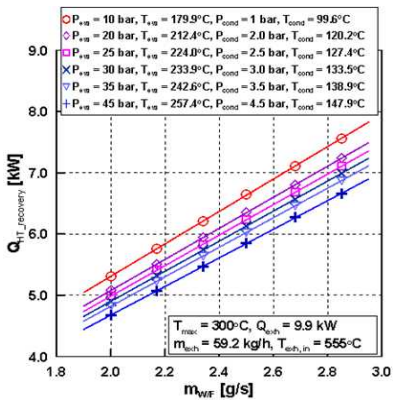

(c) Heat recovery

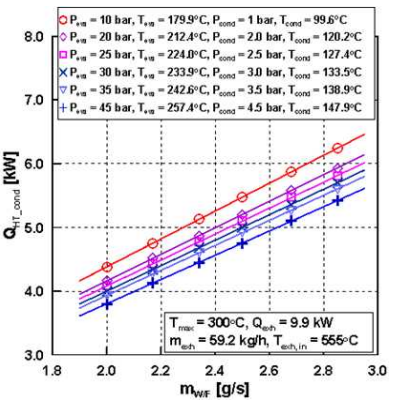

(d) Heat dissipation

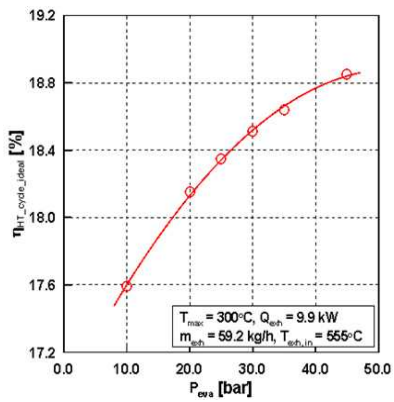

(e) Cycle efficiency

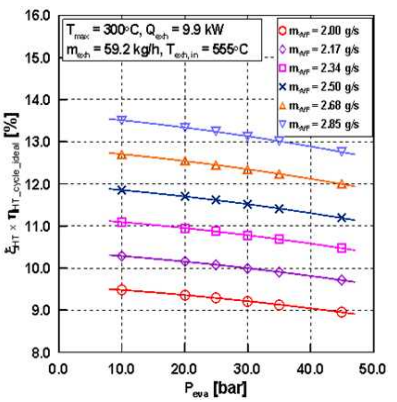

(f) Re-generative power ratio

Figure 2.7 Calculation results for HT loop design (80 km/h)

Figure 2.6 (b) shows the heat recovery rates of the HT loop for the cases of Figure 2.6 (a). In the range of the exhaust gas temperature of 140 ~ 160 ℃, the heat recovery rate is distributed around 65%. The design specifications for the core components are calculated by the cycle analysis program. Figure 2.6 (c) and (d) represent the heat recovery to the HT boiler or the system and the heat dissipation from the HT condenser to the exterior. The heat recovery is about 15 ~ 17 kW and the heat dissipation is about 12 ~ 14 kW in the above range. The theoretical cycle efficiency is shown according to the evaporation pressure in Figure 2.6 (e). The area of the T-s or P-h diagram enlarges as the evaporation pressure increases, which results in the cycle efficiency increase. Figure 2.6 (f) shows the ideal re-generative power ratio according to the evaporation pressure and the mass flow rate. A multiplication of the ratio and the exhaust gas heat means the ideal re-generative power from the cycle. The ideal re-generative power is 2.93 kW from the exhaust gas heat of 25.2 kW when the ratio is 11.9%. The losses at the expander and the power transmission device, et cetera should be considered.

Figure 2.7 shows an example of the calculation results for HT loop design for the recovery at the off-design point of the vehicle speed of 80 km/h. Since the maximum temperature of HT loop working fluid is fixed as 300 ℃, the LT loop working fluid can reach the cycle maximum temperature of 120 ℃ as at the design point. Thus, the reference range of the exhaust gas outlet

temperature from the HT boiler is around 150 ℃. The heat recovery is distributed around 60%. The heat recovery is about 5~6 kW and the heat dissipation is about 4~5 kW in the range. The theoretical cycle efficiency in Figure 2.7 (e) is identical with Figure 2.6 (e), since the maximum temperature and expansion ratio are fixed. The ideal re-generative power is 1.07 kW from the exhaust gas heat of 9.9 kW when the ideal re-generative power ratio is 10.9%. On the other hand, the energy density decreases with increasing evaporation pressure of the cycle over the ranges of working fluid mass flow rates and heat source conditions as shown in Figure 2.8. Energy density of a cycle has been calculated by division of regenerative power by working fluid mass flow rate. The trade-off relation between the cycle efficiency and the energy density should be considered in order to establish the effective cycle design.

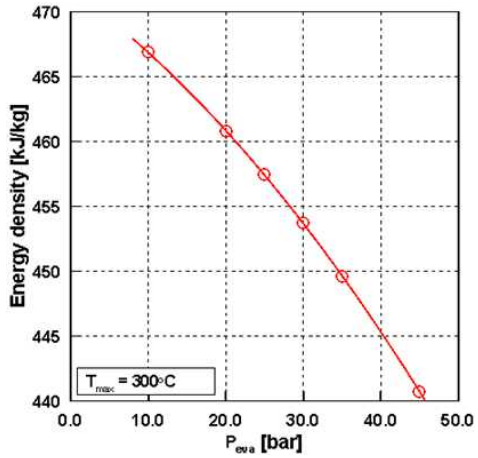

Figure 2.8 Energy density according to the evaporation pressure

Waste heat from the engine coolant and residual heat dissipated from the HT loop are recovered in the heat recovery heat exchangers of the LT loop (See Figure 2.9). The heat dissipation from the LT loop is consequently the subtraction of the re-generative power from the sum of the heat recovery.

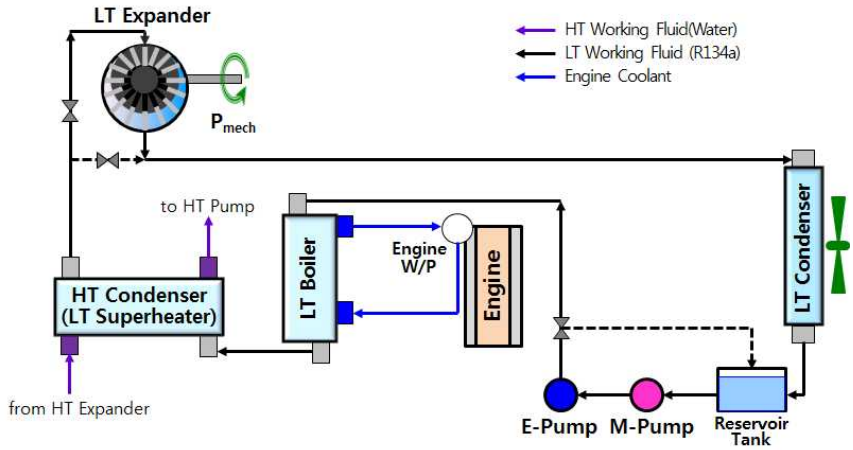

(a) LT loop cycle layout

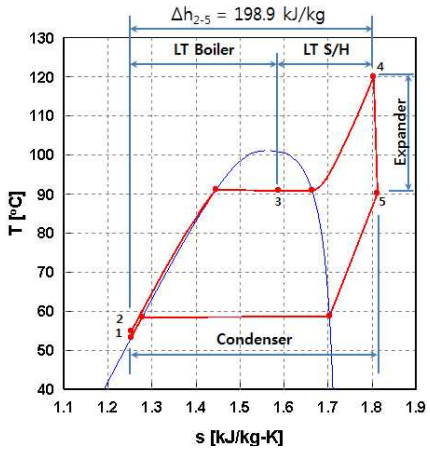

(b) T-s diagram

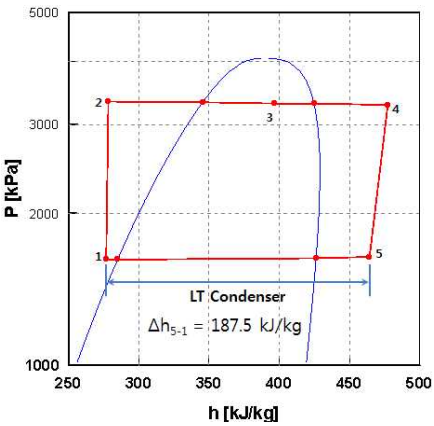

(c) P-h diagram

Figure 2.9 LT loop Rankine cycle design concept

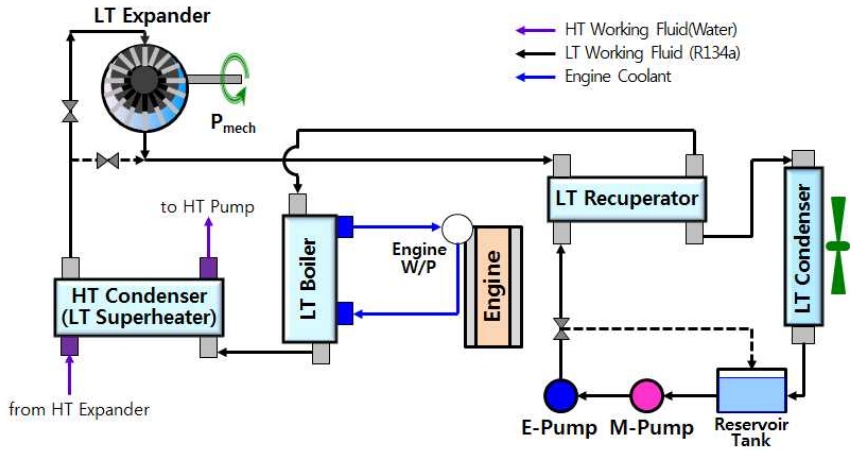

(a) LT loop cycle layout

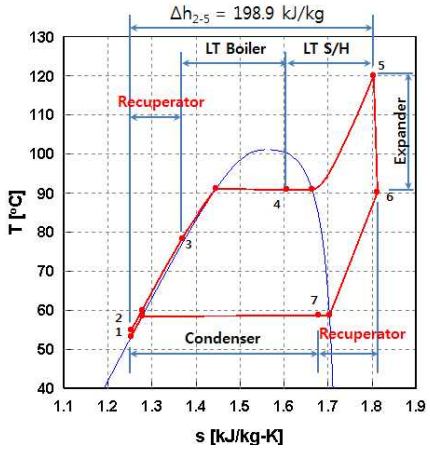

(b) T-s diagram

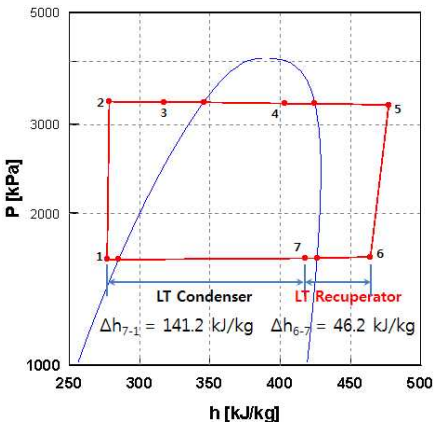

(c) P-h diagram

Figure 2.10 LT loop Rankine cycle design concept - Recuperator considered

At the design point, the heat recovery to the LT loop and the heat dissipation to ambient are about 31 kW and 28 kW, respectively. The mass flow rate of working fluid over 150 g/s for an air-cooled heat exchanger of a passenger vehicle.

Moreover, the heat transfer rate over 20 kW is an excessive amount for these circumstances.

However, an introduction of a heat exchanger can reduce the burden of heat dissipation requirements as shown in Figure 2.10. A recuperator can be located between the LT pump and the LT boiler. In the recuperator, the working fluid the working fluid in the low temperature liquid state from the LT pump exchanges heat with the working fluid in the relatively high temperature vapor state from the LT expander.

In view of the low temperature side of the working fluid, the waste heat is recovered in the LT recuperator; in view of the vapor, it is cooled before it enters the air-cooled LT condenser. Thus, the size of the LT condenser is greatly reduced by adopting the recuperator in the LT loop.

The design of HT and LT cycles has been conducted in consideration of the system target fuel economy on the basis of the characteristics analysis of the heat source. Table 2.5 shows the calculation results from the cycle design with respect to the heat source conditions according to the vehicle speed. The HT loop recovers a part of waste heat from exhaust gas. The LT loop recovers a part of waste heat from the engine coolant and heat dissipation from the HT loop. The expander output is obtained from a multiplication of the heat recovery, the cycle efficiency, and the expander efficiency. An additive multiplication of the transmission efficiency yields the regenerative power.

Table 2.5 Prediction of engine efficiency improvement

Vehicle speed (km/h)	60		80		100		120	
Engine output (kW)	6.7		12.7		16.4		26.7	
Loop	HT	LT	HT	LT	HT	LT	HT	LT
Waste heat (kW)	5.7	6.8	9.9	10.2	15.1	16.5	25.2	27.0
Heat recovery (kW)	3.2	5.8 +2.4	5.9	10.9 +4.3	9.3	13.6 +6.9	16	19.5 +11.5
Theoretical efficiency (%)	18.2	7.90	18.2	7.99	18.2	8.09	18.2	8.15
Expander efficiency (%)	70	60	73	65	73	65	75	67
Expander output (kW)	0.41	0.39	0.78	0.79	1.24	1.08	2.18	1.69
Transmission efficiency (%)	95	95	95	95	95	95	95	95
Regenerative power (kW)	0.39	0.37	0.74	0.75	1.17	1.02	2.07	1.60
Engine efficiency improvement (%)	11.3		11.7		13.4		13.7	

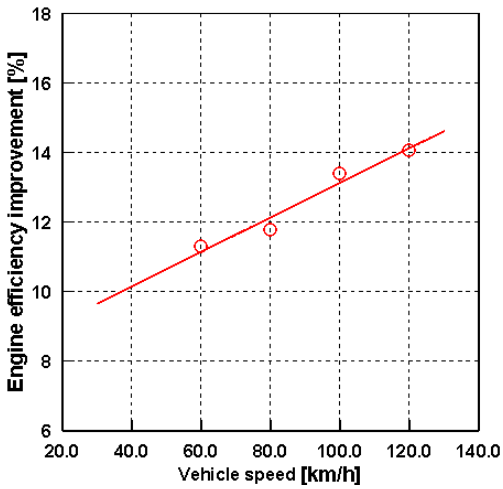

Figure 2.11 Engine efficiency improvement according to vehicle speed

The engine efficiency improvement is calculated by a division of summation of the regenerative power from HT and LT cycles by the engine output. The trend of the fuel efficiency improvement according to the vehicle speed can be estimated as shown in Figure 2.11.

The target fuel economy improvement of the dual loop engine waste heat recovery system is 12% at the highway fuel economy test mode of EPA (Environmental protection agency) of United States. The test mode has a duration of 765 seconds and an average speed of 77.7 km/h. The engine efficiency improvement has been predicted as about 12.0% considering the speed distribution and the trend estimation above.

2.3.4 Dual-loop System Layout

Figure 2.12 shows the final layout design of entire system layout, which consists of HT loop for recovering waste heat from high temperature exhaust gas and LT loop for recovering waste heat from relatively low temperature engine coolant.

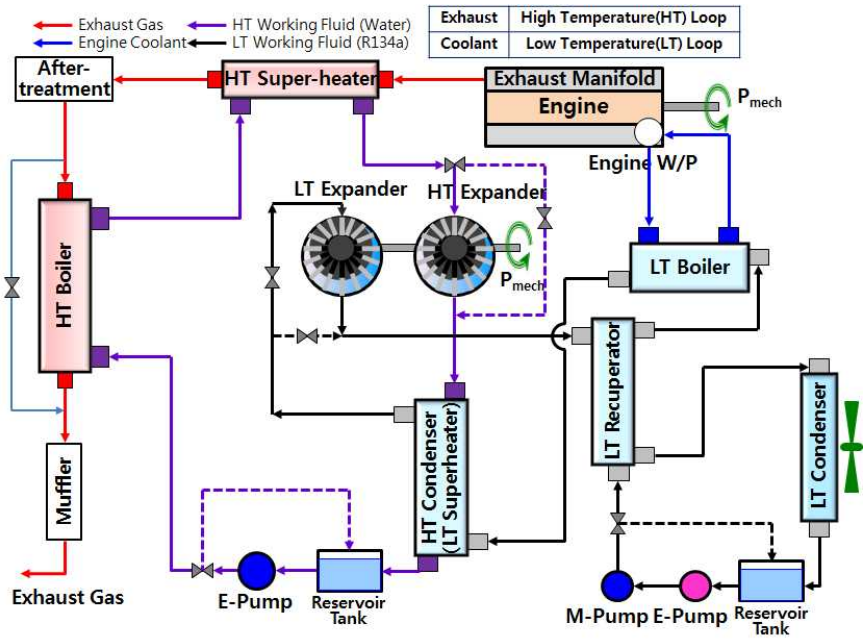

Figure 2.12 Layout of the dual-loop waste heat recovery system

The working fluid compressed to a high pressure by an electric pump generates superheated vapor at the HT boiler and the HT superheater on the exhaust-gas line. It does expansion work in the expander, and condenses in the HT condenser. The waste heat recovery system is used as an auxiliary power of the engine

via a belt connected to the engine crankshaft and the power transmission device and power is obtained from the expander.

At the design stage of the cycle of the HT loop, the reliability aspects of the expander are considered first. The primary factors in the reliability design of the expander are the pressure and temperature of the working fluid entering the expander, which are the highest pressure and the maximum temperature of the system, respectively.

The pressure and the mass flow rate of the working fluid are controlled by an electric expansion valve and an electric pump according to the waste heat conditions of the exhaust gas. Thus, the temperature of the working fluid at the inlet of the expander is controlled by adjusting the mass flow rate of the working fluid.

The HT loop cycle has a considerably high high-pressure of 25 bar. The expansion ratio is 10, and the condensation temperature is 127.4 ℃. Thus, the HT pump inlet temperature of the working fluid is so high temperature of 122.4 ℃, even though sub-cool is 5 ℃, that the reliability design of the pump is important. The required power is very small, considering the high pressure and low pressure, and the flow rate of the working fluid. The flow rate of the working fluid of HT loop is 6.4 g/s when the heat recovery is set as 16 kW from HT boiler and HT superheater, and the heat dissipation of the HT condenser is set as 13.5 kW. For the purpose of the pump design according to the exhaust gas

conditions, the flow rate at the required discharge pressure should be designed than the amount above considering the flow controlling bypass valve.

Since the inlet temperature of the heat source in the LT loop is 100 ℃, the evaporation temperature of the working fluid is set as 90.8 ℃. Thus, the evaporation pressure is set as 32.8 bar; the condensation pressure and temperature are set as 16.4 bar and 58.7 ℃, respectively considering the ambient air temperature with the expansion ratio of 2.

In the design of the cycle of the HT loop, the temperature of the working fluid exiting the HT condenser is in the range of 120 ~ 140 ℃ (122.4 ℃ at the design point), which is generally higher than the temperature of the engine coolant. Therefore, the heat from the HT condenser can be recovered. Hence, the HT condenser works as a superheater for the LT loop. Because two separate loops are connected by the HT condenser, the design and control of the system cannot be separated. As shown in Figure 2.12, the LT boiler and the HT condenser are connected in series. That is, the HT condenser is an important heat exchanger that plays a role of a superheater to heat up the working fluid to the superheated state in the LT loop, and another role of a condenser in the HT loop. The flow rate of the working fluid of LT loop is 156 g/s when the heat recovery is set as 13.4 kW from LT boiler and 11.5 kW from LT superheater.

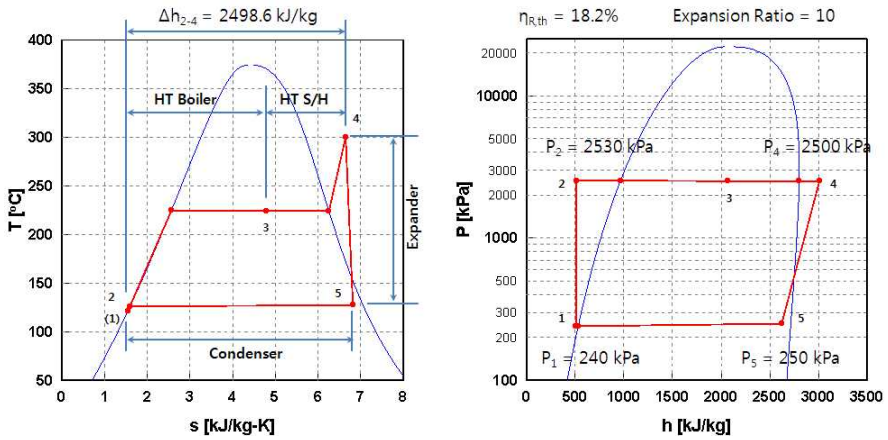

(a) T-s diagram (b) P-h diagram

Figure 2.13 HT loop cycle diagram

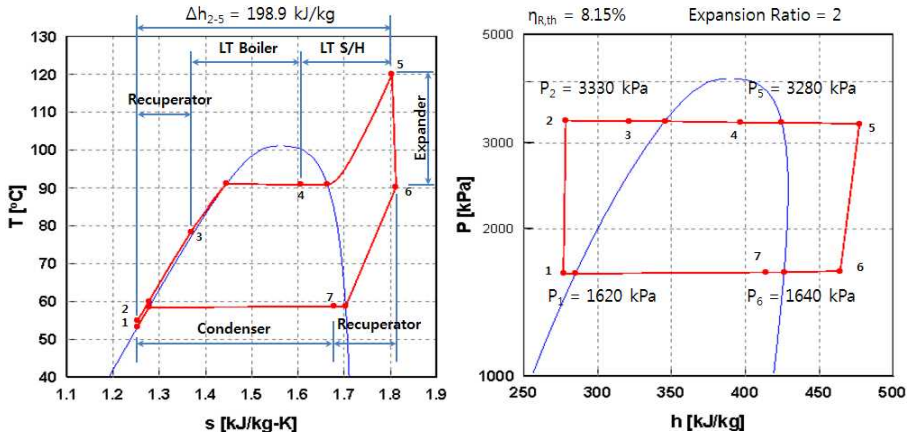

(a) T-s diagram (b) P-h diagram

Figure 2.14 LT loop cycle diagram

The T-s diagrams and P-h diagrams of the HT and LT loops are shown in Figures 2.13 and 2.14. The ideal efficiency of the water cycle is calculated to be 18.2%; the refrigerant cycle 8.15%.

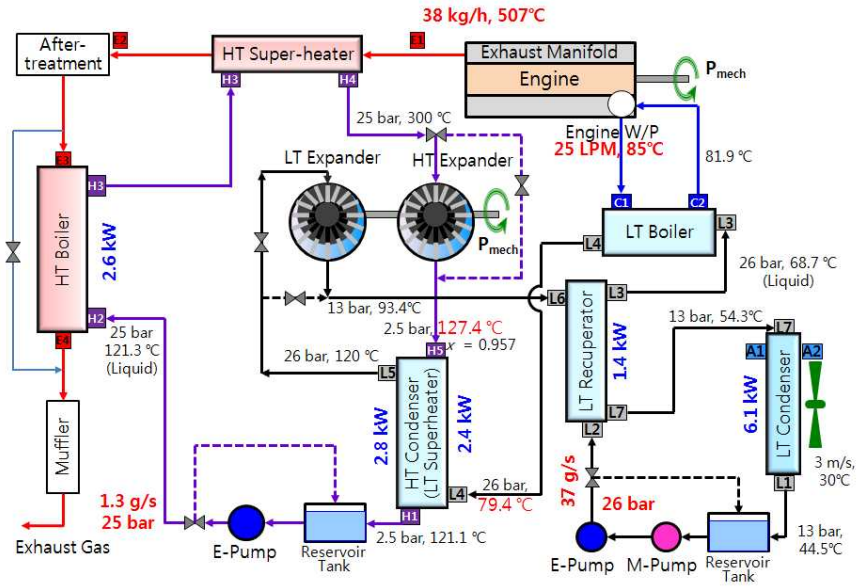

Figure 2.15 Layout of the system at vehicle speed of 60 km/h

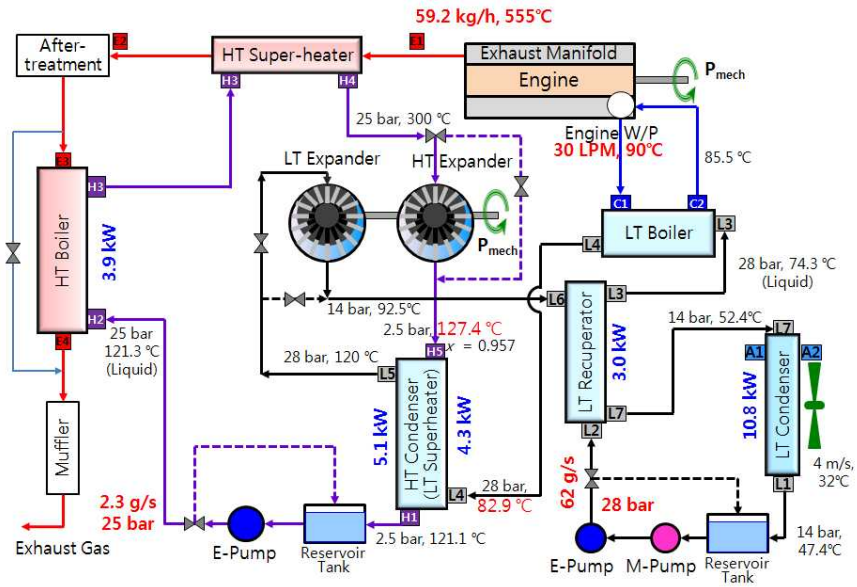

Figure 2.16 Layout of the system at vehicle speed of 80 km/h

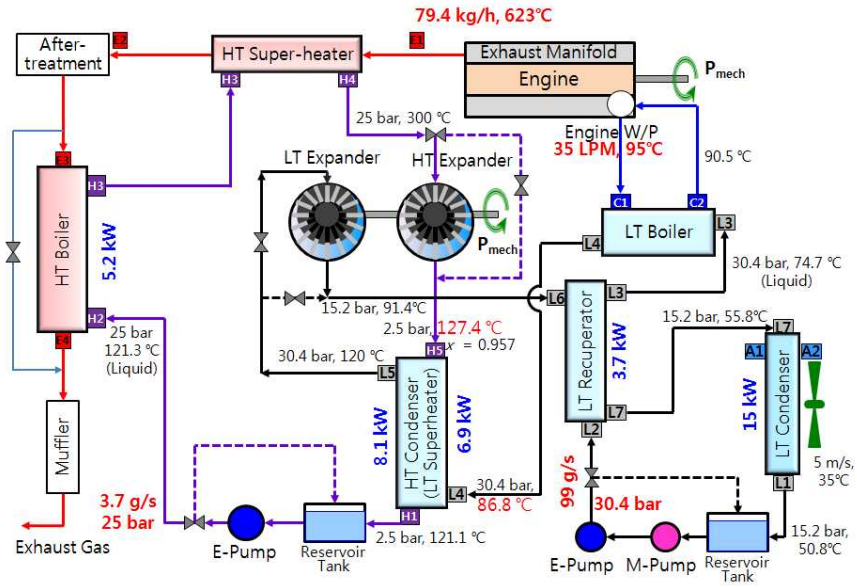

Figure 2.17 Layout of the system at vehicle speed of 100 km/h

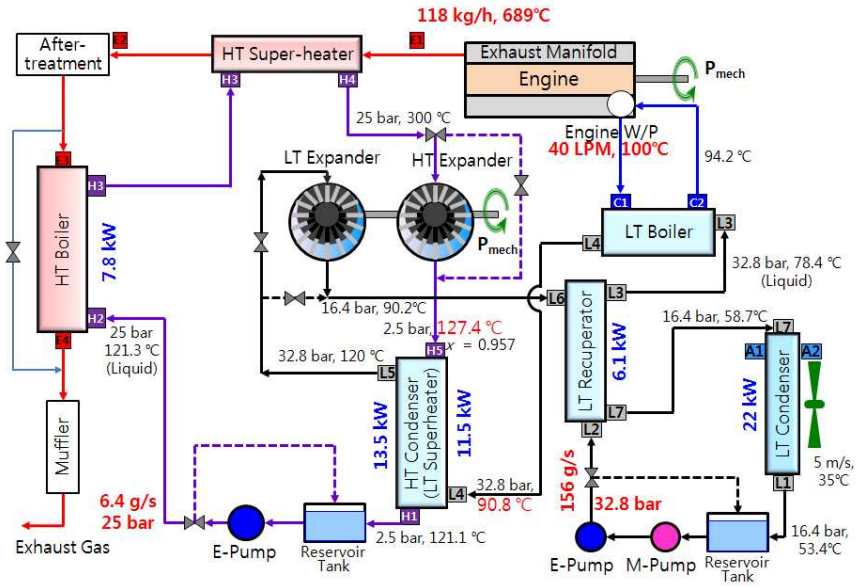

Figure 2.18 Layout of the system at vehicle speed of 120 km/h

Figures 2.15 to 2.18 show the conditions of heat source for working fluid to recover the waste heat and states of the working fluid at all points in the system layout at various vehicle speed conditions. The temperature level and the mass flow rate of the exhaust heat source increases with increasing vehicle speed. The engine coolant conditions and heat dissipating conditions also increase as the speed increases. At steady operating conditions, the exhaust gas exit temperature from the exhaust manifold keeps high temperature, which enables the HT loop cycle maintain the maximum temperature of 300 ℃. Heat recovery with varying heat source conditions is controlled by adjusting the mass flow rate of the HT working fluid; and the same for the LT working fluid.

Chapter 3

Design Process of a High Temperature Boiler

3.1 Role of HT Heat Recovery Exchangers

What should be considered fundamentally in the construction of the waste heat recovery system is the amount of the waste heat recovered to be used into the Rankine cycle. While the waste heat recovery system has a form of fixed type in the industry, it is essential to configure the system layout for an automobile engine considering stable operation and variability according to the change in driving mode in the actual vehicle.

The working fluid at high pressure and low temperature recovers waste heat from exhaust gas, and evaporates to be at super-heated state in the one or more waste heat recovery heat changers depending on the system configuration. In this study, the waste heat recovery system has two waste heat recovery heat exchangers such as HT boiler and HT superheater.

The exhaust gas loses heat to the working fluid side resulting in a continuous temperature drop, while the pressurized working fluid inflows into the HT boiler, recovers the heat to be hotter, and reaches a saturation temperature where an isothermal phase

change occurs. The saturated working fluid flows into the HT superheater, and undergoes another phase change to be superheated vapor. Figure 3.1 shows the behavior of the HT working fluid, water, in the HT boiler shell by use of the performance prediction program for the HT boiler, with the conditions of inlet sub-cool of 5℃ of the low pressure, and outlet quality of 0.603.

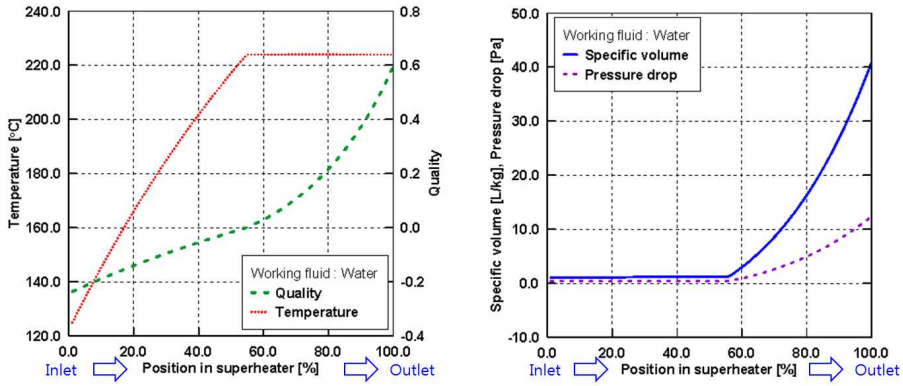

(a) Quality and temperature (b) Specific volume and pressure drop

Figure 3.1 Behavior of the working fluid in the HT boiler

The HT superheater has a function of superheating the working fluid to the maximum system temperature, however, it has to be installed in a confined space close to the engine exhaust manifold. Therefore, it is important to design the HT superheater to maximize the heat transfer performance and minimize the volume occupied. The HT boiler heats up the pressurized liquid

water from the HT pump to be sufficiently saturated state. It is connected onto the exhaust duct after the HT superheater and the catalytic converter, therefore, it has the height and width limits affected by the engine bottom structure. However, as shown in Figure 3.2, there is quite sufficient space in the longitudinal direction.

3.2 Design Conditions for an HT Boiler

For the design of the HT boiler, the amount of the heat recovery to the HT loop system is the most important function of it. The secondary point is the pressure drop at the exhaust side by which the engine exhaust system and maybe the engine itself are affected depending on the exhaust gas temperature resulting from the heat recovery performance.

The mass flow rate of the HT working fluid, water, at the design point and in the whole range are so small that the pressure drop at the water side is not considerable.

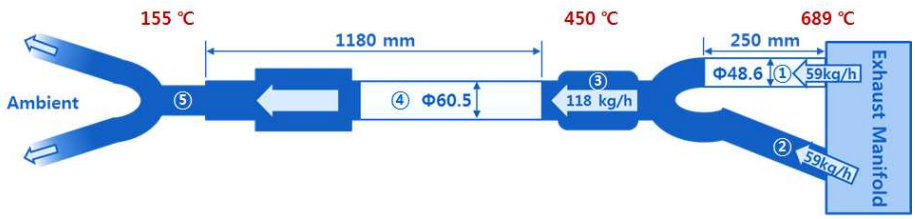

Figure 3.2 Exhaust system of the target vehicle

As shown in Figure 3.2, the HT superheater has only about 250 mm of its length, which is located between the exhaust manifold and the converter (location ①). However, the HT boiler has the larger space of about 1.2 m in the middle of the exhaust duct (location ④).

The exhaust gas condition at the design point is the high-speed driving condition at 120 km/h. In this condition, the exhaust

mass flow rate is 118 kg/h, and the temperature of the exhaust gas entering the HT superheater is 689 ℃. The exhaust gas entering the HT boiler is expected to be at about 450 ℃, taking into consideration cooling at the superheater and heat dissipation from the exhaust system, including a catalytic converter.

A variety of heat exchanger types have been investigated to set a direction of design for highly-efficient compact HT boiler as a heat exchanger recovering waste heat from exhaust gas.

3.3 Concept Design for an HT Boiler

The first design concept is a 'Wavy Fin and Helical Coil' type circular heat exchanger (called as HTB #1). The small flow rate of the working fluid has called forth the concept of a circular tube with a small cross-sectional area. The second one is a 'Circular Shell and Spiral Tube' type (HTB #2). A bundle of the heat transfer enhanced spiral tubes are supported by flow guiding baffles in a circular shell. The third is a 'Rectangular Shell and Spiral Tube' type (HTB #3). The unique design concept of the rectangular shell has been aroused taking the state and conditions of the working fluid at the inlet region into account.

3.3.1 Design of Fin and Helical Coil type

For the first conceptual design, a long tube with a small circular cross-section has been set as the structure of the heat recovery heat exchanger for the HT working fluid to be sufficiently heated and evaporated. The tube can probably have a form of a bundle of zigzag coil. However, it is difficult to produce and connect the zigzag coils enduring the high pressure of the working fluid, moreover, in the confined room. Hence, from the concept of removing a part of duct in the exhaust system, the exterior housing of the HT boiler has a shape of cylinder in which a bent coil in a form of a helical spring.

A round tube with a outer diameter of 3/4" has been inserted into a circular housing having a helical coil shape by bending. Two set of wavy fins are placed adjacent to the round coil tube, that is, inside and outside the tube, respectively. which become the flow paths of exhaust gas. The wavy fin presents improved heat transfer performance than a plain corrugate fin. Thin plates are formed as a can. The smaller can is placed inside the inner wavy fin. The larger can is placed between outside of the inner fin and inside of the round coil tube. The cans support the inner fin at brazing in the production and guide the exhaust gas only through the wavy fins.

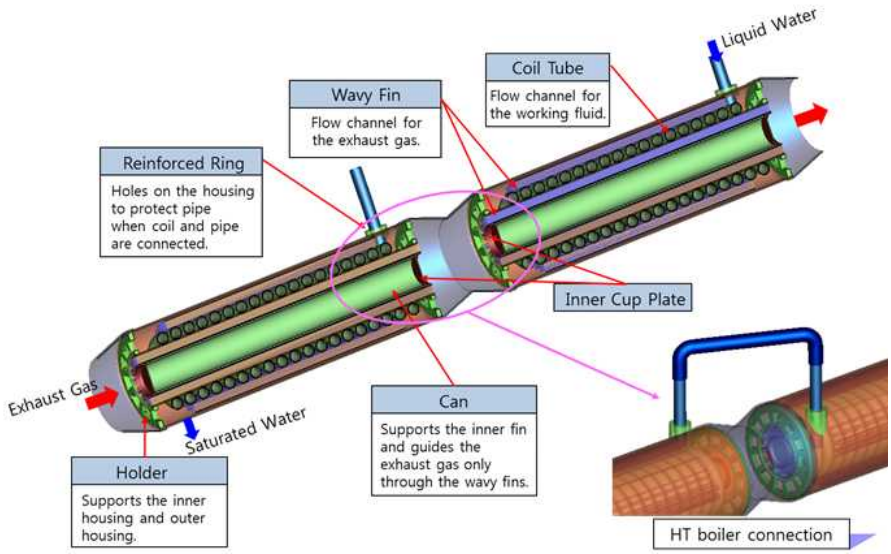

Figure 3.3 Concept design for HT boiler (#1)

Cup plates are placed on the inlet and outlet part of the thin

plates rolled as a can, which introduces exhaust gas to inflow easily. In addition, holders are placed on the inlet and outlet to make the exhaust gas flow uniform while supporting the exterior housing and the outer can plate. The coil tube can not be out of the housing. The coil tube is packaged in the housing with reinforced rings at the inlet and outlet of the working fluid channel. Tube connectors are inserted into the hole of the reinforced rings which protect the connectors at steady connection with the housing. The coil tube is limited in the length to be produced as the standard tube, however, the longitudinal limit in the exhaust gas is not great. Therefore, the structural design has been modified to have two cylindrical heat exchangers in series. Figure 3.3 shows the conceptual design draft for the helical coil type HT boiler which has a counter-flow structure with the exhaust gas and the working fluid herein.

3.3.2 Design of Circular Shell & Spiral Tube type

The structural design improvement has been conceived focusing on maximizing the heat transfer effect of the exhaust gas and the working fluid in a limited size and besides, the durability and productivity are taken into account. The defect of the fin and helical coil is the lesser contact area between the exhaust gas and working fluid channels. The heat transfer area of a shell and spiral tube type heat exchanger is enlarged more significantly than the previous model. The key concept of the heat exchanger is the flow guiding baffles which lead the working fluid in a form of zigzag flow.

The high temperature exhaust gas is introduced into the HT boiler and exchanges heat with the working fluid passing through a bundle of spiral tubes. Spiral grooves in the tube serve to increase the heat transfer area, and the convective and total heat transfer coefficients by the turbulence enhancing geometry. The baffles maximize the heat transfer effect through the increase in the lengths of the flow paths by being arranged in a certain interval and vertical symmetry in the shell, which makes the working fluid flows in zigzags. Several holders are inserted in the shell to give exact location of the baffles and facilitate the assembly of the gas tubes with baffles during production. In consideration of the productivity of the spiral tubes, the HT boiler has a form of two cylindrical heat exchangers in series.

Figure 3.4 shows the conceptual design of the cylindrical shell and spiral tube type HT boiler.

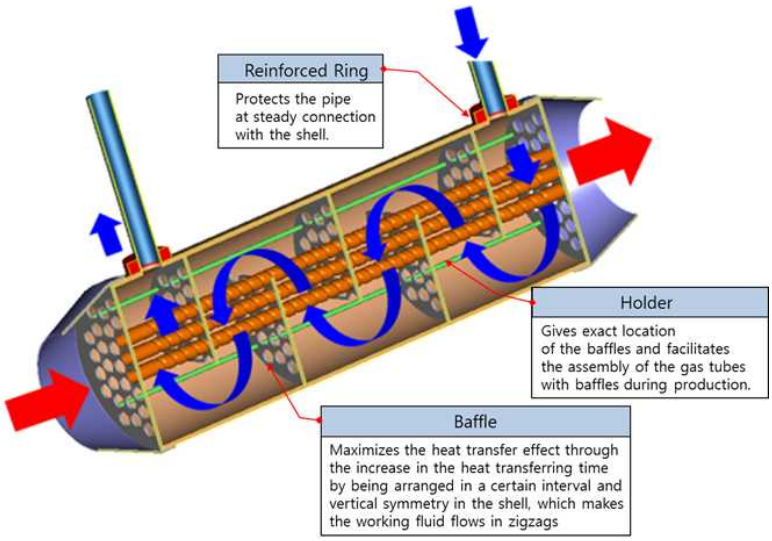

(a) Shell and tube structure

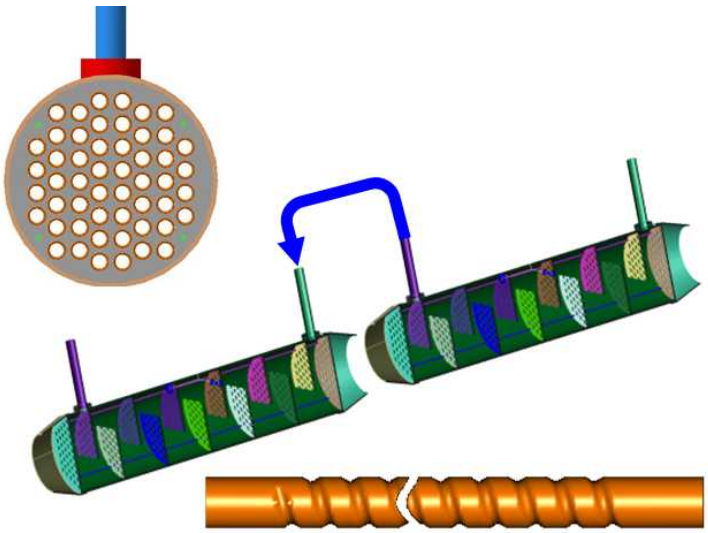

(b) Cross-sectional view and two-cylinder construction

Figure 3.4 Concept design for HT boiler (#2)

3.3.3 Design of Rectangular Shell & Spiral Tube type

The working fluid of very small flow rate should exchange heat sufficiently at the liquid state in a shell & spiral tube type heat exchanger which has somewhat wide flow channel for the working fluid. Total tube length needs to be reduced considering the packaging in the actual vehicle.

In this study, the shell and spiral tube HT boiler has got a new concept geometry with a rectangular exterior. The cross-section of the heat exchanging core is designed as a rectangular.

As shown in Figure 3.1, the working fluid enters at the liquid state and after gaining heat of a certain amount, it reaches the saturation state at which the working fluid has gradually growing specific volume.

In the rectangular cross-section, the flow channel working fluid is separated as a liquid state part and a saturation state part to reduce the cross-sectional area for the purpose of increase of the flow velocity of the working fluid of low volume flow rate. Three rows of the small cross-sectional area channel in the lower part increases the flow velocity of the working fluid at the liquid state, in order to reach the saturation state quickly. A row has 5 small and long room for only two exhaust gas tubes. The working fluid passes through all the channels in this part, back

and forth, and to the upside. In the upper part, the cross-sectional area is enlarged, since the increase in the quality at the saturation state, increases the specific volume greatly. The rectangular baffles guides the working fluid to form a horizontal zigzag flow among the 53 tubes. The more baffles reduce the cross-sectional area of the working fluid in the upper part.

The total tube length has been reduced in order to reduce the exhaust gas pressure drop and the space in the exhaust system occupied by itself.

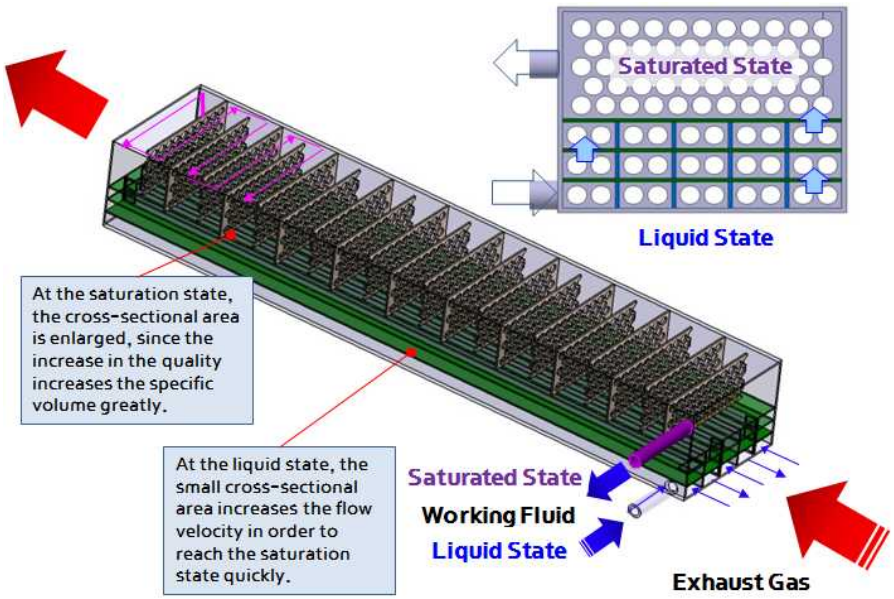

Figure 3.5 Concept design for HT boiler (#3)

3.4 Analytical Design of HT Boiler

A 1D program has merit that it can resolve the problem of phase change analysis which cannot be easily solved in 3D commercial codes. In general zero-D programs, exactly 1D where is only a single cell in the analytical range, can predict by analytical methods such as LMTD (log mean temperature difference) or ε -NTU (effectiveness - number of transfer units). However, the zero-D program predicts as the properties of the high temperature and low temperature fluids undergo linear change from the inlet to the outlet. Actual temperature (, and any other properties) of the fluids reveals the nonlinear curves changing the slope in the analytical range, of course, behaving three-dimensionally. Yet, for analysis of heat exchangers, the 1D streams are dominant in both fluid flows. Although the 1D program maybe simplify some details in the actual flow situation, it can simulate the heat transfer process by tracing both fluids in their own channels. Moreover, it is hard for zero-D program to simulate the phase change in no more than 1 cell, since there are complex routines as latent heat and sensible heat in the phase change region.

The behavior of the working fluid in a boiler in the waste heat recovery system is already described above, and shown in Figure 3.1. Figure 3.6(a) shows temperature profiles in a counter-flow heat exchanger. The heat exchange analytical model can be

established using equations (3.1) and (3.2), which calculate the heat dissipation from the high temperature fluid and the heat recovery to the low temperature fluid in kth calculation cell. To analyze the whole heat exchanger, connections of these cells with physical calculations, lots of iterations and balancing the heat dissipation and the heat recovery each other.

$$Q_{d,k} = \dot{m}_H \overline{c_{p,H,k}} \left(T_{H,k,in} - T_{H,k,out} \right) \tag{3.1}$$

$$Q_{r,k} = \dot{m}_L \overline{c_{p,L,k}} \left(T_{L,k,out} - T_{L,k,in} \right) \tag{3.2}$$

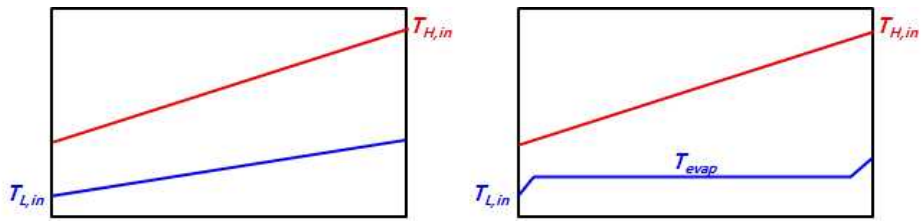

(a) General (sensible heat) (b) Phase change (latent heat)

Figure 3.6 Temperature profiles in heat exchangers

However, the temperature of the heat source lowers gradually as it loses heat in a boiler of a Rankine cycle, but the low temperature working fluid undergoes phase change where the fluid gains heat without change of the temperature, shown in Figure 3.6 (b). In this case, equation (3.2) which calculate sensible heat in each cell cannot be used. Instead, equation (3.3) which calculate latent heat, that is, enthalpy difference is used in pairs

with equation (3.1). As shown in Figure 3.7, temperatures are arranged in the grid at the high temperature side and enthalpies, instead of temperature, are set at the low temperature side.

Generally the method of ε-NTU is used to calculate the heat transfer rate where the required data are not sufficient to calculate by LMTD method. In this case, the required data are the outlet temperature of the high temperature fluid and the outlet enthalpy of the low temperature fluid [Kays84].

$$Q_r = \dot{m}_L \left(h_{L,k,out} - h_{L,k,in} \right) \tag{3.3}$$

$$Q_k = \epsilon_k C_{min,k} \left(T_{H,k,in} - T_{L,k,in} \right) \tag{3.4}$$

$$NTU_k = \frac{UA_k}{C_{min,k}} \tag{3.5}$$

Tracing the fluids with increasing cell number, the equations (3.4) and (3.5) are solved using equation (3.6) which calculates the total heat transfer rate in each cell. The convective heat transfer coefficients h_i and h_o are dependent upon the geometry of flow channel and thermal conditions. The evaporation process has been simulated by use of the correlations proposed by Gungor et al. [Gungor86]. The pressure drop is also one of the most important performance characteristics of the heat exchanger. The pressure drop of both fluid side are calculated in the cell with growing cell numbers, that is, tracing the fluids, taking into account the

variable properties such as temperatures, absolute pressures, densities, velocities, etc. The effects of sudden contraction at the inlets and sudden expansion at the outlets are all considered as shown in equation (3.7) which Kays *et al.* proposed for fluid flow through the heat exchanger [Kays84].

$$\frac{1}{UA} = \frac{1}{\mathrm{h}_i A} + \frac{\delta_t}{kA_t} + \frac{1}{\mathrm{h}_o A} \tag{3.6}$$

$$\Delta P = \frac{G^2}{2\rho_i}\left[\left(K_c + 1 - s^2\right) + 2\left(\frac{\rho_i}{\rho_o} - 1\right) + f\frac{A_{tot}}{A_s}\frac{\rho_i}{\rho_m} - \left(1 - s^2 - K_e\right)\frac{\rho_i}{\rho_o}\right] \tag{3.7}$$

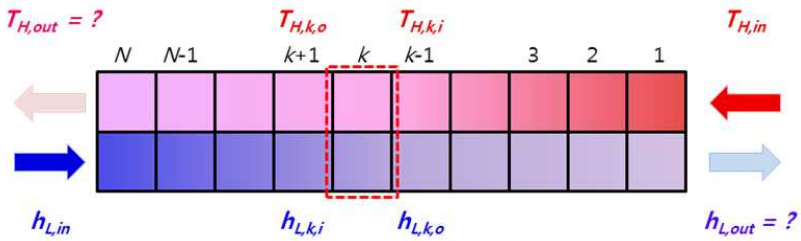

(a) One dimensional counter-flow fluids in their grid

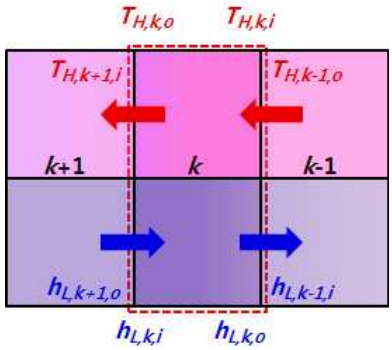

(b) Simplified control volume for heat exchange calculation *k*th

Figure 3.7 Schematic of calculation cells for latent heat exchange

3.4.1 Fin & Helical Coil type Design Program

A core part in the fin and helical coil has a coil-shaped round tube and two exhaust gas flow paths consisted of wavy fins inside and outside of the tube. The first HT boiler model has two core parts in series connection. The HT boiler performance design program is constructed based on a single core heat exchanger. This program enables to analyze the HT boiler in various arrangements of the core parts such as one or more in series connection by applying the inlet and outlet conditions.

The Exhaust gas from exhaust manifold inflows the HT superheater, transfers the waste heat and lowers its temperature. And it lowers the temperature about 100 ℃ through the catalytic converter, then enters the HT boiler. The working fluid from HT condenser has the temperature at the degree of sub-cool of 5 ℃, pressurized at the HT pump, and enters the HT boiler. The high temperature exhaust gas and the low temperature working fluid compose a counter-flow heat transfer process inside the HT boiler. These processes are took into account as the analytical conditions in the performance design program.

The one-dimensional heat recovery performance design and analysis program has been developed to design a fin and helical coil type HT boiler in Basic language, following the procedures shown in Figure 3.8. The working fluid is selected at the first dialog window. The helical coil and overall geometrical data of

the HT boiler are inputted at the second dialog window. The geometrical data for the wavy fins are then inputted. After inputting the geometrical data and operating conditions of an HT boiler, the inlet pressure losses are calculated. The exhaust gas temperature profile across the flow channel is assumed as a linear one at the first iteration where the outlet temperature of the exhaust gas is assumed as an average value of the inlet temperatures of both fluids. Then, the processes of heat transfer of the working fluid and the exhaust gas and the change of phase are simulated cell by cell, through the helical coil tube.

After that, the exhaust gas inlet temperatures of all cells are rearranged from a combination of the exhaust gas outlet temperatures at the current iteration and the previous iteration with adjusting of a relaxation factor. As the residuals converge to zero or close to the tolerance, the exhaust gas temperature profile forms a reasonable curve. If the calculation satisfy the criteria, the program quits the iteration and shows various performance data on the result window and temperature profiles of the counterparts on the graph window. A couple of dialog windows of geometrical input data are shown in Figure 3.9.

Each calculation cell of the helical coil tube has been assumed as a unit cell of a straight tube with an equivalent length adjacent to the wavy fins curled in concentric circles. Dong *et al.* proposed performance correlations for wavy fins [Dong07, Dong13]. The Dean number that represents curvature effect for a

curved pipe is considered for calculating the pressure drop of the working fluid, which P. Naphon *et al.* (requoted H. Ju *et al.*) proposed for several cases as following [Naphon06].

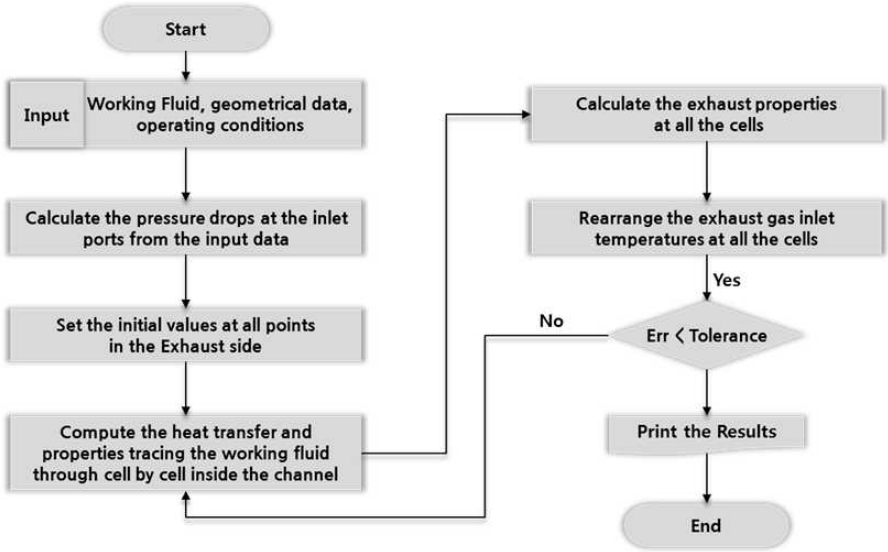

Figure 3.8 Flow chart of the design program for the HT boiler

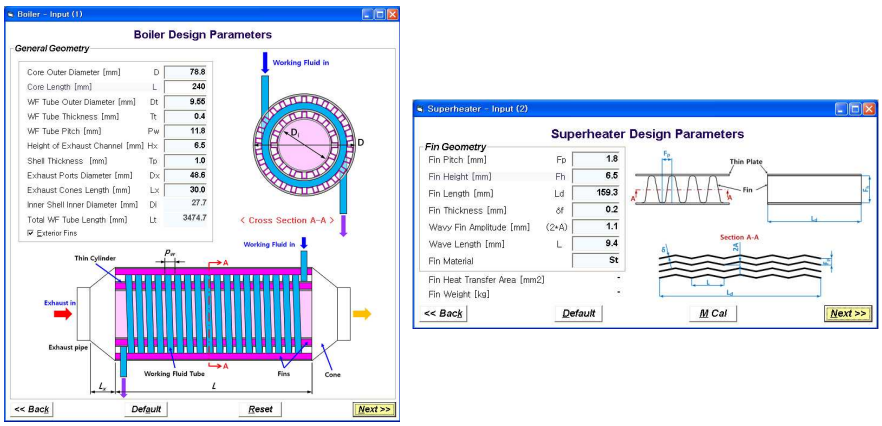

Figure 3.9 Design program for fin & helical coil heat exchanger

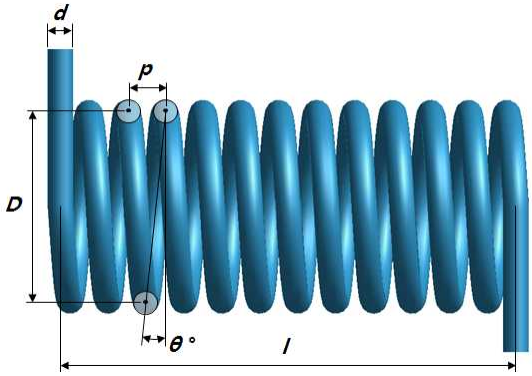

(a) Geometry of a helical coil tube

(b) Equivalent tube

Figure 3.10 Equivalent tube concept for the helical coil

$$\mathrm{De} = \mathrm{Re}\sqrt{\frac{d}{D}} \tag{3.8}$$

In case of $\mathrm{De} < 11.6$,

$$f_{straight} = \frac{16}{\mathrm{Re}},\ \frac{f_{curved}}{f_{straight}} = 1$$

In case of $\mathrm{De} > 11.6$, $\mathrm{Re} < \mathrm{Re}_{crit}$,

$$f_{straight} = \frac{16}{\mathrm{Re}},\ \frac{f_{curved}}{f_{straight}} = 1 + 0.015\mathrm{Re}^{0.75}\left(\frac{d}{D}\right)^{0.4}$$

Case else ($\mathrm{De} > 11.6$, $\mathrm{Re} > \mathrm{Re}_{crit}$),

$$f_{straight} = \frac{0.0791}{\mathrm{Re}^{0.25}},\ \frac{f_{curved}}{f_{straight}} = 1 + 0.11\mathrm{Re}^{0.23}\left(\frac{d}{D}\right)^{0.14} \tag{3.9}$$

3.4.2 Cylindrical Shell & Spiral Tube type Design Program

A shell and tube heat exchanger has a cylindrical appearance, in general. Lots of that type has a bundle of tubes in the shell and flow guiding baffles, which are expected to enhance the structural strength of the heat exchanger. The exhaust gas tubes of the HT boiler are in shape of the round tube with spiral grooves for enhanced heat transfer performance. It is similar to the previous section that the cylindrical shell and spiral tube type HT boiler performance design program is constructed based on a single core heat exchanger.

The heat exchanging core has a zigzag channel of the working fluid consisting of the inner surface of the exterior shell, the outer surface of the numerous spiral tubes, and flow guiding baffles. The geometries of flow channels of both fluids are simplified to configure the one-dimensional calculation grid as described in Figure 3.7. The exhaust gas flow channel is regarded as a single tube with corresponding heat transfer area, cross-sectional area, and mass flow rate. The working fluid flow channel is simplified as it forms a straight counter-flow against the exhaust gas in corresponding path length for the calculation of heat transfer. In order to calculate the pressure drop on the working fluid side, the program utilizes the correlation established by E. Gaddis *et al.* about the pressure drop on the

fluid in the shell of shell and tube heat exchangers with baffles [Gaddis97].

$$\Delta P_{W/F} = \left(n_{baffle} - 1\right) \Delta P_C + 2\Delta P_{CE} + n_{baffle} \Delta P_F + \Delta P_S \,, \qquad (3.10)$$

where ΔP_C is the pressure drop in a cross flow section, ΔP_{CE} is the pressure drop in an end of cross flow section, ΔP_F is the pressure drop in a counter flow or turning section, and ΔP_S is the pressure drop in both inlet and outlet ports [Gaddis97]. For the pressure drop at bends, the correlations from Domanski *et al.* have been used [Domanski08].

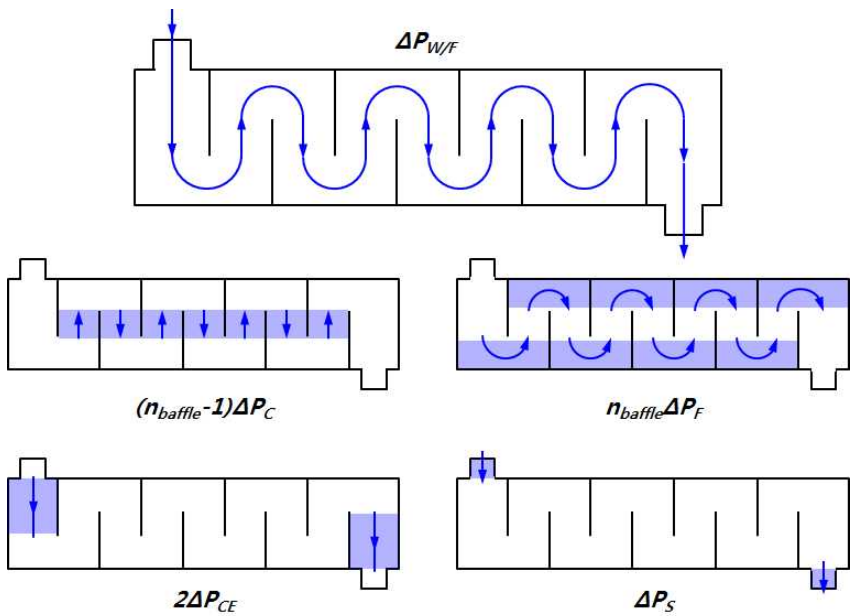

Figure 3.11 Flow sections for pressure drop calculation

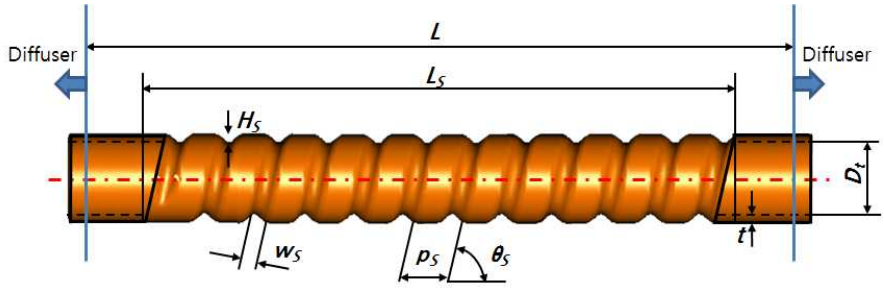

Figure 3.12 Geometry of spiral tube for exhaust gas

Heat transfer and pressure drop characteristics have been investigated for turbulent flow in the spiral tubes by M. M. Mehta and M. R. Rao with the severity factor, $\phi = H_s^2/(p_s D_t)$ [Mehta79]. The Nusselt number and friction factor for spiral tubes have been correlated within a range of Reynolds number from 10,000 to 80,000:

$$\mathrm{Nu}_s = 0.029\exp(-16\phi)\mathrm{Re}_{Dh}^{0.8\exp(-25.5\phi)}\mathrm{Pr}^{0.4} \tag{3.11}$$

$$f_s = 0.0791\exp(-92\phi)\mathrm{Re}_{Dh}^{0.25\exp(-215\phi)}. \tag{3.12}$$

The range has been widen by P. G. Vicente *et al.* [Vicente04] from 1500 to 90,000 as:

$$\mathrm{Nu}_s = 0.374\phi^{0.25}\left(\mathrm{Re}_{Dh} - 1500\right)^{0.74}\mathrm{Pr}^{0.44} \tag{3.13}$$

$$f_s = 1.53\phi^{0.46}\mathrm{Re}_{Dh}^{0.16} \tag{3.14}$$

The effect of sudden contraction and expansion has been considered at the inlet and outlet ports using the correlations proposed for two-phase flow by Chen *et al.* [Chen07, Chen09] The operating conditions and environment for the HT boiler are the same as described in the previous section. The basic calculation procedures are based on the algorithm of Figure 3.8.

After selecting the working fluid at the first dialog window, the geometrical data of the baffles and exterior size of the HT boiler are inputted at the second dialog window. The geometrical data for the spiral tubes are then inputted. The heat transfer between working fluid and exhaust gas, and the phase change are simulated cell by cell, through the zigzag flow and the spiral tubes assumed as in a one-dimensional axis. A couple of dialog windows of geometrical input data are shown in Figure 3.13.

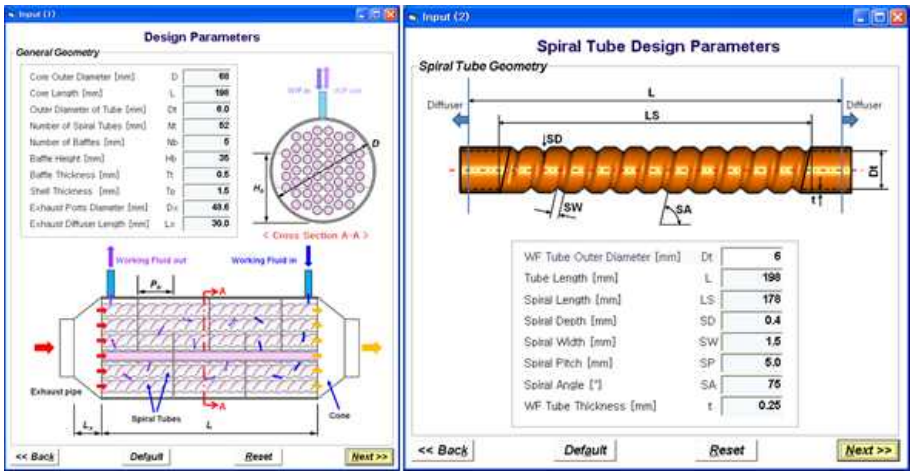

Figure 3.13 Design program for shell & tube heat exchanger

Figure 3.14 shows temperature profiles of the exhaust gas and working fluid in a cross-flow heat exchange as an example of graphical result window. The graph includes quality profile of the working fluid in the shell along the flow passage.

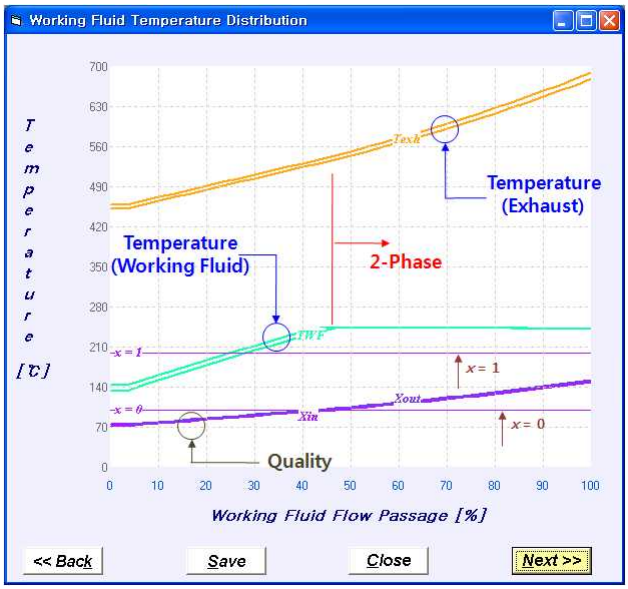

Figure 3.14 An example of graphical result window

An application example for a parametric study is shown in Figure 3.15. Concerning about the baffles, an increase of the number of them increases the heat transfer performance and the pressure drop simultaneously, and increases the heat transfer area slightly. As the heat transfer enhances, the exhaust gas outlet temperature goes down so that the specific volume and, thus, the pressure drop at the exhaust gas side decrease.

The independent variable in Figure 3.15 (a) is the number of

baffles; the baffle pitch depends on the number. In order to show in a single graph, the performance data are divide to be dimensionless factors by the maximum value in the calculation range. For example, when the total length of the HT boiler with a single core is 600 mm and the boiler has 15 baffles, the baffle pitch is 37.5 mm. A trade-off or balancing point has been settled on the 23 baffles. In other words, a single core of the HT boiler with two core has a 11 baffles and the baffle pitch is 25 mm, respectively. The number determined above is not only from balancing of the two performance factors but also from consideration of the structural strength of the boiler.

The height ratio, the ratio of segment baffle height to the inner diameter of the shell, is another important parameter to be decide to balance heat transfer and pressure drop. If the baffle is very small, the baffle fails to function. On the other hand, if the baffle height is close to the diameter, the working fluid gains tremendous pressure drop or fails to flow further. Therefore, there must be a balancing point in the height ratio also. The range of the heigh ratio has been set as from 50% to 93%. The heat recovery, the pressure drops at both fluids and the total heat transfer area are calculated as dimensionless factors. If the height ratio of baffle increases more than 85%, the heat recovery performance is insignificant, but the pressure drop increases sharply. The height ratio should be not more than 85%, but the structural strength should be considered to determine it also.

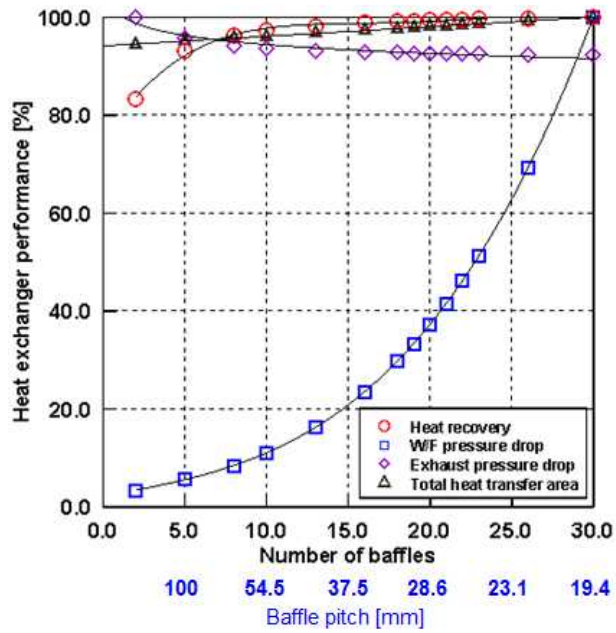

(a) Number of baffles (or pitch of baffles)

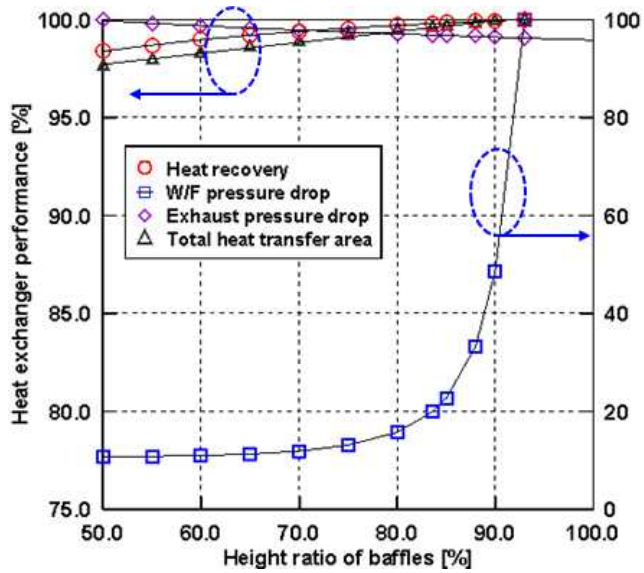

(b) Height ratio of baffles

Figure 3.15 Parametric study for geometry of HT boiler

3.4.3 Rectangular Shell & Spiral Tube type Design Process

For the rectangular shell and spiral tube type HT boiler, it is very difficult to set a one-dimensional analysis program, since the flow channels at the liquid state, e.g., in the lower inlet part, affect one another so that the interactions are exposed in a three-dimensional grid. However, if the working fluid in the lower inlet part is at the liquid state, the phase change calculation can be put aside for a while.

In this section, a three-dimensional thermal flow analysis has been conducted for the lower inlet part which has 15 working fluid flow sections and 30 exhaust gas tubes: The lower inlet part has 3 steps in which 5 flow sections exist. Two spiral tubes are allocated in each flow section. The working fluid passes straightly through a flow section, turns to the neighbor section and flow in the direction opposite to the previous section. The flow sections in which the working fluid passes through and turns are arranged side by side and step by step. Consequently, the temperature of working fluid in each flow section affects another adjacent sections, and affected greatly by the temperatures of the exhaust gas tubes.

At the first flow section, the working fluid forms a parallel flow with the exhaust gas and passes through to the end of the flow section. The working fluid turns to the second flow section

and forms a counter flow with the exhaust gas, passes through, and turns to move to the next flow section. The working fluid moves upward after five sections. It repeats the passes, turns and moving up. Then, the working fluid moves to the saturation region and forms cross-flows with exhaust gas in a zigzag movement.

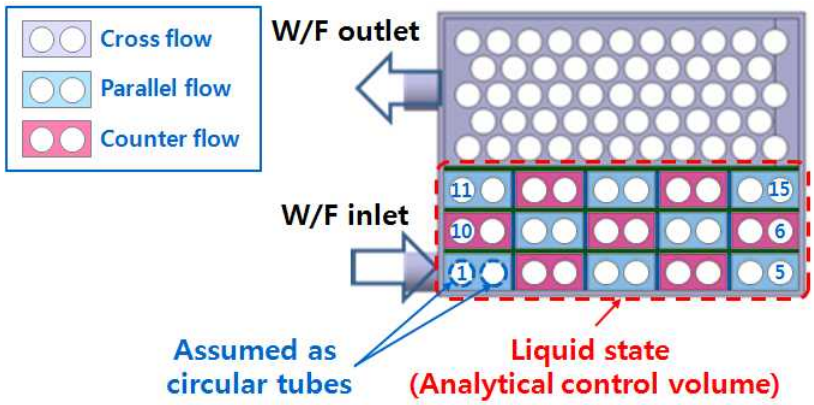

Figure 3.16 Analytical control volume for liquid working fluid

As shown in Figure 3.16, the analytical control volume is restricted as the 15 flow sections of longitudinal dimension of 440 mm. The function of the liquid flow sections is obtaining the heat required for the working fluid to be the saturation state. The exhaust gas tubes are assumed to be round tubes without any grooves on the surfaces in order to simplify and effectively conduct a full model analysis of the liquid flow sections. Another assumption is that the liquid working fluid undergoes not phase

change but temperature change with sensible heat from around 122 ℃. In fact, the saturation temperature is 224 ℃ at the pressure of 25 bar so that the working fluid undergoes only temperature change about 102 ℃. At the design point, the working fluid of mass flow rate of 6.4 g/s requires about 2.86 kW. The exhaust gas inlet temperature has been set as 450 ℃. The heat transfer performance at liquid state has been analyzed using a commercial CFD program (Fluent 6.3).

The analytical results are shown in Figure 3.17. The pressure distribution in a side view is shown in Figure 3.17(a). The velocity distribution in a plan view at the first step is shown in Figure 3.17(b). The average velocity in the working fluid sections is predicted as about 0.15 m/s. Figure 3.17(c) shows the temperature distributions in a plan view at all steps. The second step is under the influence of temperatures of the first and the third steps, by which the working fluid in the second step is rather adversely affected resulting in temperature decrease along the flow path in the step. However, the working fluid temperature increases along the path in the third step. The heat recovery from the exhaust gas is predicted as 2.8 kW at the liquid state. Considering the spiral tubes which can enhance heat transfer about 30%, it is expected for the working fluid to be able to reach the two phase enough.

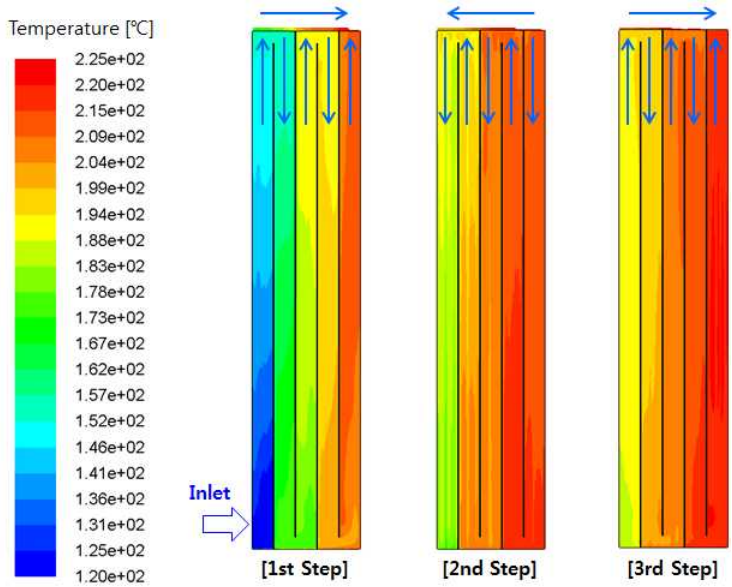

(a) Temperature distribution (plan view)

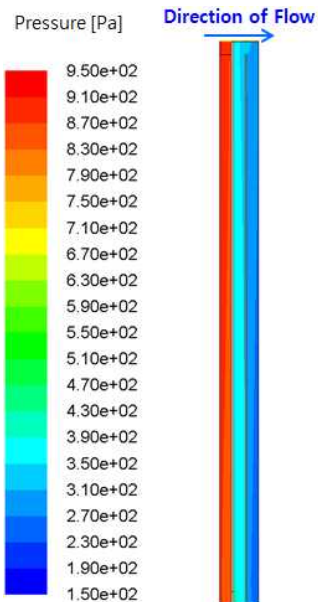

(b) Pressure (side view)

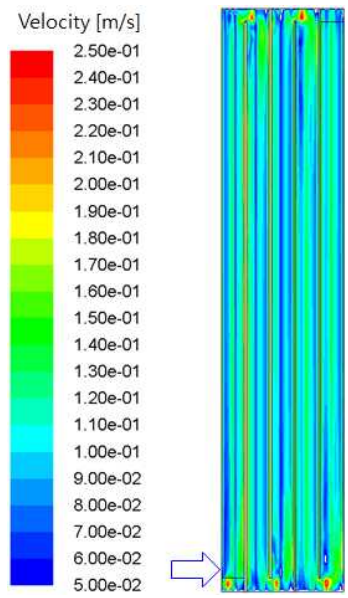

(c) Velocity (plan view)

Figure 3.17 CFD results for liquid state

3.5 Drafts of the HT boilers

Three drafts of the HT boiler have been established via 1D and/or 3D thermal flow analytical simulations.

The draft of the fin & helical coil tube type HT boiler (#1) has been derived from a concept design and thermal flow analysis by the developed prediction program as shown in Figure 3.18. Total length of the boiler is 630 mm, the outer diameter of the shell is 78.8 mm, and two helical coil tubes are connected in series.

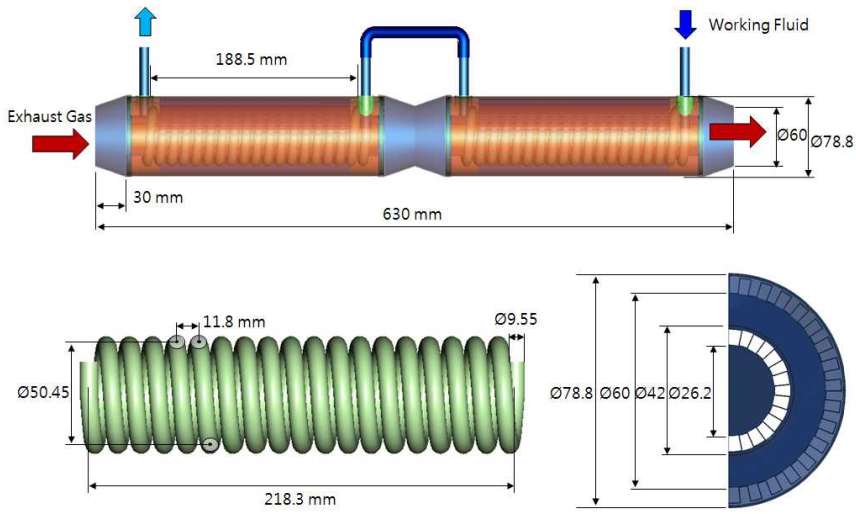

Figure 3.18 Draft of the fin and helical coil type HT boiler (#1)

The draft of the circular shell & spiral tube type HT boiler (#2) has been derived as shown in Figure 3.19. Total spiral tube length is 600 mm, the outer diameter of the shell is 78.8 mm, and two cores are connected in series.

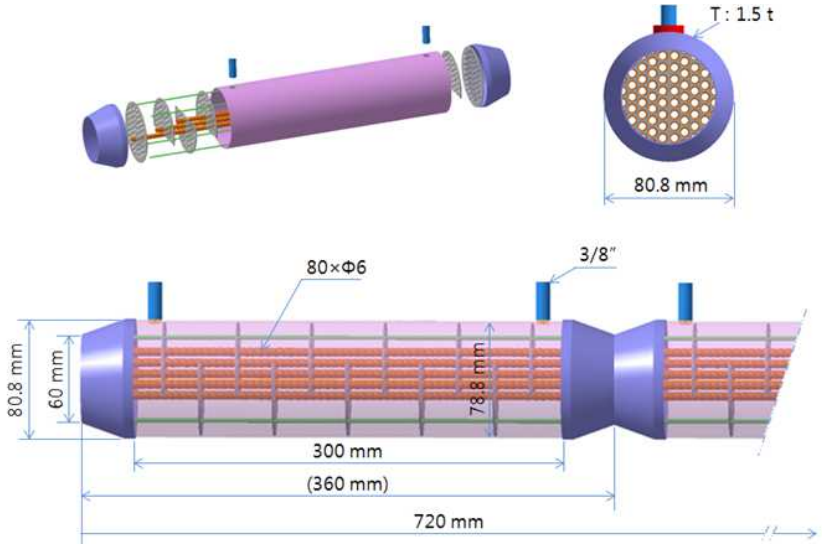

Figure 3.19 Draft of the circular shell and spiral tube type HT boiler (#2)

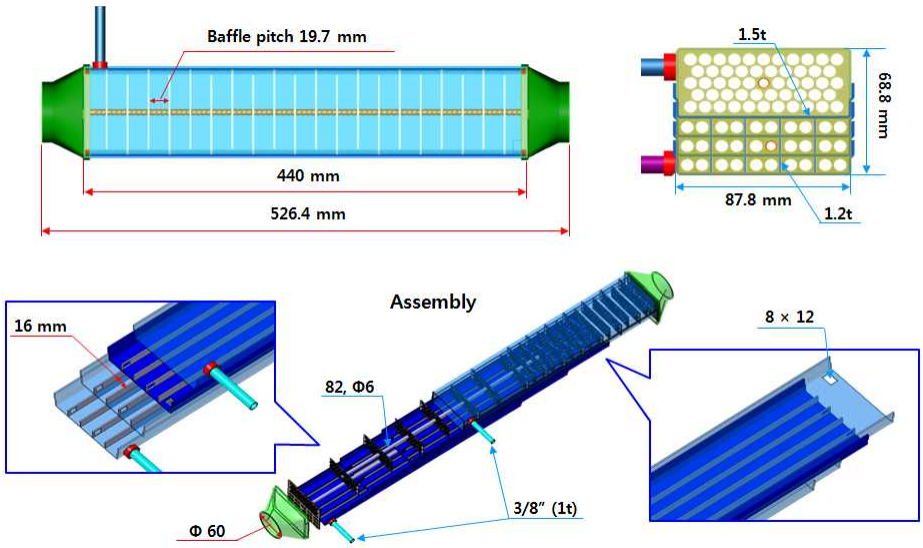

Figure 3.20 Draft of the rectangular shell and spiral tube type HT boiler (#3)

The draft of the rectangular shell & spiral tube type HT boiler (#3) has been derived as shown in Figure 3.20. Total length of the boiler is 526 mm, the spiral tube length is 440 mm and the boiler has a single core.

3.6 Performance Evaluation

3.6.1 Experimental Apparatus

The apparatus for performance evaluation is roughly sectioned into the HT loop and LT loop lines, and the HT loop line for the HT boiler evaluation is configured as shown in Figure 3.21. The HT loop line consists of the exhaust gas line that simulates the exhaust gas conditions of vehicles and the secondary line to recover waste heat from the exhaust gas line. To simulate the exhaust gas, an indirect heating system wherein compressed air at the actual exhaust gas pressure is sent to a heat exchanger in the LPG gas furnace is adopted.

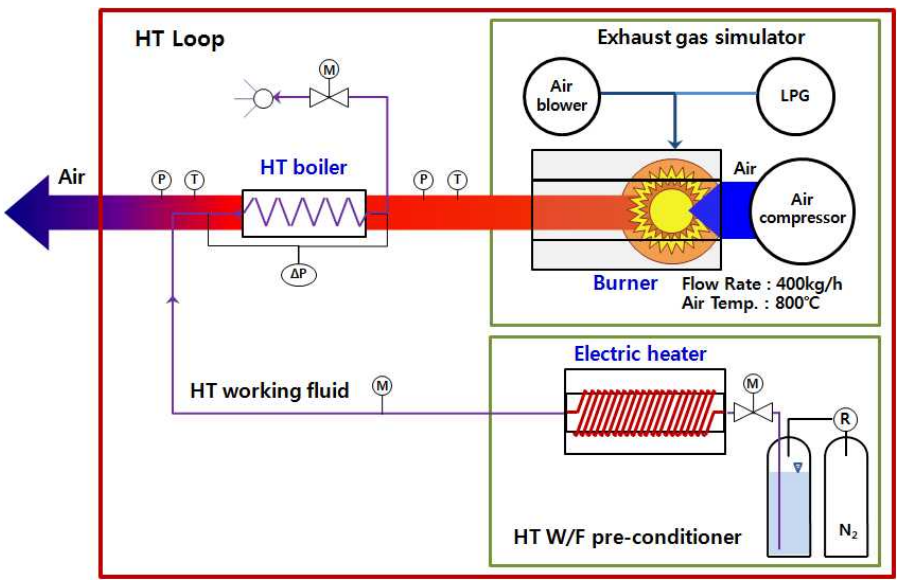

Figure 3.21 Schematic diagram of the experimental apparatus

A scroll-type compressor of 120 HP-class power is used to supply compressed air; it can generate a mass flow rate of up to 400 kg/h and pressure of up to 590 kPa, and can raise the temperature of the compressed air up to a maximum of 800 ℃.

Distilled water is used as the working fluid. Liquid working fluid of high temperature and high pressure is pressurized by the fill pressure of nitrogen gas. The pressurized working fluid is heated by an electric heater and enters the HT boiler in a liquid state. The pressure and the mass flow rate of the working fluid are controlled by the regulator of the pressure vessel and the metering valve mounted at the front of the electric heater. The mass flow rate is measured in the liquid state by a flowmeter in front of the boiler sample. The pressure and temperature at both the inlet and exit ports are measured by absolute pressure sensors and K-type thermocouples mounted on the fore and rear sides of the sample. The state or phase of the working fluid is predicted through the REFPROP program. A differential manometer is employed to accurately measure the pressure drop, along with the pressure sensors. The available range of measurement of the absolute pressure sensors is up to 100 bar with an accuracy of ±0.1%, and that of the differential manometer is up to 0.69 bar with an accuracy of ±0.25%. The mass flow rate of the working fluid is measured by connecting flowmeters with measurement ranges of 0.05~0.5 L/min and 0.2~2.0 L/min, respectively, in parallel and fitting a 3-way valve

in order to enable precise measurement of the mass flow rate; the flowmeters are selected according to the range of the mass flow rate.

In the exhaust gas line, the temperatures are measured by K-type thermocouples fitted at the fore and rear sides of the sample, and the pressure drop is measured by a differential manometer with a maximum range of 2.0 bar and a tolerance of ±0.25%. The mass flow rate of the exhaust gas is measured by connecting a flowmeter with a low range of measurement of 0.25 ~ 75 nm^3/h and one with a high range of 70 ~ 350 nm^3/h in parallel in order to enable precise measurement of the mass flow rate; the flowmeters are also selected according to the range of the mass flow rate. The heat dissipated from the exhaust gas side in the boiler sample is calculated by using the measured temperature change and mass flow rate of the exhaust gas. The heat balance is checked by calculating the recovered heat at the working fluid side and comparing the heat on the other side.

3.6.2 Experimental Conditions and Methods

Regarding the performance design conditions of the HT boiler, the state of the working fluid at the exit is unclear since it is in the region of two phases in which liquid and vapor coexist. Therefore, in the actual experiment, the exit condition of the HT boiler is set as a superheat of 5 ℃; the inlet condition is set as a sub-cool of 5 ℃; as shown in Figure 3.22, the mass flow rate satisfying this condition can be found.

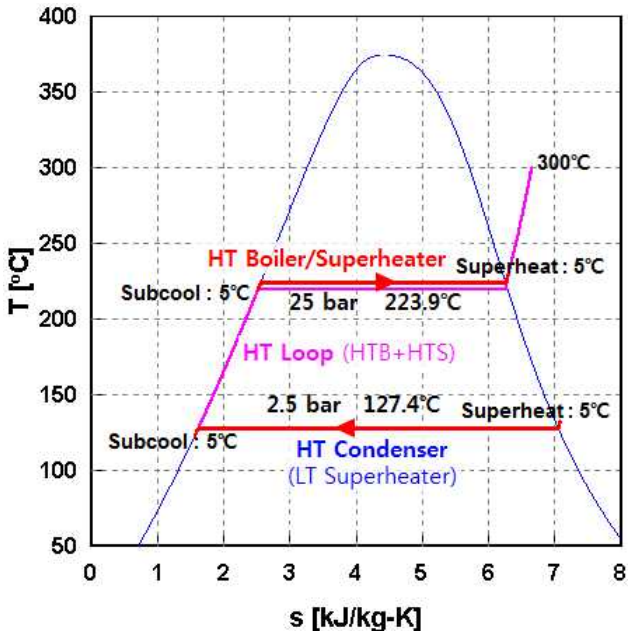

Figure 3.22 Experimental conditions for the heat exchangers

For the performance evaluation of the HT boiler #1 prototype, the mass flow rate of the exhaust gas has been varied as 60, 80,

100 and 118 kg/h, respectively, and the exhaust gas inlet temperature has been varied as 400, 450, 500 and 689 ℃ taking into consideration that the inlet temperature of exhaust gas into the HT boiler would be about 450 ℃. Regarding the exhaust gas conditions, the experiment has been carried out by varying the evaporation pressure of the working fluid as 10, 25, 35, 40 bar. Under these conditions, the heat recovery of the HT boiler sample from the exhaust gas and the pressure drop of both fluids have been evaluated.

After the evaluation of the effect of the evaporation pressure, the evaporation of the working fluid has been fixed as 25 bar for the HT boiler #2 and #3 prototypes. The mass flow rate of the exhaust gas has been the same as for the HT boiler #1, the temperature has been varied as 450, 500, 550 and 600 ℃. Thus, the design point conditions of the HT boiler such as exhaust gas inlet temperature of 450 ℃, exhaust gas mass flow rate of 118 kg/h, and working fluid evaporation pressure of 25 bar have been satisfied for all prototypes. And the assessment of the prototypes at a variety of off-design points have been conducted.

3.6.3 Experimental Results

The prototypes and their experimental installation are presented for the three types of the HT boilers in Figure 3.23.

(a) Fin and helical coil type model (#1)

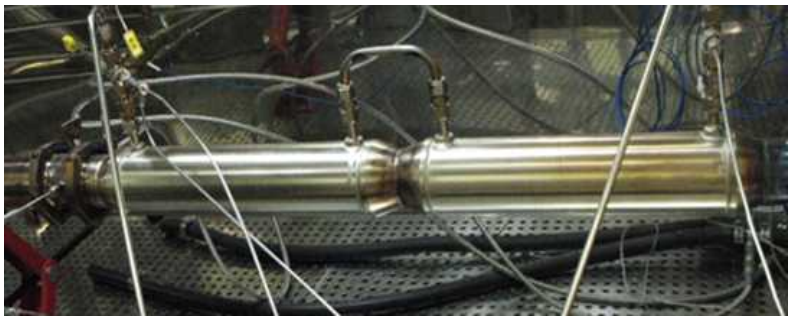

(b) Circular shell and spiral tube type model (#2)

(c) Rectangular shell and spiral tube type model (#3)

Figure 3.23 Prototypes and experimental mounting on rig

Figure 3.24 shows the variation of the heat recovery of the HT boiler #1 with the evaporation pressure of the working fluid and the inlet temperature of the exhaust gas. The mass flow rate of the working fluid increases linearly with the inlet temperature of the exhaust gas, and the heat recovered increases almost linearly. For the same inlet temperature of the exhaust gas, since the evaporation temperature decreases according to the decrease in the evaporation pressure of the working fluid, the temperature difference between the exhaust gas and the working fluid increases to reveal the increasing trend in the heat recovery. The heat recovery is 10.3 kW when the exhaust gas inlet temperature is 689 ℃ and the evaporation pressure is 25 bar, assuming the HT boiler recovers the waste heat from the exhaust gas alone. However, when the exhaust gas inlet temperature to 450 ℃ and the evaporation pressure is 25 bar, which are the conditions on the assumption that the HT superheater exists before the HT boiler in the exhaust line, the heat recovery is no more than about 4.67 kW, which is an insufficient amount for the HT boiler. This information can be utilized to make up the layout of the heat recovery system.

Figure 3.25 shows the exhaust gas side pressure drop with respect to the inlet temperature of the exhaust gas at the same mass flow rate of the exhaust gas. The exhaust gas pressure drop increases with the exhaust gas temperature at the same working fluid pressure since a higher temperature lowers the density of

the exhaust gas. The pressure drop of exhaust gas is 2.64 kPa at the design point of the HT boiler as exhaust gas inlet temperature of 450 ℃ and mass flow rate of 118 kg/h.

Figure 3.26 depicts the pressure drop at the working fluid side according to the evaporation pressure. The mass flow rate of the working fluid decreases with increasing evaporation pressure; therefore, the pressure drop exhibits a decreasing trend. At the design point, the pressure drop of the working fluid is 4.46 kPa.

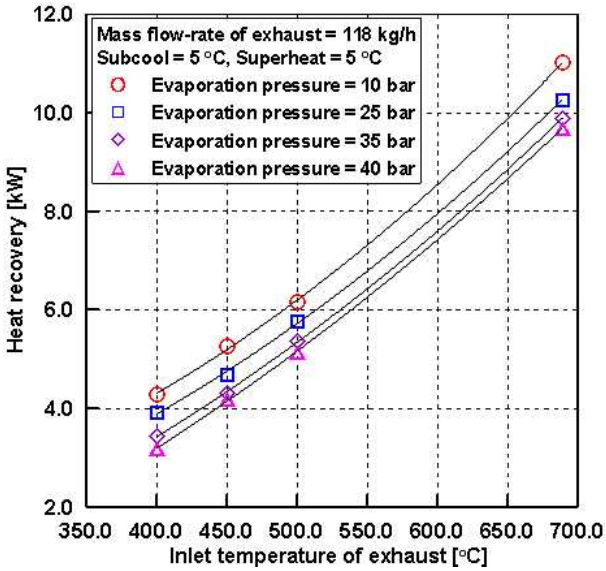

Figure 3.24 Heat recovery according to evaporation temperature of HT boiler model #1

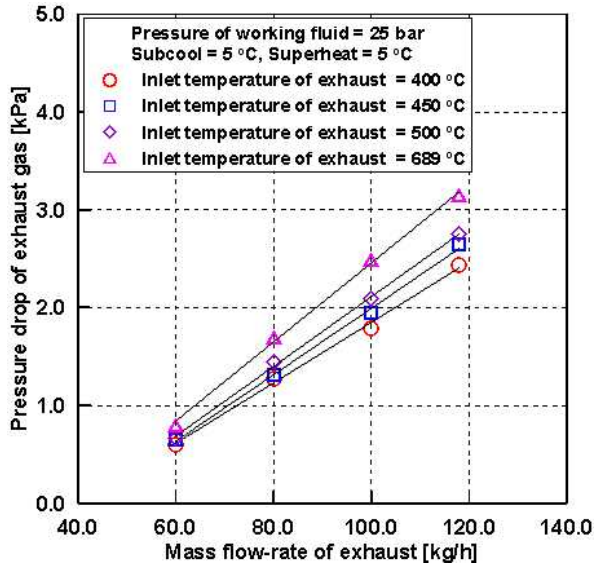

Figure 3.25 Pressure drop of exhaust gas according to mass flow rate of exhaust gas of HT boiler model #1

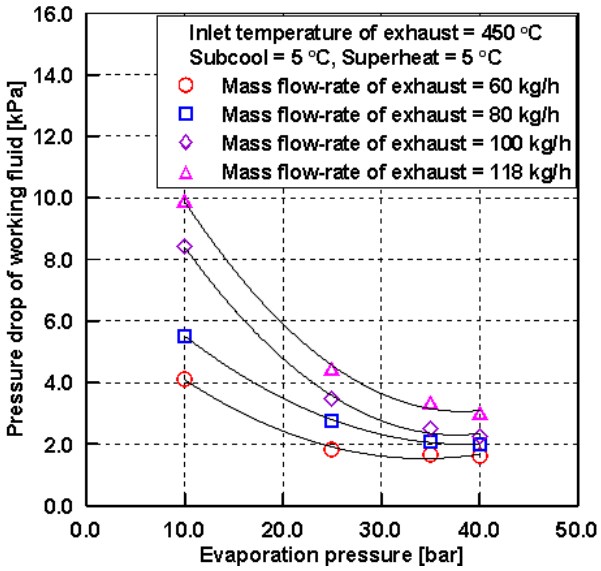

Figure 3.26 Pressure drop of working fluid according to evaporation pressure of HT boiler model #1

A one-dimensional computational fluid dynamics analysis has been performed by setting the conditions described above for the circular shell and spiral tube type HT boiler (#2) before an experiment. An experiment under above conditions has been conducted with the prototype of HT boiler (#2). The comparison data are shown in Figures from 3.27 to 3.29 for verification of the feasibility of the design program.

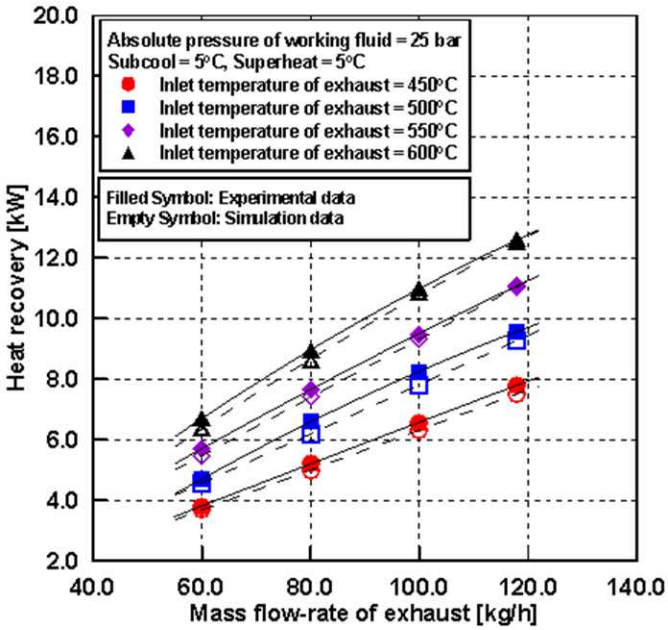

Figure 3.27 Heat recovery of HT boiler model #2

Figure 3.27 shows the heat recovery characteristics in accordance with the temperature and flow rate of exhaust gas. The hollow symbols mean the prediction values and the solid symbols mean the experimental data. The experimental heat

recovery is 7.79 kW at the design point. It is remarkably improved value in comparison with the fin and helical coil type HT boiler (#1). The predicted data by the design program shows the error of －6.3 ~ -0.4% over the range of the temperature and flow rate of exhaust gas. The data match mutually within 3% on overage.

The comparison data between prediction and experiment are shown in Figure 3.28 for exhaust gas pressure drop according to the exhaust gas flow rate at the design point exhaust gas temperature of 450 ℃. The exhaust gas pressure drop is 4.11 kPa at the flow rate of 118 kg/h. The analytical data represent the tendency of the lower prediction value than the experimental data with errors of about -15 ~ 8%.

The pressure drop characteristics of the working fluid are presented as the experimental results in Figure 3.29 with respect to the mass flow rate of the working fluid entering the HT boiler in comparison with the prediction data. The pressure drop at the design point is 1.23 kPa. Whereas the predicted data through analysis shows a tendency to increase more or less sharply, the experimental data has a somewhat dull slope. The pressure drop represents an error of about 18% at the design point of the exhaust gas flow rate of 118 kg/h. As the working fluid mass flow rate reduces, a decline in the prediction data becomes larger.

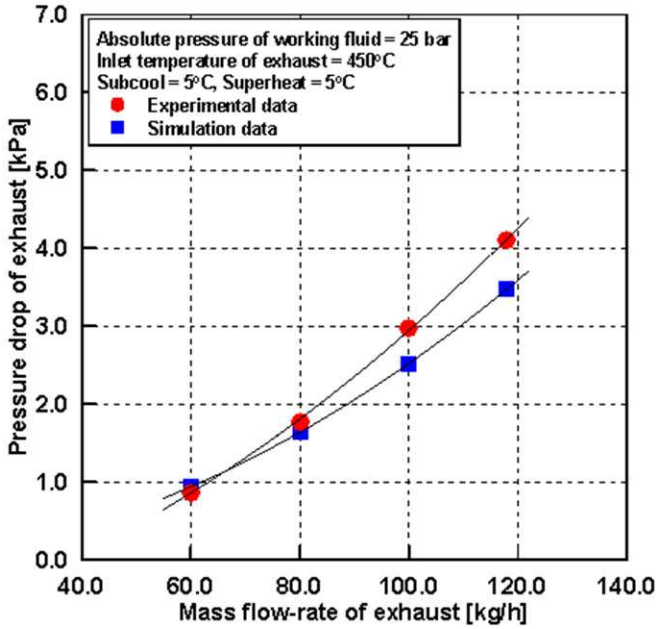

Figure 3.28 Exhaust gas pressure drop of HT boiler model #2

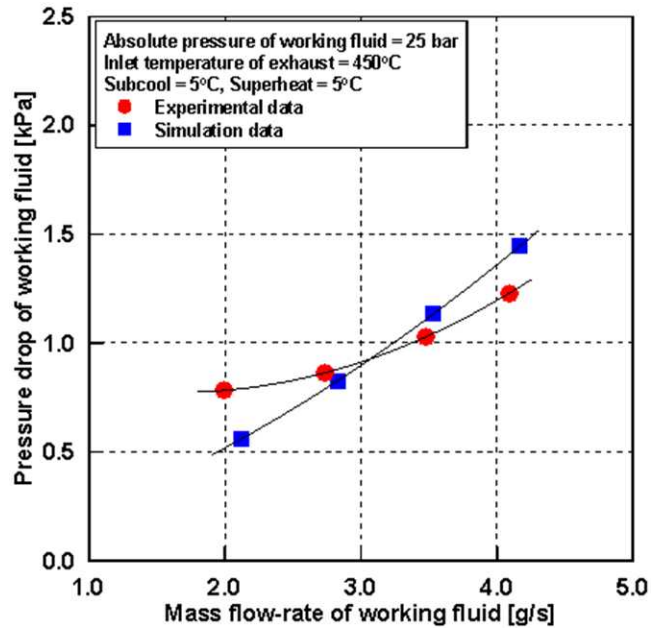

Figure 3.29 Working fluid pressure drop of HT boiler model #2

The performance data has been obtained through an experiment for the prototype of the rectangular shell and spiral tube HT boiler (#3) as shown in Figures 3.30 to 3.32. The experimental conditions are the same as those for the circular shell and spiral tube HT boiler.

Figure 3.30 shows the heat recovery from various conditions of the exhaust gas in temperature and mass flow rate including almost all the cases which the HT boiler could possibly undergo. The heat recovery increase as the heat source increases nearly linearly. The heat recovery at the design point is 7.81 kW, which is almost same as the circular shell and spiral tube model, even though the volume and the length of the rectangular one is largely reduced. In front of the HT boiler, the HT superheater plays a role of the heat recovery heat exchanger recovering the exhaust gas waste heat at the highest level such as about 700 ℃. However, the exhaust gas temperature can exceed to the level of 800 or 900 ℃. The upper region of Figure 3.30 shows the excessive heat source range. In case that the HT superheater discharges still excessive exhaust gas heat, the HT boiler recovers the amount of heat shown in the graph. When the vehicle speed is 100 km/h, the mass flow rate of the exhaust gas is about 79.4 kg/h. If the exhaust gas inlet temperature is 450 ℃, the heat recovery performance is 5.29 kW, while the heat recovery requirement is 5.19 kW. Heat recovery requirement of 3.92 kW is also satisfied for the condition of vehicle speed of 80 km/h.

The pressure drop characteristics on the exhaust gas side are shown in Figure 3.31. The pressure drop increases linearly with the increase of the mass flow rate of the exhaust gas, however, the differences between the pressure drop in various temperature conditions are very little. The pressure drop on the exhaust gas side is 3.49 kPa at the design point.

Figure 3.32 shows the pressure drop characteristics on the HT working fluid side. The pressure drop increases as the working fluid mass flow rate with respect to the heat recovery caused by the temperature difference between the heat source and the working fluid. The pressure drop on the working fluid side is 2.43 kPa at the design point.

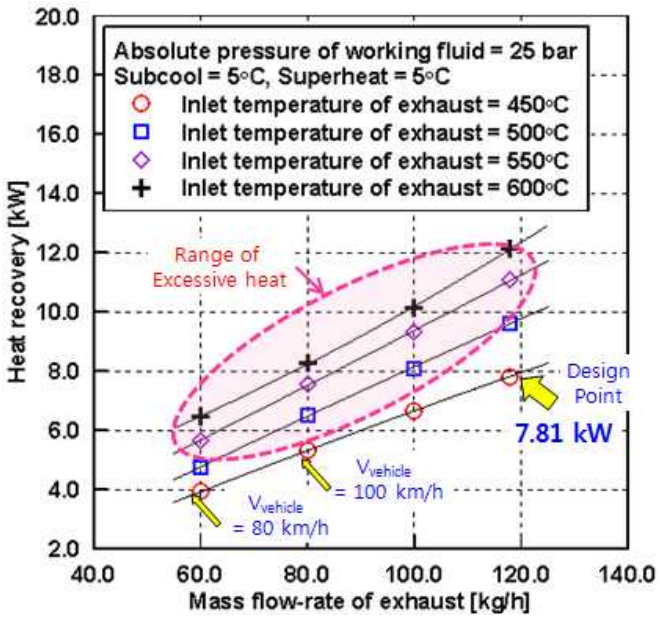

Figure 3.30 Heat recovery of HT boiler model #3

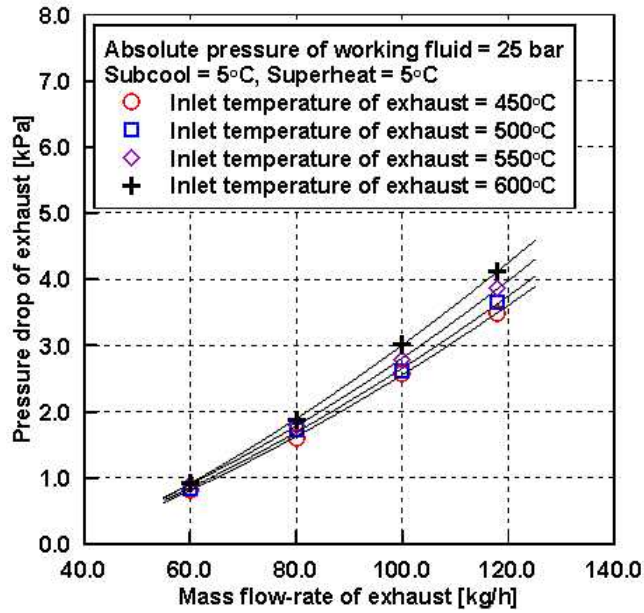

Figure 3.31 Exhaust gas pressure drop of HT boiler model #3

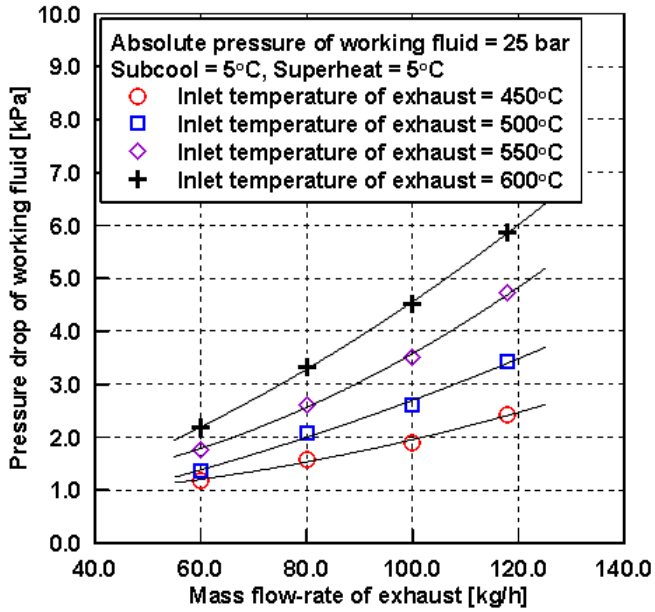

Figure 3.32 Working fluid pressure drop of HT boiler model #3

Figures 3.33 to 3.35 show comparisons of the experimental results of three prototypes and another comparisons of the experimental and simulation results of the circular shell and spiral tube model (#2).

As shown in Figure 3.33, the heat recovery data are compared in varying mass flow rate of the exhaust gas at the working fluid pressure of 25 bar and the exhaust gas inlet temperature of 450 ℃. The rectangular and circular shell and spiral tube models surpass the fin and helical coil model in heat recovery performance more than 30% over the exhaust gas mass flow rate range. The the exhaust gas conditions include the design point at vehicle speed of 120 km/h and the off-design points such as vehicle speed of 80 and 100 km/h. The rectangular one represents the best performance, however, a slight difference of 1.7% with the circular one. The simulation error rate is 3.8% on average over the range.

The exhaust gas pressure drop behaviors of three models are compared in Figure 3.34. The fin and helical coil type model shows the smallest pressure drop, which is about 31% smaller than that of the circular shell and spiral tube type model. The rectangular model shows about 10.9% less than the circular shell and spiral tube model. At the full range of exhaust gas flow rate, the pressure drop data of the circular shell model show an error rate of 7.6% on average between the experiment and the simulation.

The working fluid pressure drop data are compared in Figure 3.35. The fin and helical coil model shows about 3.2 times of the circular shell model and about 1.8 times of the rectangular shell model. The helical coil has a long flow path and a smallest cross section for the working fluid so that the working fluid loses its pressure much more by frictional flow resistance in the coil tube. The pressure drop of the rectangular model is about 1.8 times of the circular model since the liquid flow section of the small cross sectional area affects the pressure loss. However, the amount of the pressure drop of the working fluid is so low that it is negligible and it does not need to be considered significantly.

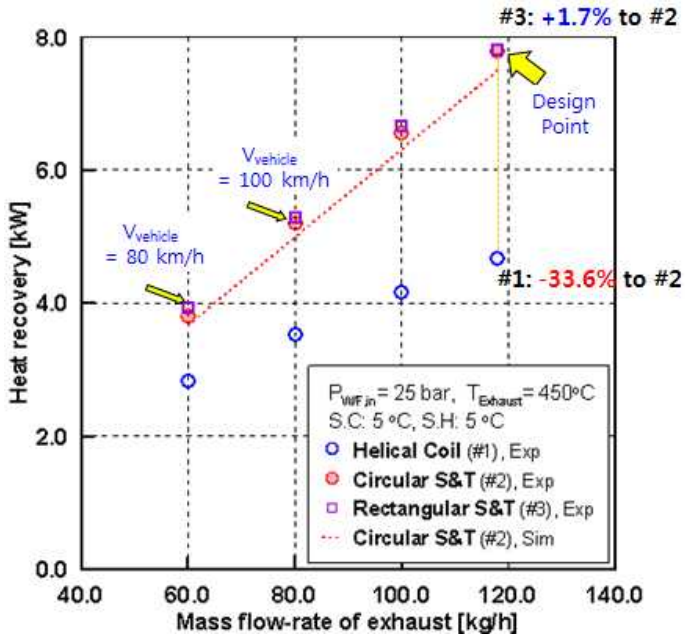

Figure 3.33 Heat recovery of 3 models

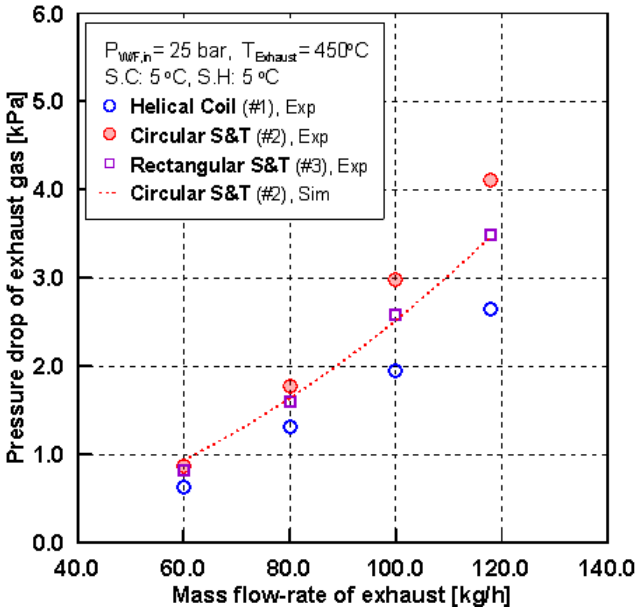

Figure 3.34 Exhaust gas pressure drop of 3 models

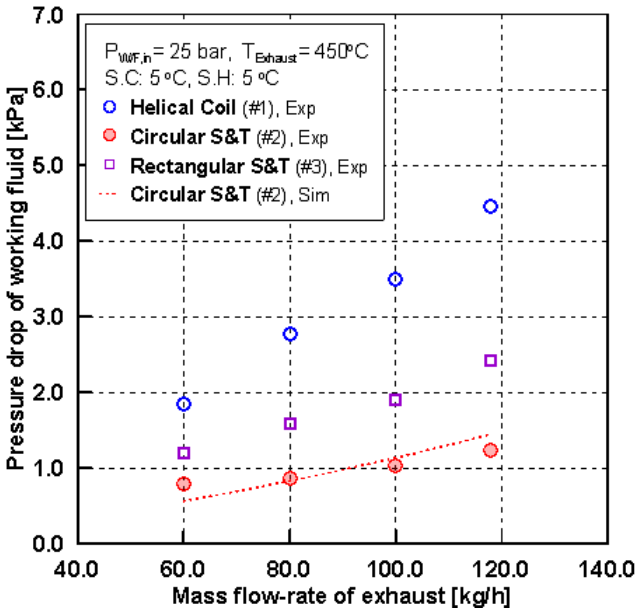

Figure 3.35 Working fluid pressure drop of 3 models

In an aspect of the heat recovery performance, the rectangular boiler is most advantageous among the models on the basis of the volume occupied. Consequently, the most adequate type for the HT boiler in the wast heat recovery system is the rectangular shell and spiral tube.

In case that the heat energy is excessive, it is advantageous in view of reliability and safe for the HT boiler to have a portion of the exhaust gas bypassed. The rectangular HT boiler is placed side by side with the exhaust gas by-pass duct and connected with Y-ducts at both ends as shown in Figure 3.36. The bypass valve is connected near the exhaust inlet, which works when the excessive heat source flows.

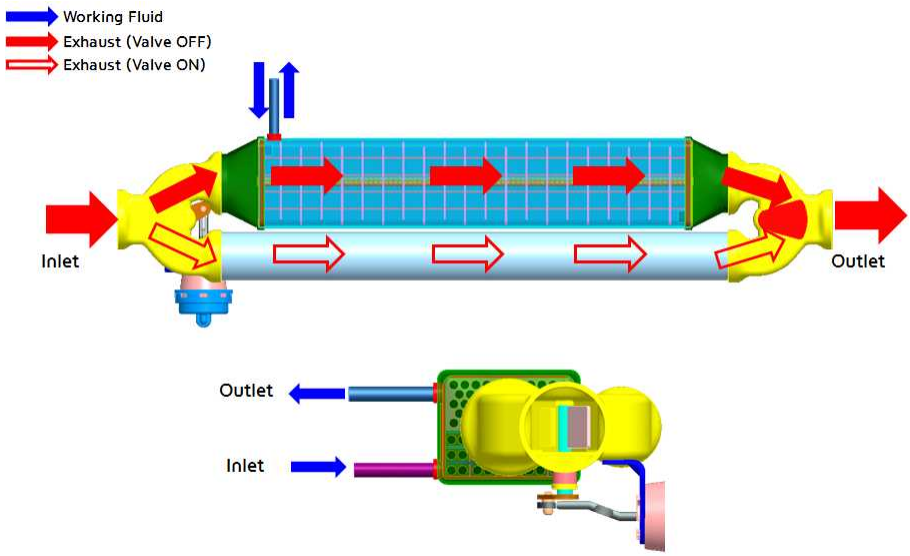

Figure 3.36 Bypass valve construction with the HT boiler

Table 3.1 Comparison of design and performance of HT boilers

Model	#1	#2	#3
Type	Fin & Helical Coil Tube	Circular Shell & Spiral Tube	Rectangular Shell & Spiral Tube
Exterior	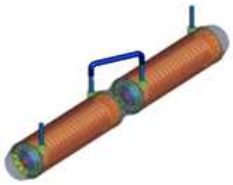	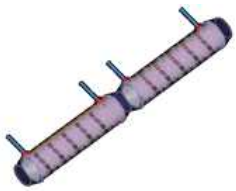	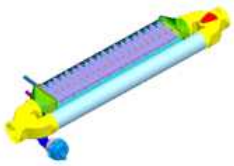
Cross-section	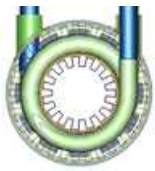	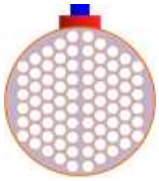	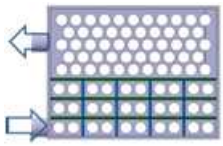
Size and Volume	*L*×*D*×*D*. 510×78.8×78.8 mm^3 Volume: 2,949 cc	*L*×*D*×*D*. 660×78.8×78.8 mm^3 Volume: 3,681 cc	*L*×*W*×*H*. 440×87.8×68.8 mm^3 Volume: 2,883 cc
Performance	*Q*. 4.67 kW ΔP_{exh}: 2.64 kPa	*Q*. 7.79 kW ΔP_{exh}: 4.11 kPa	*Q*. 7.81 kW ΔP_{exh}: 3.49 kPa

The comparison of the design concept and performance data are shown in the table 3.1. The helical coil tube type has wavy fins for the exhaust gas flow adjacent to coil tube for the working fluid flow. The cylindrical body has been devised to replace a part of the exhaust duct with the boiler, while maintaining the conventional design of the exhaust system. However, the contact area of coil and wavy fins is so insufficient

for heat recovery from exhaust gas to working fluid that the performance of the helical coil boiler is the most inferior of three models. Two shell and spiral tube models present similar heat recovery performance, however, the rectangular model has only 72.4% of the circular model in the volume occupied. In other words, taking into account of the volume occupied, the rectangular shell and tube HT boiler shows the best heat recovery performance. The energy density of the fin and helical coil tube type is 1.58 kW/L at the design point, that of the circular shell and spiral tube type is 2.12 kW/L, and that of the rectangular type is 2.71 kW/L. The rectangular model has significantly reduced the length of the HT boiler into a compact form to be mounted on the exhaust system. The pressure drop on the exhaust side is reduced by the length of the heat exchanger core in the rectangular shell and spiral tube model. The rectangular model satisfies the heat recovery requirements at various vehicle speeds.

3.7 Conclusion

In this chapter, several heat exchanger types have been investigated to derive a design process for highly-efficient compact HT boiler as a heat exchanger recovering waste heat from exhaust gas with minimized exhaust gas pressure drop. A unique design concept has been aroused taking the state and conditions of the working fluid at the inlet region into account. The results obtained through this process are as follows:

The one-dimensional analytical approach has been used to conduct a variety of parametric studies for geometrical variables through the performance prediction program developed in this study. The program has been also used to predict the heat recovery performance over the range of the heat source temperatures and mass flow rates. In order to enhance the heat recovery further, the concept of flow sections separating the liquid state and saturation state in the HT boiler has been derived. The three-dimensional analysis has been used for the performance prediction of the peculiar heat exchanger.

Although the fin and helical coil type model has been designed to be adapted to the exhaust system, the insufficient contact area has resulted in the inferior performance. The circular and rectangular shell and spiral tube models have represented better performance than the fin and helical coil type model. Comparing the circular and rectangular models, the rectangular model is the

better in heat recovery performance, yet the difference is insignificant. However, taking the volume occupied into account, the performance of the circular shell and spiral tube model is 34.2% better than that of the fin and helical coil tube model, and the rectangular type is 27.8% better than the circular shell and spiral tube type model. Consequently, the flow-sectioning rectangular model is the most efficient type for the HT boiler.

From the results of the assessment of the HT boiler prototypes, the mass flow rate of the working fluid and the subsequent heat recovery increased linearly in the cases where the inlet and exit conditions were set at fixed degrees of sub-cool and superheat.

For the same waste heat energy, the heat recovery has increased with a decrease in the evaporation pressure resulting in the increase in the temperature difference. When the temperature of exhaust gas and/or the evaporation pressure of the working fluid increases, even if the mass flow rate of the exhaust gas is the same, the exhaust gas side pressure drop shows increasing trend due to the decrease in the density of the exhaust gas.

In consideration of the fact described above, as the heat recovery performance of the heat recovery heat exchanger increases, the pressure drop at the exhaust gas side decrease. In other words, an enhancement in the HT boiler heat recovery performance cools down the temperature of the exhaust gas further, thus, the specific volume of the exhaust gas decreases followed by the decrease in the pressure drop.

Chapter 4

Design Process of Low Temperature Condenser

4.1 Role of an LT Condenser

The layout of the waste heat recovery system for gasoline vehicles applying the Rankine cycle is The LT loop is designed to recover the waste heat from the HT loop and the engine coolant, generate the auxiliary drive power, and dissipate the residual heat up to 22 kW through an LT condenser as shown in Figure 2.18 [Bae12]. The LT condenser is used to dissipate the residual heat from the whole engine waste heat recovery system.

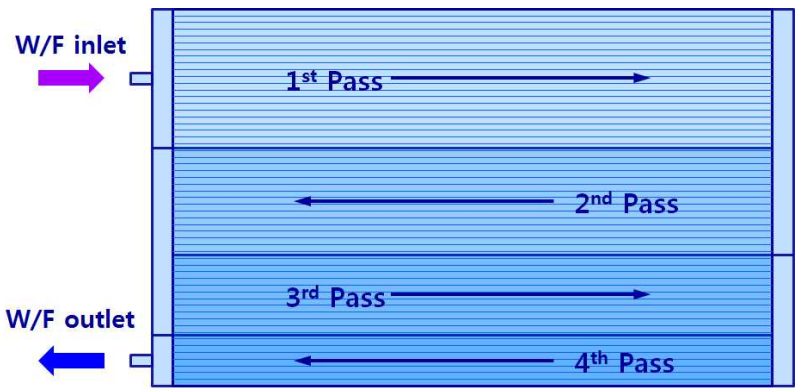

Figure 4.1 Construction of a parallel multi-flow LT condenser

The role of the LT condenser is to condense enough of the LT working fluid in a saturated or vapor state, and send it to the LT pump. Instead of using a receiver drier in the condenser model, which prevents the working fluid from being sent out in a saturated state, in case that heat transfer is insufficient, a reservoir tank is located at the outlet of the condenser.

Refrigerant R134a is selected for the working fluid of the LT loop, in order to recover waste heat from the engine coolant at about 100℃, considering the evaporation temperature, condensing pressure, cycle efficiency, and so on [Bae11]. R1234yf, an alternative refrigerant that has similar properties to R134a, can be used as a working fluid in the actual vehicle application, considering the environmental characteristics. R134a has a low evaporating temperature, so that it is advantageous to recover the engine coolant waste heat. However, since the saturation enthalpy is small, the working fluid of a significantly high flow rate of 156 g/s, i.e. 562 kg/h passes through the heat exchanger, resulting in an excessive pressure drop, while maintaining the considerably high heat dissipation required.

General condensers for air conditioning system are manufactured with four or more pass construction. Usually, when the number of passes increases, the pressure drop is increased to some extent; however, the thermal performance that can be obtained is more than 20% to 50%. For the same conditions at the inlet and outlet of the condenser, the refrigerant flow rate

increases according to the size of the heat exchanger; however, the effect of increasing the number of passes is reduced. As mentioned above, the low temperature loop of the engine waste heat recovery system needs to flow the working fluid at about 562 kg/h, which is 4.7 times larger than the general flow rate of around 120 kg/h. This means the pressure drop in the condenser of this system in identical cross-sectional areas and geometries may, arithmetically, exceed 20 times that of the general condenser. On the other hand, the tremendous pressure drop with diminishing effect of increased passes causes deterioration of the pressure of the refrigerant inside the micro-tubes, resulting in decreased heat dissipation performance. According to the evaluation of a 4-pass condenser for this system, the pressure drop was more than 3 bar, which is quite a large value, considering the operating pressure of about 16 bar, and a factor of loss in various aspects, such as the driving force of the refrigerant, and thermal performance. Consequently, the primary goal is to reduce the pressure drop in the condenser.

In addition, enhancement of heat dissipation of the LT condenser would lead to a deterioration of front end air flow resulting in the increase of fan power consumption. However, the low pressure loss lowers power consumption of the working fluid pump, and high heat dissipation increases the efficiency of the cycle. Therefore, the design optimization of the LT condenser can be obtained from this trade-off relation.

4.2 Design Conditions for an LT Condenser

A distinct point of an LT condenser, from general condensers in the conventional air conditioning system, is that most portion of the working fluid is in a saturated state. Due to the fact that an enormous flow of working fluid passes through to release much of the heat, the reduction of pressure drop of the working fluid is a big challenge for design engineers. In addition, whereas a receiver drier is normally mounted just before the final pass, there is no receiver drier in an LT condenser. There is a reservoir tank after the condenser outlet, to reduce the air flow resistance of the front end.

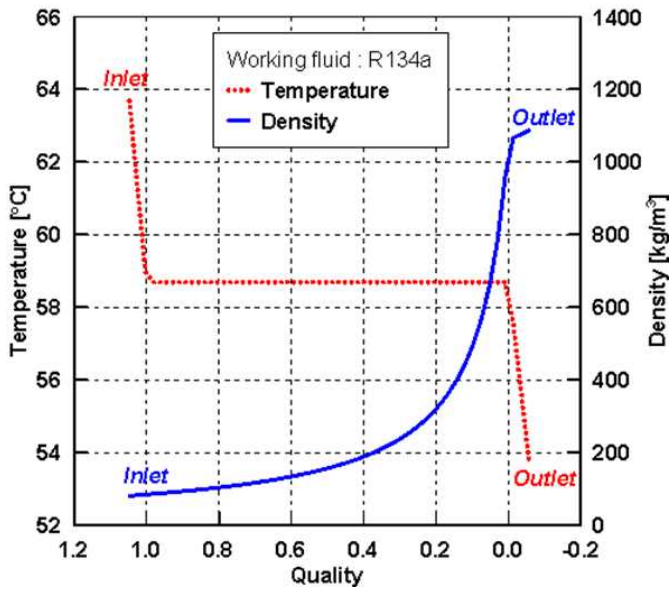

Figure 4.2 Behavior of properties of the working fluid in the micro-tubes through phase change

Figure 4.2 shows the behavior of the LT working fluid, R134a, in the condenser tubes with the conditions of inlet superheat of 5℃, and outlet sub-cool of 5℃. The important points for the optimized design of the LT condenser are as follows: first of all, the pressure drop is greater, due to the lower density at the area adjacent to the inlet pipe inside the uniformly shaped tubes, than in other areas. And, the pressure drop decreases with the increase in the number of tubes. Finally, the flow rates of the working fluid in the tubes are non-uniform, by the flow distribution in the headers. The maldistribution of the flow in the tubes may greatly affect the heat dissipation performance and pressure drop of the low temperature condenser.

For the purpose of the design of the pressure drop reduction, a technique is required to evaluate the effects of the design factors such as the number of passes, arrangement of the number of working fluid tubes on each pass, fin geometry, and core size of the heat exchanger. A commercial CFD analysis tool is capable of predicting detailed flow distribution for complex geometries, but it cannot adequately simulate the phase change process yet. On the other side, the performance prediction code is one-dimensional, but it can simulate the phase change from the superheated through saturated to sub-cooled states, and enables a quick verification of the effect of the change of a design factor. In this study, an optimized design process has been established, by harmonizing the advantages of these two design techniques.

4.3 Design Model

Figure 4.3 shows a flow chart of the design process model of the low temperature condenser established in this study. Even if the LT condenser models have an identical exterior shape, the performances differ remarkably, depending on the number of tubes, and the arrangement of the tubes with the consequence that the arrangement of the working fluid tubes can be one of the major design factors. The performance comparison of the LT condenser was carried out according to the number of tube passes, using the 1D code, with the geometrical parameters of fin and tubes fixed. The 2-pass model has the result of reducing the working fluid pressure drop significantly, with slight reduction of heat dissipation, in comparison with the 4-pass model [Bae12]. In this study, the investigation of the performance is carried out on the 2-pass model. When the number of passes is decided, the decision of the number of the tubes in each pass remains. The procedure is performed by the 1D code.

After completing the design of the exterior and interior of the LT condenser, the flow distribution of the LT working fluid should be calculated over the tubes. It is difficult to embody the distribution through a 1D code, and therefore the geometries of the header, inlet and outlet pipes, tubes, and so on, are 3-dimensionally modeled to be analyzed using a commercial CFD program (Fluent 6.3). The effects of the positions of the inlet and

outlet pipes on the header are also evaluated by 3D analyses. The resulting flow rates of the refrigerant with respect to the tubes are input into the 1D code, a comparison of the performance of the drafts is conducted, and the conclusion of the final design draft comes at the end of the design process of the LT condenser.

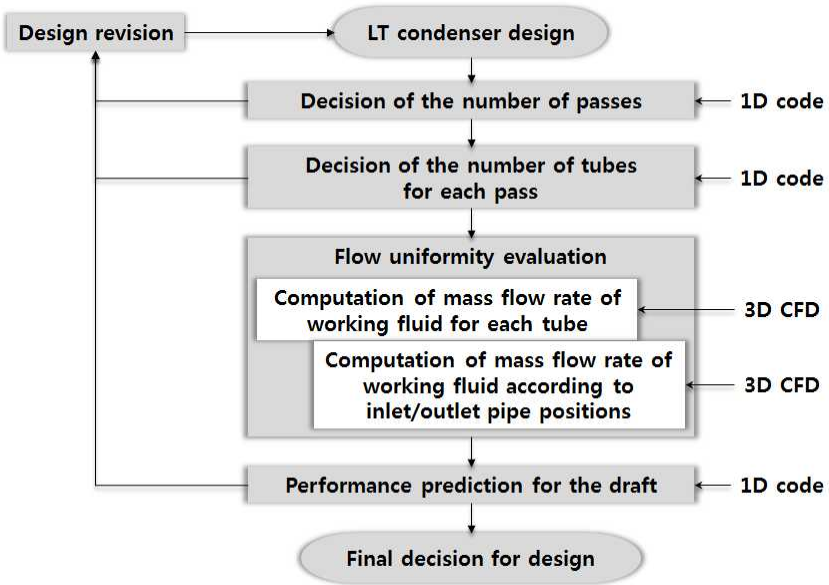

Figure 4.3 Flow chart for the design of the LT condenser

4.4 Design and Analysis Program for the LT Condenser

The LT condenser has an air-cooled parallel multi-flow structure as shown in Figure 4.1. In general, a parallel multi-flow condenser has so many parallel tubes that the working fluid inflows simultaneously and the cross-sectional area for the working fluid is large, which is structurally advantageous that the pressure dorp is reasonably low and the high-density heat transfer per unit area.

There are headers at the left and right sides of the parallel array of the working fluid tubes and air-passing louvered fins. The LT working fluid enters the inlet header, flows through the stepwise passes, and dissipates heat to the ambient air passing through the louvered fins.

The LT working fluid flows through the capillary extruded tubes and ambient air flows through the louvered fins. Both fluid form a cross flow. A control volume for the inner working fluid and outer air is set as shown in Figure 4.4. The heat transfer rates and the pressure drops according to the phase change of the LT working fluid are calculate from the finite difference method.

In this study, the numerical method has been proceeded tracing the working fluid, cell by cell, tubes to tubes, and pass to pass from the inlet to the exit direction.

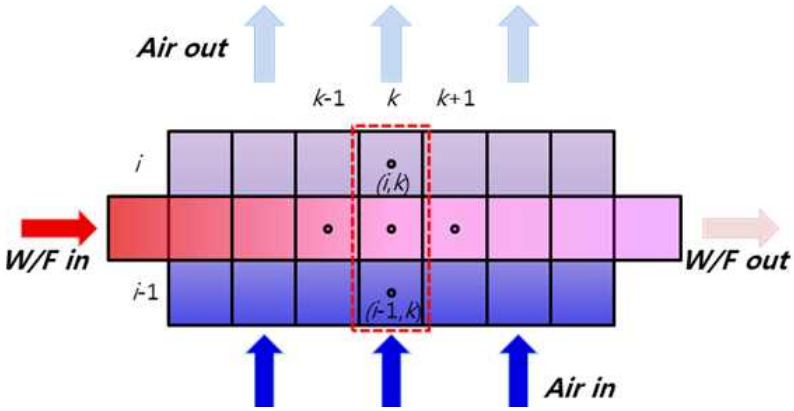

Figure 4.4 Control volume for parallel multi-flow LT condenser

The working fluid heat transfer coefficient of the single-phase region has been calculated by using the correlation as Petukhov and Kirillow [Incropera96].

$$h_k = \left(\frac{k}{D_h}\right)\frac{\mathrm{Re}_{D_h}\mathrm{Pr}\left(\frac{f_k}{2}\right)}{1.07+12.7\sqrt{\frac{f_k}{2}}\left(\mathrm{Pr}^{\frac{2}{3}}-1\right)} \tag{4.1}$$

$$0.5 < \mathrm{Pr} < 2000, \quad 10^4 < \mathrm{Re}_{D_h} < 5\times 10^5$$

The working fluid heat transfer correlation for saturation state has been obtained using the empirical equation proposed by Cavallini and Zecchin [Cavallini71].

$$h_k = 0.05\,\mathrm{Re}_{eq}^{0.8}\mathrm{Pr}_l^{0.33}\left(\frac{k_l}{D_h}\right)$$

where $\mathrm{Re}_{eq} = \mathrm{Re}_l + \mathrm{Re}_v \left(\frac{\mu_v}{\mu_l}\right)\left(\frac{\rho_l}{\rho_v}\right)^{0.5}$ (4.2)

Air side pressure drop is calculated from equation (3.7) which Kays and London proposed. The friction factor of air side louvered fins is calculated by using the equation which Chang *et al.* proposed [Chang00].

The pressure drop resulted from friction in the working fluid tube is expressed as equation (4.3) for single-phase region.

$$\Delta P_{W/F,k,1ph} = 4 f_k \frac{\delta x}{D_e} \frac{G^2}{2\rho} \tag{4.3}$$

For two-phase region, the working fluid pressure drop is expressed as equation (4.4).

$$\Delta P_{W/F,k,2ph} = \Delta P_g + \Delta P_{ac} + \Delta P_{tp} \tag{4.4}$$

where the pressure drop due to the gravity is

$$\Delta P_g = \int_0^z \left[\alpha \rho_v + (1-\alpha)\rho_l\right] dz,$$

the pressure drop due to the change in momentum is

$$\Delta P_{ac} = \left(\frac{G^2}{\rho_l}\right)\left[x\left(\frac{\rho_l}{\rho_v} - 1\right)\right], \text{ and}$$

the pressure drop due to the phase change is calculated by the correlation proposed by Lockhart and Martinelli [Collier94, Kim06]

as:

$$\left(\frac{\Delta P}{\Delta z}\right)_{tp} = \left(\frac{\Delta P}{\Delta z}\right)_{l} \Phi_l^2$$

where $\Phi_l^2 = 1 + \frac{21}{X} + \frac{1}{X^2}$, $X = \left(\frac{1-x}{x}\right)^{0.9} \left(\frac{\rho_v}{\rho_l}\right)^{0.5} \left(\frac{\mu_l}{\mu_v}\right)^{0.1}$.

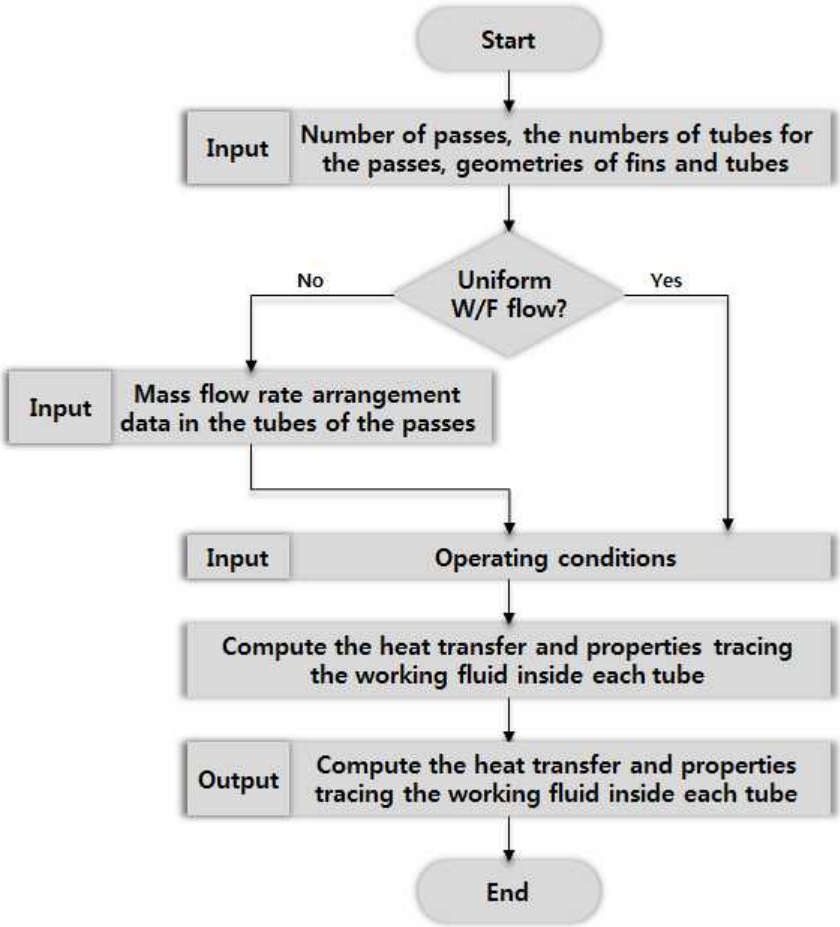

Figure 4.5 Flow chart of the design program for the LT condenser

The one-dimensional heat dissipation performance design and analysis program was developed to design an air-cooled condenser in Basic language, following the procedures shown in Figure 4.5.

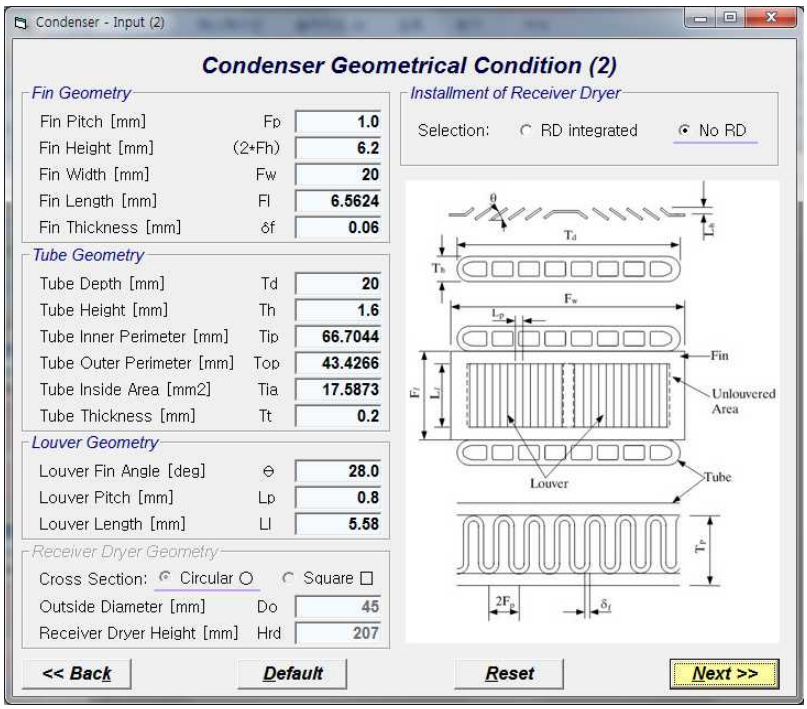

Figure 4.6 Geometrical input window of the 1D code

After inputting the geometrical data and operating conditions of an LT condenser (Figure 4.6), the processes of heat transfer of the working fluid and ambient air, and the change of phase are simulated, through the trace of the working fluid in the tubes. Finally, various performance data and the distributions of the

properties, such as pressure, temperature, velocity, specific volume, quality and so forth, are shown in the two-dimensional graphic windows (Figure 4.8). The code is actually two-dimensional 1D code.

After determining the number of passes and the numbers of tubes in the corresponding passes, the ratios of mass flow rate per tube are input to conduct the performance prediction. If the flow data from 3D analysis are input in the dialog window shown in Figure 4.7, the flow uniformity of each pass is calculated, and appears in real-time. The user can confirm the flow distribution, with values of summation and average of the ratios of the flow rates in the real-time calculation window. The 1D analysis program in this study tracks all the interior phase changes in the micro-tubes.

Once the calculation processes are completed, the performance calculation results data are shown in the series of results windows. This study also developed visual contour graphics, to observe at a glance the distributions of temperature, pressure, velocity, and so forth, of the working fluid inside the tubes. Figure 4.8 displays an example view of the resulting contour window, which reveals the effects of the number of passes and tubes on the performance, with the assumed uniform velocity and temperature of ambient air onto the LT condenser.

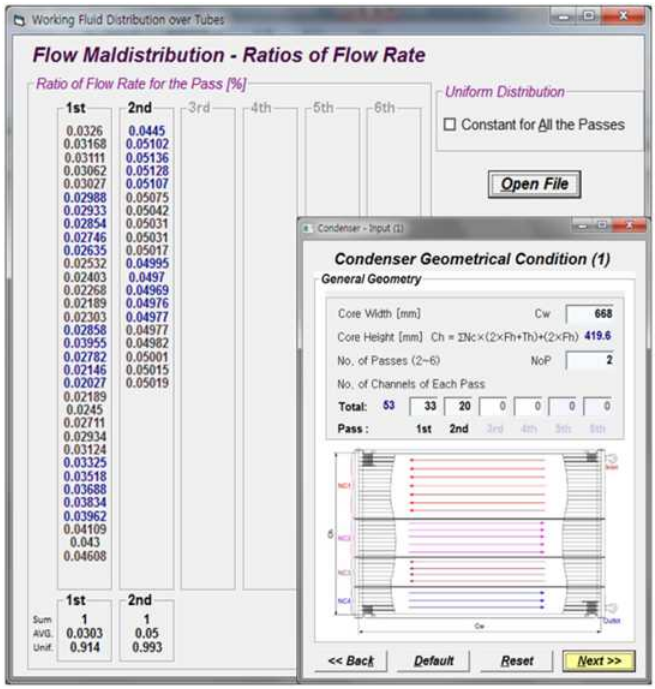

Figure 4.7 Dialog windows of the 1D code

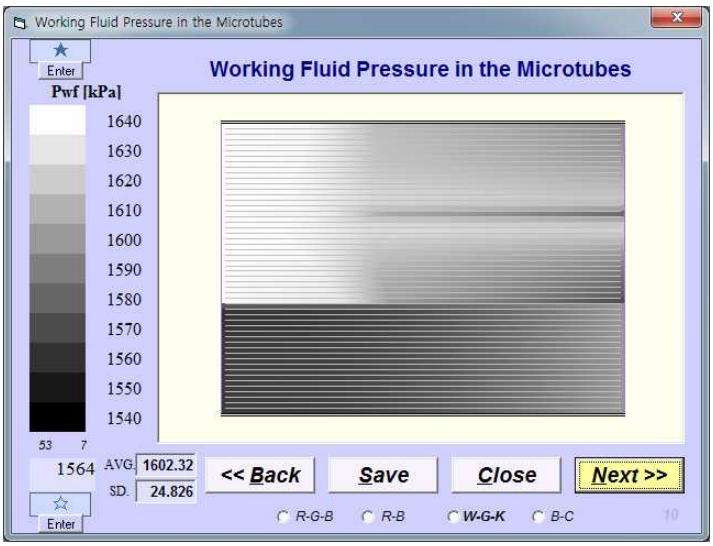

Figure 4.8 Pressure distribution in the tubes of the LT condenser

4.5 Design and Analysis

The analytical design was performed for an LT condenser through the above processes.

4.5.1 Decision of the Number of Passes

When the number of tubes in a condenser is fixed, a larger number of passes elongates the flow path of the working fluid in the heat exchanger and may enhance the heat dissipation performance. However, a smaller number of tubes allocated in a pass increases the pressure drop due to increased flow rate of the working fluid. Thus, a smaller value is advantageous in view of the number of passes.

A comparison of the experimental results of LT condenser prototypes is shown in Figure 4.21. The pressure drop of the 2-pass condenser is less than half (44.8%) of the value of the 4-pass condenser of identical geometry at the design point. However, the difference of heat dissipation between the two models is not significant.

4.5.2 Arrangement of the Numbers of Tubes

The total number of the tubes is 53 for the new design model. Compared with the first model, the tube geometry and the total number of the tubes are changed; however, this section focuses on the numbers of tubes etc., leaving the changes aside at this point.

The effects of the numbers of the tubes were analyzed at the design point, with the number of passes determined as 2. First, the flow rates are assumed to be uniform, throughout the entire tubes per pass. The calculations were carried out using the 1D code, for the decision of the optimum range of the numbers of tubes.

Although the inlet state of the working fluid is a saturated state with a quality of 0.942 at the design point, the superheated-state inlet conditions were also considered. In other words, the inlet state conditions of the refrigerant R134a are specified as superheat of 20℃, superheat of 5℃, and quality of 0.942, respectively, which cover almost the entire operation range of the LT condenser. The performance predictions were performed by finding the mass flow rates satisfying the conditions mentioned above at the inlet and the sub-cool of 5℃ at the exit with the inlet pressure of the refrigerant of 16.4 bar, conventional air-cooled condenser conditions of ambient air temperature of 35℃, and air velocity of 5 m/s.

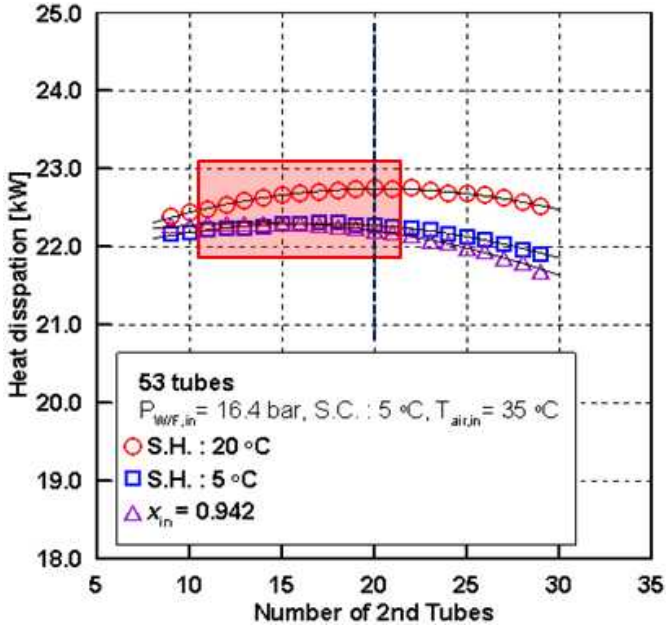

Figure 4.9 Comparison of heat dissipation (Uniform flow)

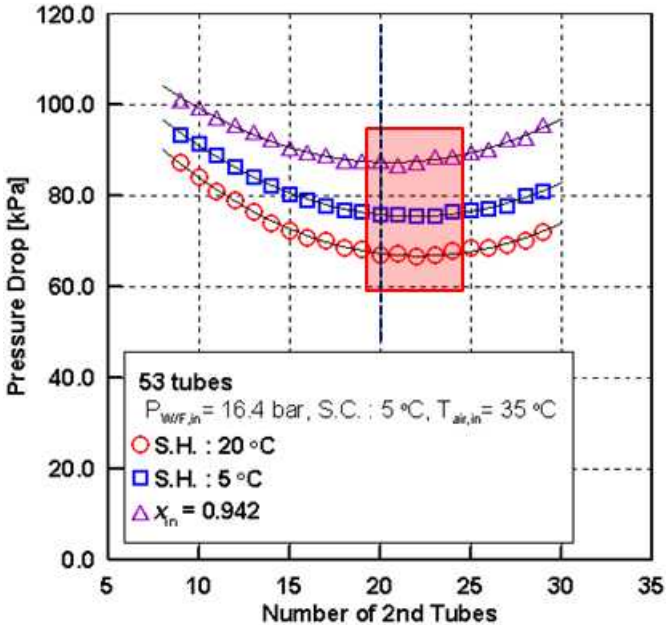

Figure 4.10 Comparison of pressure drop (Uniform flow)

Figure 4.9 shows the heat dissipation according to the number of tubes of the second pass, with respect to the inlet conditions. The highlighted ranges of the heat dissipation are slightly different for the conditions; however, the optimum range of the number of the second pass tubes is generally between 12 and 22.

Figure 4.10 shows a comparison of the pressure loss of the LT working fluid according to the arrangement of the tubes, with respect to the inlet conditions. When the inlet and exit conditions are the same and even if the flow rates split into the tubes are all uniform, the pressure drop differs not less than 20 kPa, with respect to the arrangement of the number of the tubes in the passes. The optimum range of the number of second pass tubes lies between 19 and 24.

Consequently, the optimum point of the number of second pass tubes is determined to be 20, at which the LT condenser can reduce the pressure loss while maintaining the heat dissipation.

4.5.3 Assessment of the Flow Uniformity

The above consideration has a limitation that the assumption of uniform flow differs from the actual condition. A commercial three-dimensional CFD program was used to take the flow distribution over the tubes into account. Flow uniformity is a measure of non-uniformity of velocities passing through a certain cross section. The 3D analysis was conducted without any phase or temperature change, in order to investigate the influence of the geometries alone. Figure 4.11 shows an example of the resulting flow distribution from 3D analysis. With a constant density in the analysis domain, the flow uniformity can be expressed as follows:

$$\sigma = 1 - \sum_{i=1}^{N} \frac{\left| q_i - \bar{q} \right|}{2N\bar{q}} \tag{4.5}$$

The basic model of the LT condenser has an inlet pipe in the midst of the first pass, and an outlet pipe at the bottom of the second pass. Based on the number of the second pass, the flow uniformity assessment was carried out for the 7 cases of 7, 12, 17, 19, 20, 22, and 27 (#1, #2, #3, #4, #5.1, #6, and #7 respectively) including the influence of gravity; the results are shown in Figure 4.12. This graph shows the ratios of the mass flow rate of the LT working fluid, from the top tube of the first pass, to the bottom tube of the second pass, for the cases mentioned above.

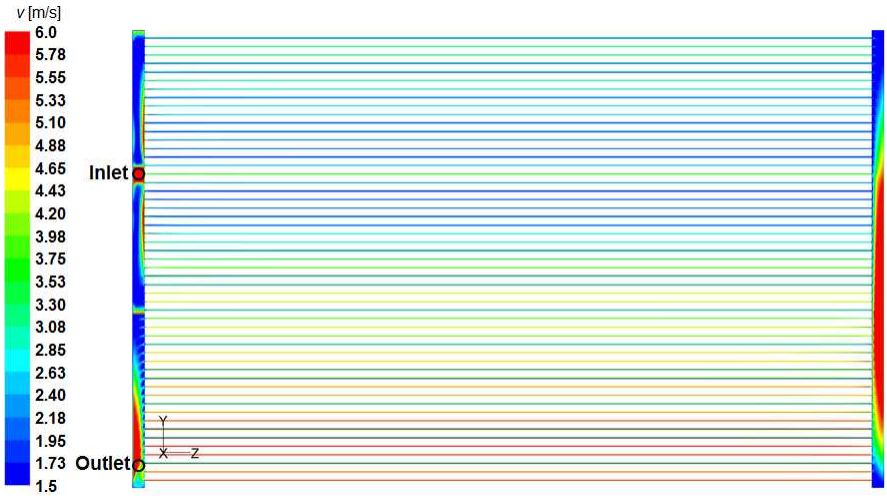

Figure 4.11 Velocity distribution in the tubes via 3D program

Since the inlet pipe is located in the midst of the first pass, a portion of the flow surges into the adjacent tubes; however, considerable portions of the flow concentrate in both the top and bottom sides quite symmetrically. The bottom side of the header has slightly more flow due to gravity.

Table 4.1 Flow uniformity according to the tube numbers

Case 1st 2nd	#1 46 7	#2 41 12	#3 36 17	#4 34 19	#5.1 33 20	#6 31 22	#7 26 27
σ_1	0.851	0.874	0.908	0.909	0.914	0.923	0.943
σ_2	0.994	0.982	0.965	0.956	0.954	0.946	0.921

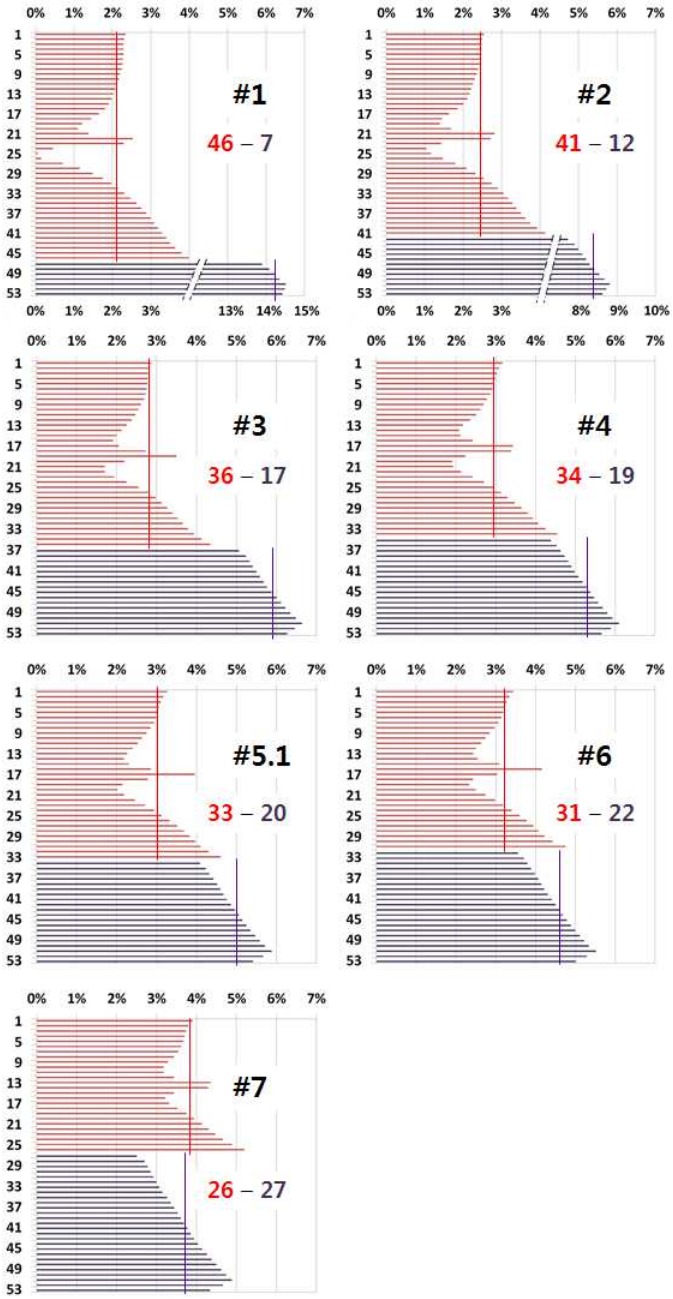

Figure 4.12 Comparison of flow uniformity (by tubes)

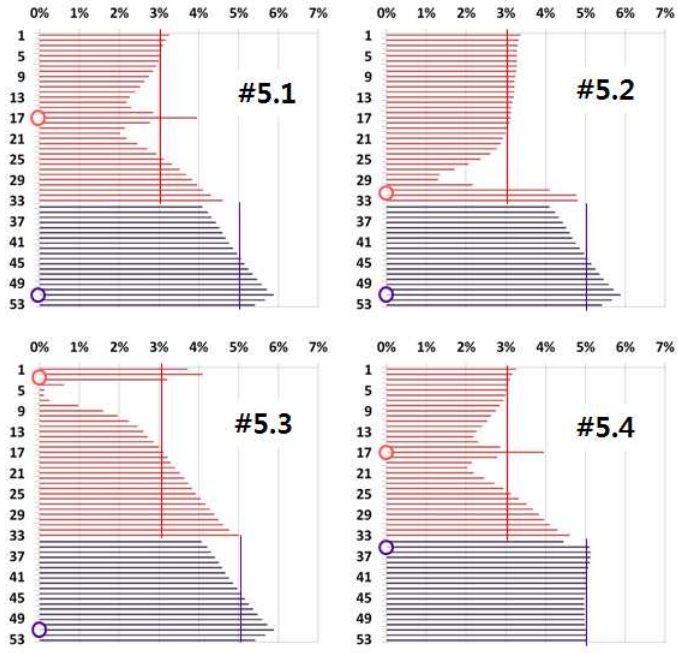

Figure 4.13 Comparison of flow uniformity (by pipes positions)

As the number of the first pass tubes increases, the inclination reinforces so that even almost zero flow is found in some cases. In the second pass, the mass flow rate increases towards the outlet pipe. This means that most of the flow after the first pass concentrates at the bottom of the second pass, which requires an analysis of the effect of the location of the pipes on the performance.

Table 4.1 shows the flow uniformities for 7 cases and two passes. The flow uniformity of the first pass increases with the decrease of the number of first pass tubes; the flow uniformity of the second pass decreases slightly with the increase of the number of the second pass tubes.

Table 4.2 Flow uniformity according to the positions of pipes

Case 1st 2nd	#5.1 Middle Bottom	#5.2 Bottom Bottom	#5.3 Top Bottom	#5.4 Middle Top
σ_1	0.914	0.918	0.819	0.914
σ_2	0.954	0.955	0.954	0.993

An analysis was made into the effect of the location of the inlet and outlet pipes on the flow distribution, using the 3-dimensional CFD program. Figure 4.13 shows the results of the analysis of the location of the inlet and outlet pipes, with the number of second tubes fixed as 20. As mentioned above, the basic model (#5.1) has an inlet pipe at the top, and an outlet pipe at the bottom of the header. Variations are the location of the inlet pipe at the bottom (#5.2), at the top (#5.3), and the outlet pipe at the top (#5.4) of the corresponding pass.

The uniformity values are shown in Table 4.2. In view of the effect of the location of the inlet pipe, the middle (#5.1) and bottom (#5.2) locations have nothing with the flow uniformity of the first or second pass; the top (#5.3) location has remarkably non-uniform flow distribution; moreover, there are some tubes adjacent to the inlet pipe in which little of the working fluid flows. The outlet pipe shows a good uniformity of over 99% with the location at the top of the second pass.

4.5.4 Decision for the Optimum Design Draft

A numerical analysis of heat transfer and fluid flow for considering the flow maldistribution in the working fluid tubes was carried out via 1D code for the low temperature condenser, for the 10 cases investigated above.

The inlet conditions were based on the system design point, i.e. the ambient air temperature of 35℃, working fluid inlet pressure of 16.4 bar, and working fluid inlet temperature of a superheat of 5 ℃. The ambient air velocity has been set as 5 m/s, and the working fluid mass flow rate has been 156 g/s; however, the situations that lack air flow and/or working fluid flow were also considered.

Figures 4.14 to 4.15 show a comparison of the heat dissipation and pressure drop respectively, given velocity of ambient air as 5 and 3 m/s, while the working fluid mass flow rate is 156 g/s, according to the 10 cases. The analysis result data are shown as relative values, i.e. the maximum value for the heat dissipation, and the minimum one for the pressure drop, are shown as 100% for each operating condition, e.g., individual ambient air velocity and flow rate. As shown intuitively, the models of #1 and #2 are disadvantageous for both heat dissipation and pressure drop. Abnormally tremendous pressure drops caused by small numbers of the 2^{nd} pass tubes affect the heat transfer performance.

And, The model in which the inlet pipe is located at the top,

and whose flow uniformity was the lowest (#5.3), displays also the lowest performance of heat dissipation.

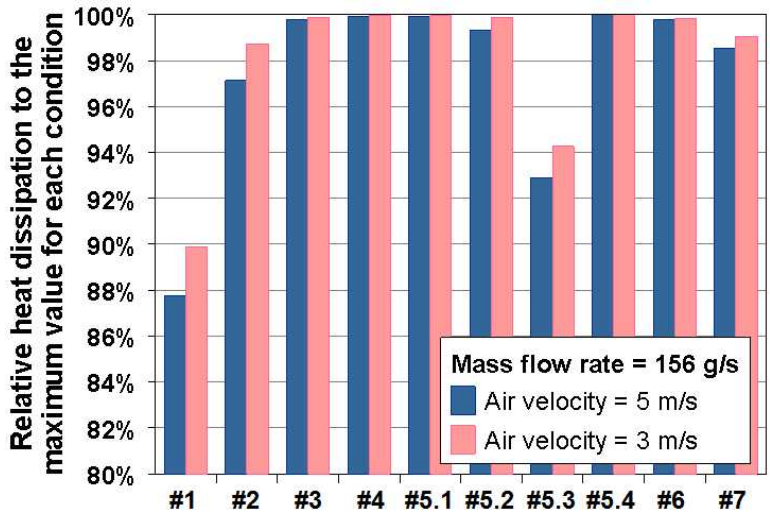

Figure 4.14 Heat dissipation comparison (flow rate: 156 g/s)

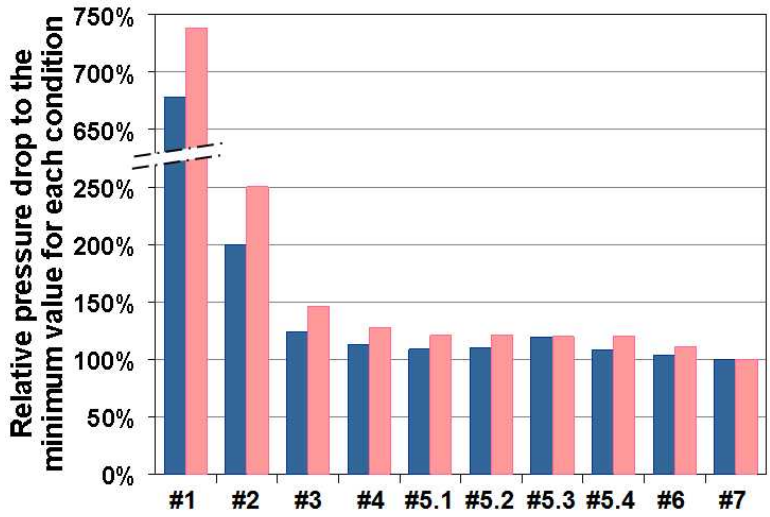

Figure 4.15 Pressure drop comparison (flow rate: 156 g/s)

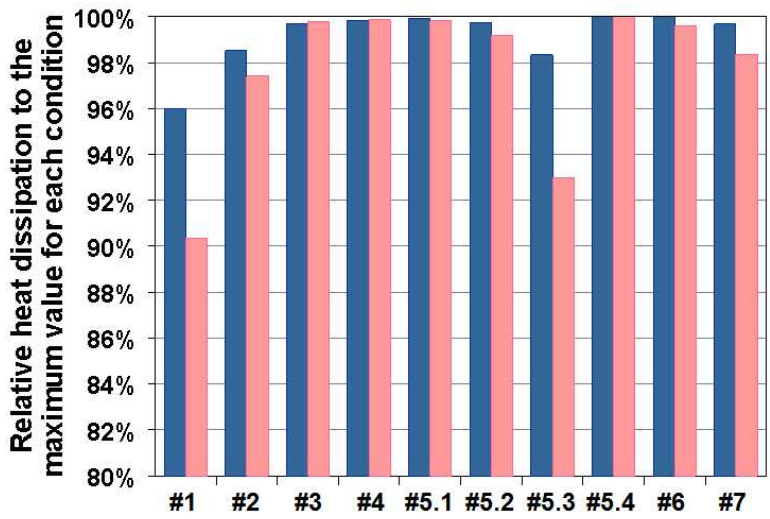

Figure 4.16 Heat dissipation comparison (flow rate: 100 g/s)

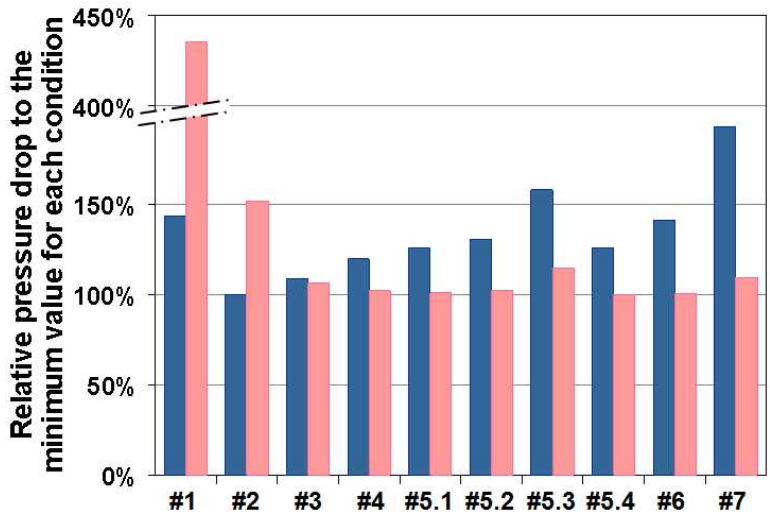

Figure 4.17 Pressure drop comparison (flow rate: 100 g/s)

Through the models of #3 to #6, the pressure loss behaviors are similar to one another, except for #5.3 model, which is rather

disadvantageous.

Figures 4.16 and 4.17 show a comparison of the performance of the LT condenser similar to that shown in Figures 4.14 and 4.15, while the working fluid mass flow rate is 100 g/s. The additional weakness appears in the performance of model #7. The top inlet pipe model represents the lowest heat transfer rate again, and the highest pressure drop in the reasonable comparison models of #3 to #6. On the other hand, two models that have 20 tubes in the second pass and have the inlet pipe at the middle, show the best heat dissipation: the outlet pipe at the top (#5.4), and the one at the bottom (#5.1).

All through the design process described above, the selected models are ones that have tubes of 33 in the first pass, and 20 in the second pass, and inlet pipe in the middle (#5.4, #5.1), which are expected to represent the optimal performance.

4.6 Experimental Results

The prototype of the LT condenser was set on a test rig as shown in Figure 4.18. The inlet pipe is located in the middle of the 1st pass, and the location of the outlet pipe can be altered at the top or bottom of the 2nd pass.

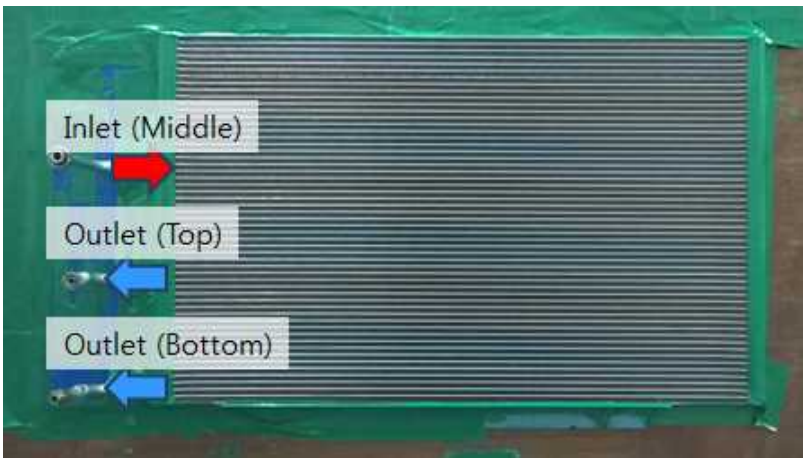

Figure 4.18 Configuration of the performance test rig

The experiment was conducted at the design point, i.e. the inlet pressure of the refrigerant was 16.4 bar, the inlet superheat was set as 5℃, and ambient air temperature was 35℃. The air velocity varied from 1 to 5 m/s. The adequate mass flow rate of the working fluid was found at which the sub-cool of 5℃ was satisfied.

Figure 4.19 shows a comparison of the heat dissipation results of the experiment, and the simulation, at the design point for the

two selected models (#5.4 Middle - Top, and #5.1 Middle - Bottom). Although all the values match within 1%, the simulated predictions by flow distribution are closer to the experimental values, than ones by uniform flow. The heat dissipation values estimated from the experiment are similar, i.e. 22.12 kW and 22.17 kW, respectively.

For the purpose of graphical presentation, the simulation results for the working fluid in the tubes of 2 models are shown in Figure 4.20. In the middle of the end of the 1st pass, an area of slightly low temperature occurs in each case, due to the flow mal-distribution.

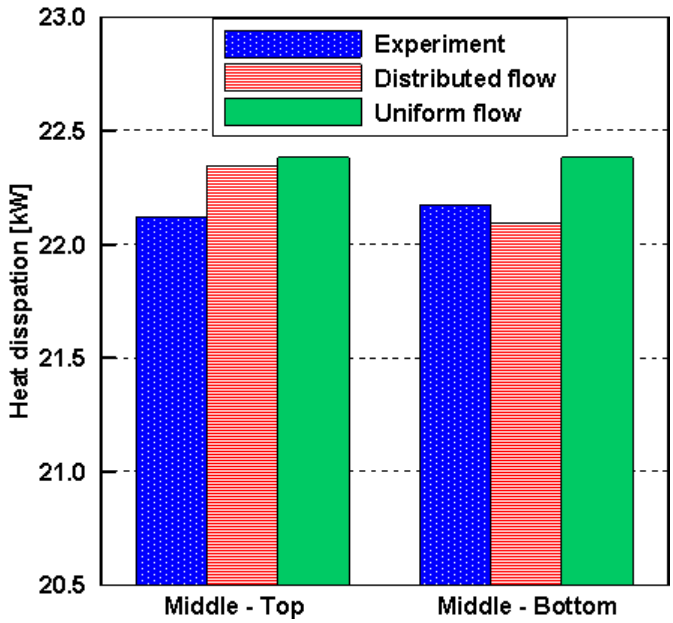

Figure 4.19 Comparison of experimental performance with simulation (#5.4: Middle - Top, #5.1: Middle - Bottom)

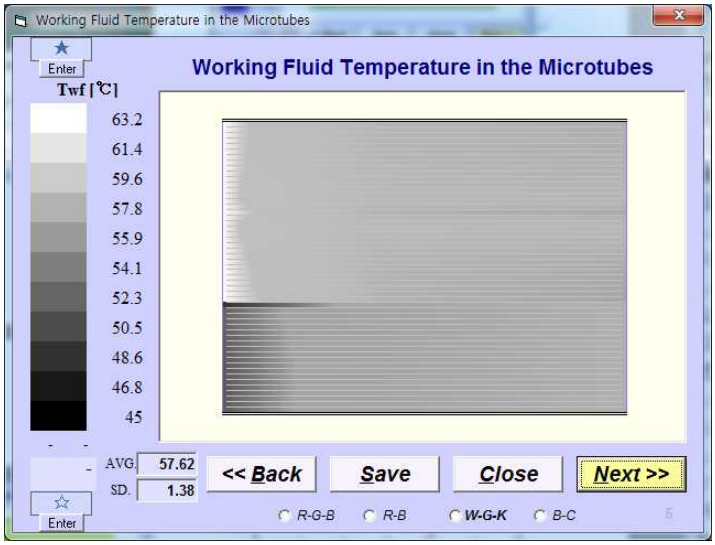

(a) Middle - Top configuration (#5.4)

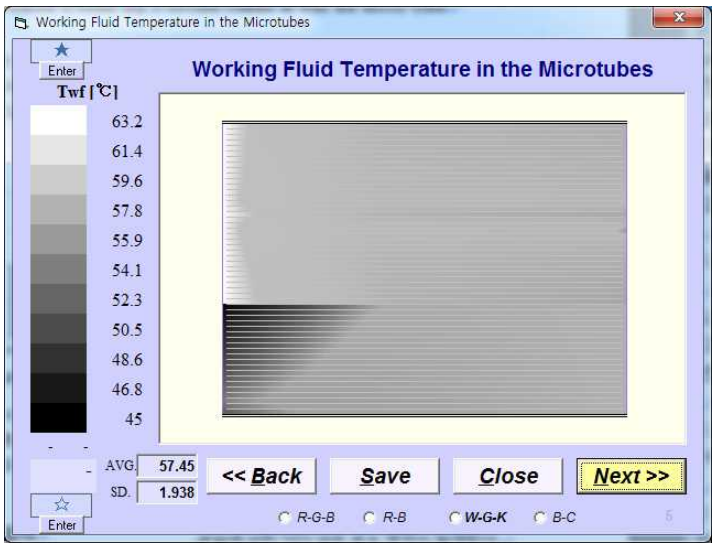

(b) Middle - Bottom configuration (#5.1)

Figure 4.20 Working fluid temperature distribution (simulation)

Though both models have similar heat dissipation and pressure

drop, the Middle - Top model (Figure 4.20 (a)) has relatively uniform flow distribution at the exit, and the Middle - Bottom model (Figure 4.20 (b)) has concentrated flow to the bottom at the same region. The #5.4 model is somewhat advantageous from the aspect of the flow uniformity; however, the uniformity at this region has no significant effect on the performance. As mentioned above, the system has a reservoir tank at the outlet of the condenser, for the purpose of preventing the saturated vapor from flowing into the working fluid pump. However, when the working fluid is not fully condensed in variable operating conditions, flow resistance may abruptly occur temporarily with the outlet pipe at the top position. Consequently, the #5.1 model was selected for the optimum design, which has the outlet pipe at the bottom.

Figure 4.21 shows a comparison of the experimental results of 4-pass and 2-pass prototypes that have the same cross-sectional geometry of tubes (total tube number is 55), and another comparison of the experimental and simulation results of the current model (#5.1 model, total tube number is 53) that has enhanced cross-sectional areas of tubes. The 2-pass models have slightly better heat performance over air velocity range. The 2-pass model has relatively low deterioration of performance caused by a rise of pressure drop, so that the heat dissipation increased by 4% or more rather than the 4-pass model.

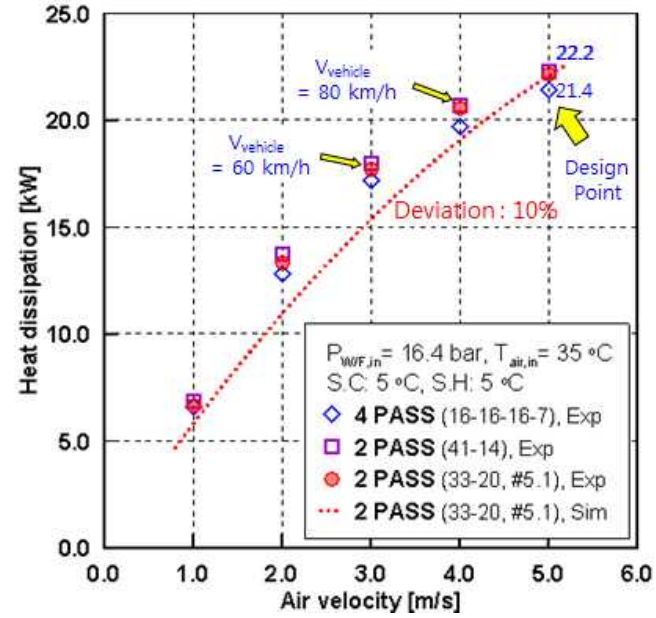

(a) Heat dissipation

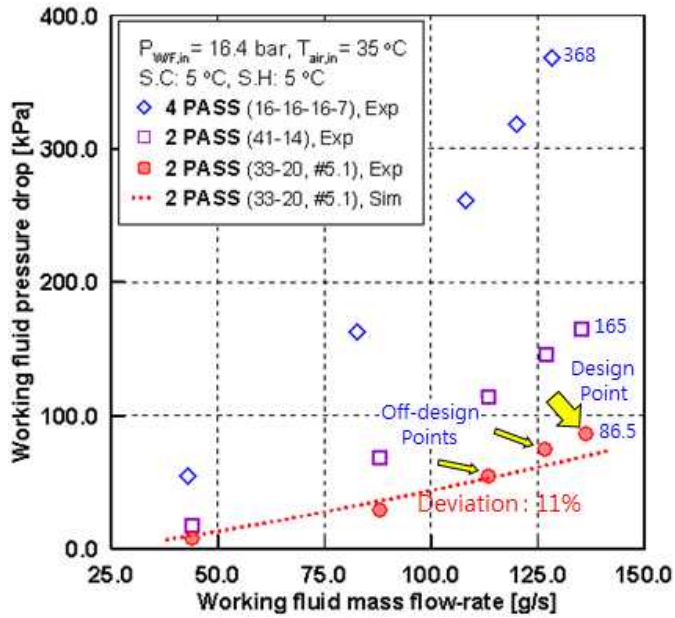

(b) Working fluid pressure drop

Figure 4.21 Experimental results comparing 3 models

Air velocity of 3, 4, and 5 m/s imply the cycle conditions at the vehicle speed of 80, 100, and 120 km/h, respectively. The lower air speed range implies the lower range of the vehicle speed.

The pressure drop of working fluid of the 4-pass model was 368 kPa at the design point; however, the model that has reduced passes to 2 showed a greatly reduced pressure drop, i.e. 165 kPa. Only reducing the number of passes decreases 55.2% of the working fluid pressure drop.

The 53-tube models in the previous chapter (#1 to #7) could have a reduced pressure drop of around 100 kPa, since they have larger cross-sectional areas of tubes than the 55-tube models. Further optimum design (#5.1) for the reduction of the working fluid pressure drop enabled a reduction in the pressure drop to about 86 kPa. The optimum design model represents drastically reduced pressure drop and satisfies heat dissipation requirements.

The entire design process decreased the pressure drop by 62%, exclusive of the influence of the cross-sectional areas. The analysis data of heat dissipation coincided with the experimental ones within 1% at the design point. At the full range of air velocity, the heat dissipation data show an error rate of 10% on average, and the pressure drop data show an error rate of 11% on average.

4.7 Conclusion

This chapter has dealt with a design process that reduces the pressure drop of an air-cooled LT condenser in an engine waste heat recovery system, while maintaining the heat dissipation performance. The results obtained through this chapter are as follows:

The optimum performance design was peformed for the pressure drop reduction of a parallel multi-flow type air-cooled condenser using a own 1D design program.

In the dual-loop engine waste heat recovery system, the flow rate of the low temperature loop working fluid, or refrigerant, is considerably larger, than in a conventional automotive air conditioning system. Therefore, new design methodology is needed to reduce the pressure drop at the refrigerant side. The larger the number and the cross-sectional areas of tubes, the more the pressure drop is reduced. After these features are fixed, the number of passes should be minimized at first, and the numbers of tubes onto the passes is arranged, and the locations of the inlet and outlet pipes are determined through the design procedures.

The number of passes and arrangement of the number of tubes have a significant effect on the pressure drop, even if the condenser geometry is identical in appearance. An increase in the number of passes does not enhance the heat dissipation

performance but increases the pressure drop so that the performance gets worse instead. In other words, a reduction of number of passes decreases the pressure drop at working fluid side, thus the heat dissipation slightly increases consequently.

The pressure drop differs about 2 to 7 times according to the ambient and working fluid conditions by the arrangement of the number of tubes. As a result, the heat dissipation deteriorate about 4.0 ~ 12.2% according to the conditions.

The locations of the inlet and outlet pipes on the header affect the flow uniformity of the working fluid in the tubes remarkably, and as a result, the performance differed by 7% for the heat dissipation, and 46% or more for the pressure drop.

The optimum design is selected as the 2-pass model, in which the tubes are arranged as 33-20 (62%-38%), the inlet pipe is located in the middle of the header, and the outlet pipe is in the bottom.

The experimental investigation has been performed in a limited range of prototypes and conditions. The 1D code was made available to use the data of frontal air distributions of velocity and temperature; however, throughout the scope of this paper, all the distributions are assumed to be uniform. Some experimental data offsets seem to have arisen from this fact.

The working fluid pressure drop could be affected by phase change in the tubes. For more accurate research, further two-way analytical coupling would be necessary, i.e. investigation reflecting

the interactive effect of the geometry (commercial 3D) and phase change (own 1D code).

Chapter 5

Conclusion and Future Works

Recent worldwide trend of automotive technology proceeds toward the development of the technologies which are able to satisfy the regulations and customer's demand for eco-friendly, highly efficient, low fuel consumption and in short term. The drastic improvement of fuel efficiency of conventional internal combustion engine vehicles and hybrid vehicles by use of The technology that re-generates the power from the waste energy is a very realistic and useful alternative. There are a variety of limitative environmental conditions for heat recovery from heat sources and heat dissipation to circumstances at low energy level in adaptation of Rankine cycle technology to vehicles. The conditions are mostly the temperatures and pressures of the heat sources, the working fluids, and the circumstances or ambient. It is important for the waste heat recovery system to secure stable operation in spite of the change in driving mode in the actual vehicle.

A waste heat recovery system containing two Rankine cycles has been constructed to be installed on vehicles in order to improve the fuel efficiency, which is initiated and designed by 1D and/or 3D analytical design approach. The own 1D programs have been made for design of heat exchangers in this study; the

3D program used for design is a general-purpose commercial code (Fluent 6.3).

First of all, selections of the working fluids satisfying the limit conditions are the very first essential procedure in system design. The one-dimensional cycle analysis program has contributed to select the working fluids of the cycles considering the amount, level, and type of the heat source, cycle efficiency, size of the core components, reliability design, system cost, safety and environmental aspects. In this study, the system have been configured as a dual loop system in which water, the high temperature loop working fluid, recovers waste heat from exhaust gas, and refrigerant, the low temperature loop working fluid, recovers waste heat from coolant. The highest pressure has been limited to 25 bar, and the maximum temperature has been limited to 300 ℃. Under these conditions, the ideal cycle efficiency is predicted to be about 18.6% for HT loop, and 8.15% for LT loop. From the design process of cycles and system layout, the engine efficiency improvement has been predicted as 12.0% out of the engine power gathering these regenerative powers from HT and LT loops at EPA highway mode.

A design process has been conducted to seek an optimal structure of the heat recovery heat exchanger. The working fluid in the HT boiler experiences a phase change from liquid state to saturated state. At a liquid state, the specific volume of the working fluid is so small that the cross-sectional area must be

small, otherwise it would not recover sufficiently the waste heat. On the other hand, at a saturated state, the specific volume of the working fluid grows with the quality, i.e., the cross-sectional area of the heat exchanger can be larger than at a liquid state. Focusing on this point, three structural concepts have been established, designed via 1D and 3D analytical design process, embodied as prototypes, and assessed by experiments. The installation of HT boiler at the exhaust system has been designed as the structure that exhaust gas can be bypassed in accordance with the variation of the transient engine conditions when the energy source is excessive for the waste heat recovery system. The performance of the rectangular model is 27.8% better than the circular model, and is 71.5% better than the fin and helical coil tube model in view of heat recovery considering the volume occupied. The rectangular model satisfies the heat recovery requirements over the heat source range.

For the heat dissipating core, LT condenser, a novel design process model has been built, so that the pressure drop is reduced, while the heat transfer performance is maintained at a target. The refrigerant has small saturation enthalpy, so that excessive mass flow rate of the LT working fluid causes an enormously large pressure drop of the working fluid, to maintain the heat dissipation performance, which is extremely large amount as the one for an air-cooled heat exchanger in an automotive. An investigation for multi-pass structural design has

been described by inspecting the number of passes, and the arrangement of the numbers of tubes, in order to enhance the flow uniformity, and reduce the pressure drop of the working fluid. Reducing the number of passes from 4 to 2 makes the pressure drop less than half, i.e., 44.8%. The optimal arrangement of passes reduces 62%, and as a result, increases 4% of heat dissipation at the design point. At various operating conditions, the pressure drop differs about 2 to 7 times by the arrangement of the number of tubes and as a result, the heat dissipation declines about 4.0 ~ 12.2%. The performance differs by 7% for the heat dissipation, and 46% or more for the pressure drop by the locations of the inlet and outlet pipes on the header.

The design process data of this study can be applied to other major parts of the engine waste heat recovery system, and expanded also to the important parts of the co-generation in industrial usage, automotive air conditioning systems and engine cooling systems.

The system and components have not been in the conventional vehicle so that the additional installation of the system would increase in the weight of the vehicle, however, many components are replaceable of the existing parts or can reduce ones. HT boiler and HT superheater are installed at the place of ducts which have been removed from the exhaust system. In addition, HT boiler is capable of playing the role of the muffler for diminution of noise so that the muffler can be reduced or

removed from the exhaust system. LT boiler, which serves to cool down the engine coolant, makes it possible to reduce significantly the size of the conventional engine radiator. In view of regeneration energy of the system, the power re-generated by the expander is used as the additional power into the engine through the power transmission device. The system control algorithm utilizing the one-way clutch shuts down the waste heat recovery system when the engine output is low and avoids the situation that the expander become the burden on the engine.

The field of the co-generation system based on Rankine cycle technology is still a beginning stage for automobile industry that any mass production has been not yet conducted. It means that the design technology of the Rankine cycle and core components are promising for the future such as a high possibility of the adaptation to the global system and components.

A waste heat recovery system is a new system that has various components such as high pressure pumps, heat exchangers, valves, and controllers for the temperatures and pressures of the working fluids, and is associated with the conventional exhaust system and the engine cooling system. The related technology from this study is considered as having a great impact on the various technologies. Since the core components of the system in this study differ considerably from the ones of other systems for automobiles in all aspects of temperatures, pressures, mass flow rates of the working fluids, the technical competitiveness can be

secured in the future new market of the engine waste heat recovery system for vehicles.

In the United States, since cargo trucks use much of yearly fuel and run a lot of long-distance travels at highway mode, Cummins Inc. analyzes that even a several percentage of fuel saving leads to the willing adoption of the waste heat recovery system no matter how much the price rises. Cummins Inc. had finished the research on heavy duty truck engine waste heat recovery in the system aspect to achieve 6% fuel economy improvement, is expected to select the company for mass production core components at the current level, and targets of more than 10% fuel economy improvement. In this trend, other commercial vehicle companies are known to be preparing for their own development [Kadota08, Wei08, Lopes12, Arunachalam12, Feru13, Shu13]. In view of the trend of car-makers, the system technology is believed to be certainly commercialized sooner or later, the market share is expected to grow exponentially in 2020. In recent years, the engine waste heat recovery system has been actively developed in the shipbuilding industry so that the development of the relevant core components are expected to have a great pervasive effect onto other industries.

Bibliography

[Ringler09] Ringler, J., Seifert, M., Guyotot, M. and Hubner, M. (2009). Rankine Cycle for Waste Heat Recovery of IC Engines. *SAE Paper* No. 2009-01-0174.

[Endo07] Endo, T., Kawajiri, S., Kojima, Y., Takahashi, K., Baba, T., Ibaraki, S., Takahashi, T. and Shinohara, M. (2007). Study on Maximizing Energy in Automotive Engines. *SAE Paper* No. 2007-01-0257.

[Teng07] Teng, H., Regner, G. and Cowland, C. (2007). Waste Heat Recovery of Heavy-Duty Diesel Engines by Organic Rankine Cycle Part Ⅱ: Working Fluids for WHR-ORC. *SAE Paper* No. 2007-01-0543.

[Heo5] Heo, H. S. and Bae, S. J. (2010). Technology Trends of Rankine Steam Cycle for Engine Waste Heat Recovery. A*uto Journal of KSAE*, 32, 5, 23-32.

[Kee10] Kee., J. D. and Lee., J. H. (2010). Technology Trends of Turbo Compound System for Engine Waste Energy Harvesting. *Auto Journal of KSAE*, 32, 5, 33-42.

[Stobart06] Stobart, R., and Weerasinghe, R. (2006). Heat Recovery and Bottoming Cycles for SI and CI Engines –A Perspective, *SAE Paper* No. 2006-01-0662.

[Freymann12] Freymann, R., Ringler, J., Seifert, M. and Horst, T. (2012). The Second Generation Turbosteamer. *MTZ Worldwide*, 2012, 2, 18-28.

[Nelson09] Nelson, C. R. (2009). "Exhaust Energy Recovery,"

Presentation at USDOE Directions in Engine-Efficiency and Emissions Research Conference.

[Ye09] Ye, L., Tong, M. W. and Zeng, X. (2009), Design and analysis of multiple parallel-pass condensers. *International Journal of Refrigeration*, 32, 6, 1153-1161.

[Sanaye11] Sanaye, S., Dehghandokht. M. (2011). Modeling and multi-objective optimization of parallel flow condenser using evolutionary algorithm, *Applied Energy*, 88, 1568-1577.

[Lopes12] Lopes, J., Douglas, R., McCullough, G., and O'Shaughnessy, R. (2012). Review of Rankine Cycle Systems Components for Hybrid Engines Waste Heat Recovery, *SAE Paper* No. 2012-01-1942.

[Kays84] Kays, W. M., London, A. L. (1984). Compact heat exchangers. *McGraw-Hill*, 3rd edition. 14-21, 35-38.

[Gungor86] Gungor, K. E., Winterton, R. H. S. (1986). A general correlation for boiling in tubes and annuli, *International Journal of Heat Transfer*, 19, 351-358.

[Dong07] Dong, J., Chen, J., Chen. Z,, Zhou, Y., Zhang, W. (2007). Heat transfer and pressure drop correlations for the wavy fin and flat tube heat exchangers, *Applied Thermal Engineering*, 27, 2066-2073.

[Dong13] Dong, J., Su, L., Chen, Q., Xu, W. (2013). Experimental study on thermal-hydraulic performance of a wavy fin-and-flat tube aluminum heat exchanger, *Applied Thermal Engineering*, 51, 32-39.

[Naphon06] Naphon, P., Wongwises, S. (2006), A review of flow and heat transfer characteristics in curved tubes, *Renewable and Sustainable Energy Reviews*, 10, 463-490. (Requoted: Ju H, Huang Z, Xu Y, Duan

B, Yu Y. (2001), Hydraulic performance of small bending radius helical coil-pipe. *J Nucl Sci Technol*, 18, 826-831.)

[Gaddis97] Gaddis, E. S., Gnielinski, V. (1997), Pressure drop on the shell side of shell-and-tube heat exchangers with segmental baffles, *Chemical Engineering and Processing*, 36, 149-159.

[Domanski08] Domanski, P. A., Hermes., C. J. L. (2008). An improved correlation for two-phase pressure drop of R-22 and R-410A in 180° return bends, *Applied Thermal Engineering*, 28, 793-800.

[Mehta79] Mehta, M.H. , Rao, M. R. (1979), Investigations on heat transfer and frictional characteristic of enhanced tubes for condensers, *Advances in Enhanced Heat Transfer, ASME*, 11-21.

[Vicente04] Vicente, P. G., Garcia, A., Viedma. A. (2004). Experimental investigation on heat transfer and frictional characteristics of spirally corrugated tubes in turbulent flow at different Prandtl numbers, *International Journal of Heat and Mass Transfer*, 47, 671-681.

[Chen07] Chen, I. Y., Liu, C. C., Lin, Chien, K. H., Wang. C. C. (2007). Two-phase flow characteristics across sudden expansion in small rectangular channels, *Experimental Thermal and Fluid Science*, 32, 696-706.

[Chen09] Chen, I. Y., Tseng, C. Y., Lin, Y. T., Wang. C. C. (2009). Two-phase flow pressure change subject to sudden contraction in small rectangular channels, *International Journal of Multiphase Flow*, 35, 297–306.

[Bae12] Bae, S. J., Heo, H. S., Park, J. S., Lee, H. Y. and Kim, C. J.

(2012). Design and Performance Evaluation of Low Temperature Condenser of Waste Heat Recovery System for Fuel Economy Improvement. *Spring Conference of KSAE*, 250-255.

[Bae11] Bae, S. J., Heo, H. S., Lee, H. K., Lee, D. H., Kim, T. J., Park, J. S., Lee, H. Y. and Kim, C. J. (2011). Performance Characteristics of a Rankine Steam Cycle and Boiler for Engine Waste Heat Recovery. *SAE Paper* No. 2011-28-0055.

[Incropera96] Incropera, F., Dewitt, P. D. (1996). Introduction to Heat Transfer, *John Wiley & Sons Inc.*, 3rd edition.

[Cavallini71] Cavallini, A., Zecchin., R. (1971). A dimensionless correlation for heat transfer in forced convection condensation, *Proceedings of the 13th International Congress of Refrigeration*, 2, 193-200.

[Chang00] Chang, Y. J., Hsu, K. C., Lin, Y. T., Wang, C. C. (2000). A generalized friction correlation for louver fin geometry, *International Journal of Heat and Mass Transfer*, 43, 2237-2243.

[Collier94] Collier, J. G., Thome, J. R. (1994). Convective Boiling and Condensation, 3rd ed., *Oxford University Press Inc.*, New York, U.S, 64-68.

[Kim06] Kim, B. J., Sohn, B. H. (2006). An experimental study of flow boiling in a rectangular channel with offset strip fins, *International Journal of Heat and Fluid Flow*, 27, 514-521. (Requoted: Lockhart, R. W., Martinelli, R. C. (1949). Proposed correlation of data for isothermal two-phase two-component flow in pipes, *Chemical Engineering Progress*, 45, 39–48.)

[Kadota08] Kadota, M. and Yamamoto, K. (2008). Advanced Transient

Simulation on Hybrid Vehicle Using Rankine Cycle System. *SAE Paper* No. 2008-01-0310.

[Wei08] Wei. D. H., Lu, X. S., Lu, Z., Gu, J. M. (2008), Dynamic modeling and simulation of an Organic Rankine Cycle (ORC) system for waste heat recovery, *Applied Thermal Engineering*, 28, 1216–1224.

[Arunachalam12] Arunachalam, P. N., Shen, M., Tuner, M., Tunestal, P. and Thern. M., Waste Heat Recovery from Multiple Heat Sources in a HD Truck Diesel Engine Using a Rankine Cycle - A Theoretical Evaluation, *SAE Paper* No. 2012-01-1602.

[Feru13] Feru, E., Kupper, F., Rojer, C., Seykens, X., Scappin, F., Willems, F., Smits. J, De Jager, B., Steinbuch, M., Experimental Validation of a Dynamic Waste Heat Recovery System Model for Control Purposes, *SAE Paper* No. 2013-01-1647.

[Shu13] Shu, G. Q., Yu, G., Tian, H., Wei, H., Liang, X., Simulations of a Bottoming Organic Rankine Cycle (ORC) Driven by Waste Heat in a Diesel Engine (DE), *SAE Paper* No. 2013-01-0851.

국문초록

복합차원 열유동 해석 기법을 통한 가솔린 자동차용 엔진 폐열 회수 시스템 열교환기의 설계 최적화

전 세계적으로 지구 온난화 및 자원 고갈에 대응하기 위한 강력한 연비 규제 정책이 확대되고 있으며, 엔진과 변속기 등의 파워트레인 기술 개발에 의한 연비 향상 기술은 한계에 도달하고 있다. 자동차의 연료 에너지 중에서 동력 발생에 사용되는 에너지는 최대 30% 수준이며 주 운전 영역에서 약 10~20%에 불과하고, 엔진 보기류의 구동과 공기 및 구름 저항까지 고려하면 실제 차량 구동에 사용되는 에너지는 10% 이하로 감소한다. 동력 에너지로 변환되지 못하고 외부로 방출되는 엔진의 폐에너지를 회수하는 엔진 폐열 회수 시스템 기술 중에서 랭킨 사이클 기술은 현재 자동차에 적용성이 가장 높은 것으로 알려져 이에 대한 연구가 각광 받고 있다.

본 연구에서는 가솔린 자동차의 연비 향상을 위해 랭킨 사이클 방식의 엔진 폐열 회수 시스템을 구성하였다. 상용 CFD 해석 프로그램은 복잡한 형상에 대한 상세 열유동 분포를 계산할 수 있지만 상변화 과정을 충분히 예측할 수 없는 반면, 사이클 및 핵심 부품에 대하여 개발한 전용 해석 프로그램을 이용하면 1차원적으로 성능을 예측하지만 상변화에 따른 작동유체 변화를 추적할 수 있으며, 형상 설계 인자들이 성능에 미치는 영향을 신속하고 다각적으로 확인할 수 있다. 본 연구에서는 이 두 가지 설계 기술의 장점을 조화시켜서 엔진 폐열 회수 시스템의 설계 및 구성을 복합차원 해석 프로세스

를 통하여 최적화하였다.

우선, 랭킨 사이클 기반의 폐열 회수 시스템은 1차원 해석 프로그램의 개발을 통하여 시작하였다. 설계 제한 조건을 충족하면서 연비 향상 효과를 극대화할 수 있는 엔진 폐열 회수 시스템 구성을 위해서 사이클 성능 예측 프로그램을 이용하여 시스템 성능 예측, 사이클 성능 설계, 핵심 부품의 설계 제원 설정을 수행하였다. 이로써 듀얼 루프 폐열 회수 시스템을 구성하였다. 작동유체의 선정 과정 또한 사이클 해석 프로그램을 통해 진행되었다. 엔진 배기로부터 폐열을 회수하는 고온측 (HT) 회로는 작동유체로 물을 선정하였고, 고온측 회로의 방열 및 비교적 저온인 냉각수로부터 폐열을 회수하기 위한 저온 측 (LT) 회로에서는 작동유체로 냉매를 선정하였다.

배기가스로부터 폐열을 회수하는 HT 보일러는 신 구조 개념으로 설계를 수행하였다. HT 보일러 내부의 작동유체는 액상에서 기상으로 상변화를 겪는데, 액상에서는 작동유체의 비체적이 매우 작으므로 단면적이 작아야 폐열을 충분히 회수할 수 있다. 반면에 포화상태에서는 건도가 상승할수록 작동유체의 비체적이 증가한다. 이러한 점에 근거하여 3가지 구조의 개념 설계를 수립하고, 1차원 성능 예측 프로그램 개발 및 3차원 상용 코드 해석을 이용한 설계 과정을 통해 시작품을 설계 및 제작하고 실험을 통하여 성능을 비교 평가하였다.

본 연구에서는 시스템 전체의 남은 열을 방출하는 LT 응축기의 방열 성능을 유지하면서 압력 손실을 저감시키는 새로운 설계 프로세스 모델을 구축하였다. LT 작동유체로 선정된 냉매는 약 100℃의 엔진 냉각수로부터 폐열 회수하기에 적합한 증발 온도를 갖추고 있지만 포화 엔탈피가 작아서 작동유체 유량이 150 g/s을 초과한다.

이 때문에 20 kW 이상의 높은 방열량 수준을 유지하기 위해서는 LT 작동유체 측의 압력 손실이 크게 증가할 수밖에 없다. 평행 다류관 구조의 LT 응축기의 압력 손실을 최소화할 수 있는 패스 수, 각 패스의 튜브 수 분배 및 유동 균일도를 유지할 수 있는 구조 설계 방안에 대해서 기술한다.

본 연구에서 다루고자 하는 사이클 설계 기술과 복합차원 해석을 통한 핵심 열교환기의 최적화 설계 과정은 자동차 폐열 회수 시스템 분야의 기술 경쟁력 확보의 초석이 될 것으로 기대된다.

주요어 : 폐열 회수 시스템, 랭킨 사이클, 열유동 해석, HT 보일러, LT 응축기, 복합차원 해석
학 번 : 2008-30855